INTERACTIONS OF CHOLESTEROL REDUCING AGENT SIMVASTATIN WITH PHOSPHOLIPID MODEL MEMBRANES

A THESIS SUBMITTED TO
THE GRADUATE SCHOOL OF NATURAL AND APPLIED SCIENCES
OF
MIDDLE EAST TECHNICAL UNIVERSITY

BY

MUSTAFA KOÇAK

IN PARTIAL FULFILLMENT OF THE REQUIREMENTS
FOR
THE DEGREE OF MASTER OF SCIENCE
IN
BIOCHEMISTRY

JANUARY 2007

Approval of the Graduate School of Natural and Applied Sciences

_____
Prof. Dr. Canan ÖZGEN
Director

I certify that this thesis satisfies all the requirements as a thesis for the degree of Master of Science.

_____
Assoc. Prof. Nursen ÇORUH
Head of Department

This is to certify that we have read this thesis and that in our opinion it is fully adequate, in scope and quality, as a thesis for the degree of Master of Science.

_____
Prof. Dr. Feride SEVERCAN
Supervisor

Examining Committee Members

Prof. Dr. Tülin GÜRAY (METU, BIOL) _____

Prof. Dr. Feride SEVERCAN (METU, BIOL) _____

Prof. Dr. Engin U. AKKAYA (METU, CHEM) _____

Prof. Dr. Faruk T. BOZOĞLU (METU, FDE) _____

Prof. Dr. Nadide KAZANCI (Ege Unv., PHYS) _____

I hereby declare that all information in this document has been obtained and presented in accordance with academic rules and ethical conduct. I also declare that, as required by these rules and conduct, I have fully cited and referenced all material and results that are not original to this work.

Mustafa KOÇAK

ABSTRACT

INTERACTIONS OF CHOLESTEROL REDUCING AGENT
SIMVASTATIN WITH PHOSPHOLIPID MODEL MEMBRANES

Koçak, Mustafa
M. S., Deparment of Biochemistry
Supervisor: Prof. Dr. Feride SEVERCAN

January 2007, 140 pages

Interactions of simvastatin with zwitterionic dipalmitoyl phosphotidylcholine (DPPC) multilamellar liposomes were investigated as a function of temperature and simvastatin concentration. And acyl chain length effect on the simvastatin-model membrane interactions was monitored with DPPC and dimyristoyl phosphotidylcholine (DMPC) lipids. All studies were carried out by two non-invasive techniques, namely Fourier transform infrared (FTIR) spectroscopy, and differential scanning calorimetry (DSC).

The results showed that as simvastatin concentration increased, the main phase transition temperature decreased, the main phase transition curve broadened, and the characteristic pretransition was disappeared for both DMPC and DPPC model membranes. All concentrations of simvastatin disordered and decreased the fluidity of phospholipid membranes.

Analysis of C=O stretching band showed that simvastatin either strengthen the existing hydrogen bonds of the glycerol skeleton closer to the head groups or caused the formation of new hydrogen bonds.

A dehydration effect caused by simvastatin around the PO_2^- functional groups in the polar part of the lipids was monitored. This dehydration effect in the gel phase was more profound than in the liquid crystalline phase for 1, 6, and 12 mol% of simvastatin concentrations.

DSC peaks broadened and shifted to lower temperature values by increasing the simvastatin concentration. For both lipids, simvastatin-induced lateral phase separation was observed in the DSC thermograms.

Any change caused by the acyl chain length difference of DMPC and DPPC lipids was not observed on the simvastatin-membrane interactions. Also, for both of the lipids similar trends were observed in the FTIR and DSC results. More profound effects of simvastatin on the less stable DMPC membranes were observed.

Key words: Simvastatin, acyl chain length effect, DMPC, DPPC, FTIR, DSC.

ÖZ

KOLESTEROL DÜŞÜRÜCÜ AJAN SİMVASTATİNİN FOSFOLİPİD MODEL MEMBRANLARLA ETKİLEŞİMLERİ

Koçak, Mustafa
Yüksek Lisans, Biyokimya Bölümü
Tez Yöneticisi: Prof. Dr. Feride SEVERCAN

Ocak 2007, 140 sayfa

Bu tezde simvastatinin dipalmitol fosfatidilkolin'den (DPPC) oluşan çok katmanlı lipozomların termotropik faz davranışı ve fiziksel özelliklerine olan etkisi sıcaklığa ve simvastatin derişimine bağlı olarak araştırıldı. Ayrıca simvastatin-model membran etkileşimlerinde asil zincir uzunluğunun etkisi DPPC ve dimirisitol fosfatidilkolin (DMPC) lipidleri kullanılarak araştırıldı. Tüm çalışmalarda katman yapısına zarar vermeyen Fourier dönüşüm kızılötesi (FTIR) spektroskopisi ve diferansiyel tarama kalorimetresi (DSC) kullanıldı.

Sonuçlarımıza göre her iki lipidin model membranları için simvastatin derişimi yükseldikçe, ana faz geçiş sıcaklığı düşmüş, faz geçiş eğrisi genişlemiş ve ön faz geçiş sıcaklığı tamamen yok olmuştur. Bunlarla birlikte tüm simvastatin derişimlerinde membranların düzensizliği artmış akışkanlığı azalmıştır.

FTIR spektroskopisinde C=O gerilme bandlarının analizine göre simvastatin kafa gruplarına yakın gliserol iskeletinde varolan hidrojen bağlarını güçlendirmiş ya da yeni hidrojen bağlarının oluşmasını sağlamıştır.

Ayrıca lipidlerin polar kısımlarındaki PO_2^- fonksiyonel gruplarının etrafında simvastatin kaynaklı dehidrasyon görülmüştür. 1, 6 ve 12 mol% simvastatin derişimlerinde bu dehidrasyon etkisi jel fazda sıvı kristal faza göre daha derin olmuştur.

Simvastatin konsantrasyonu arttıkça DSC tepe eğrileri genişlemiş ve daha düşük sıcaklık değerlerine kaymıştır. Yine her iki lipidin DSC termogramlarında simvastatin sebebli yanal faz ayrımının olduğu görülmüştür.

Simvastatin-membran etkileşimlerinde DMPC ve DPPC lipidleri arasındaki asil zincir uzunluğu farkından dolayı herhangi bir değişiklik görülmemiştir. Bununla birlikte her iki lipidin FTIR ve DSC sonuçlarında benzer eğilimler gözlemlenmiştir. Ayrıca daha az kararlı olan DMPC membranlarında simvastatin etkilerinin daha derin olduğu görülmüştür.

Anahtar kelimeler: Simvastatin, asil zincir uzunluğu etkisi, DMPC, DPPC, FTIR, DSC.

To My Brother Engin KOÇAK

ACKNOWLEDGMENTS

I am grateful to Prof. Dr. Feride SEVERCAN for her advice, encouragement, and supervision throughout my study.

I would like to thank my parents Rabia-Yusuf KOÇAK for their continuous help, support and encouragement throughout this study.

My gratitudes also go to my brother Engin KOÇAK for his patience, support, assistance and valuable help during this study and preparation of the manuscript.

Finally, I would like to thank my aunt Saniye SAYIN and her husband Mutlu SAYIN for their support and encouragement throughout the study.

TABLE OF CONTENTS

PLAGIARISM.....iii
ABSTRACT.....iv
ÖZ.....vi
ACKNOWLEDGMENTS.....ix
TABLE OF CONTENTS.....x
LIST OF TABLES ……..xii
LIST OF FIGURES …….…...xiii

CHAPTER

1. INTRODUCTION….....1

1.1 Scope and Aim of This Study……..……1

1.2 Biological Membranes….……..……...4

1.3 Molecular Motions in Lipid Bilayers……..8

1.4 Liposomes as Model Membranes……..10

1.5 Thermotropic Phase Transitions in Lipid Bilayers……12

1.6 Statins and Simvastatin…….……16

1.6.1 Simvastatin-Membrane Interactions…….27

1.7 Absorption Spectroscopy…….....29

1.7.1 Infrared Spectroscopy……...32

1.7.2 Instrumentation of Fourier-Transform Infrared Spectrometer..34

1.7.3 Infrared Spectroscopy in Membrane Research…….37

1.7.4 Advantages of Fourier Transform Infrared Spectroscopy..…38

1.8 Differential Scanning Calorimetry 39

1.8.1 Instrumentation of Differential Scanning Calorimetry…….40

1.8.2 Differential Scanning Calorimetry in Membrane Research…..42

2. MATERIALS AND METHODS……45

2.1 Reagents……45

2.2 Phosphate Buffer Preparation……45

2.3 Simvastatin Stock Solution Preparation……46

2.4 Preparation of Model Membranes……46

2.5 Sample Preparation for the FTIR Experiments……46

2.5.1 Infrared Spectral Regions Used in This Study……..47

2.6 Sample Preparation for the DSC Experiments……..53

2.6.1 Thermogram Analysis……...53

3. RESULTS……57

3.1 FTIR Studies……..57

3.1.1 Temperature Dependent FTIR Studies of DPPC Model Membranes……58

3.1.2 FTIR Studies to Monitor the Acyl Chain Length Effect Between DMPC and DPPC Lipids……75

3.2 DSC Studies……..96

4. DISCUSSION……...……...104

4.1 Simvastatin-DPPC Model Membrane Interaction……...104

4.2 Effect of Acyl Chain Length…...……108

CONCLUSION…….……..……113

REFERENCES…….……115

LIST OF TABLES

Table 1.7.1.1. Band assignments of some characteristic infrared absorbtion bands according to their wavenumbers in cm^{-1} (Stuart, 2004)……35

Table 3.3.1 Width at half height (ΔT), transition temperatures (T_m) and enthalpy of the transitions (ΔH) for DMPC liposomes are given…103

Table 3.3.2 Width at half height (ΔT), transition temperatures (T_m) and enthalpy of the transitions (ΔH) for DPPC liposomes are given…..103

LIST OF FIGURES

Figure 1.2.1 Fluid-mosaic model of a cell membrane……6
Figure 1.2.2 Chemical structure of a phospholipid……7
Figure 1.3.1 Movements of a phospholipid molecule within membranes……..8
Figure 1.4.1 a) The structure of a liposome, b) The types of liposomes…….12
Figure 1.5.1 Schematic illustration of the lamellar bilayer phases……15
Figure 1.6.1 The mammalian mevalonate pathway……...18
Figure 1.6.2 Inhibition of HMG CoA reductase by statins……...19
Figure 1.6.3 The chemical structures of the hydroxymethylglutaryl coenzyme A (HMG-CoA) reductase inhibitors……20
Figure 1.7.1 Propagation of an electromagnetic wave through space……...30
Figure 1.7.2 Typical energy-level diagram showing the ground state and the first excited state. Vibrational levels are shown as horizontal lines and rotational levels are also shown in between the two vibrational levels in the ground state. A possible electronic transition between the first vibrational level of the ground state and the second vibrational level of the first excited state is indicated by the long arrow. A vibrational transition within the ground state is indicated by the short arrow……..31
Figure 1.7.1.1 The part of the electromagnetic spectrum that is relevant to physical biochemistry……33
Figure 1.7.1.2 Types of normal vibrations for CO_2 molecule……...33
Figure 1.7.2.1 Basic components of an FTIR spectrometer……...36
Figure 1.7.2.2 Schematic of a Michelson interferometer……..36
Figure 1.8.1.1 Schematic illustration of a DSC……41
Figure 2.5.1.1 FTIR spectrum of DMPC liposomes. Upper spectrum shows the liposomes before water bands were subtracted and the spectrum below shows the liposomes after subtraction……..50

Figure 2.5.1.2 FTIR spectrum of DPPC liposomes. Upper spectrum shows the liposomes before water bands were subtracted and the spectrum below shows the liposomes after subtraction……..51
Figure 2.5.1.3 Infrared spectrum of air……..52
Figure 2.6.1 Phase Transition Thermogram of DMPC. The little peak on the left is the pretransition curve and the following one is the main transition curve. Three parameters namely the width, the main phase transition temperature and the transition enthalpy change used in the DSC analysis were indicated on the main transition curve…….55
Figure 2.6.2 Phase Transition Thermogram of DPPC. The little peak on the left is the pretransition curve and the following one is the main transition curve. Three parameters namely the width, the main phase transition temperature and the transition enthalpy change used in the DSC analysis were indicated on the main transition curve…….56
Figure 3.1.1.1 FTIR spectra of pure DPPC multilamellar liposomes in the C-H stretching region at different temperatures. The spectra were normalized with respect to the CH_2 antisymmetric stretching band located at 2920 cm^{-1}……...60
Figure 3.1.1.2 FTIR spectra of DPPC liposomes in the presence and absence of low and high simvastatin concentrations in the C-H stretching region at 41.4^{o}C. The spectra were normalized with respect to the CH_2 antisymmetric stretching band located at 2920 cm^{-1}……..61
Figure 3.1.1.3 FTIR spectra of DPPC liposomes in the presence and absence of low and high simvastatin concentrations in the 1800-1000 cm^{-1} region at 45.1^{o}C. The spectra were normalized with respect to the C=O stretching band located at 1735 cm^{-1}……...62
Figure 3.1.1.4 FTIR spectra of pure DPPC liposomes and simvastatin at low and high concentrations corresponding to 1 and 24 mol% in solution at room temperature……63

Figure 3.1.1.5 FTIR spectra of the pure DPPC and DMPC liposomes in their gel phases in the 3000-2800 cm^{-1} region. The spectra were normalized with respect to the CH_2 antisymmetric stretching band located at 2920 cm^{-1}……...64
Figure 3.1.1.6 Temperature dependence of the frequency of the CH_2 symmetric stretching mode in the presence and absence of different simvastatin concentrations for DPPC liposomes……..66
Figure 3.1.1.7 Temperature dependence of the frequency of the CH_2 antisymmetric stretching mode in the presence and absence of different simvastatin concentrations for DPPC liposomes……...67
Figure 3.1.1.8 Temperature dependence of the bandwidth of the CH_2 symmetric stretching mode in the presence and absence of different simvastatin concentrations for DPPC liposomes……..69
Figure 3.1.1.9 Temperature dependence of the bandwidth of the CH_2 antisymmetric stretching mode in the presence and absence of different simvastatin concentrations for DPPC liposomes……...70
Figure 3.1.1.10 Temperature dependence of the frequency of the C=O stretching mode in the presence and absence of different simvastatin concentrations for DPPC liposomes……..72
Figure 3.1.1.11 Temperature dependence of the frequency of the PO_2^- antisymmetric double stretching mode in the presence and absence of different simvastatin concentrations for DPPC liposomes……...74
Figure 3.1.2.1 Simvastatin concentration dependence of the frequency of the CH_2 symmetric stretching mode for DMPC liposomes at 10^oC. (*) $P < 0.05$……....77
Figure 3.1.2.2 Simvastatin concentration dependence of the frequency of the CH_2 symmetric stretching mode for DPPC liposomes at 29.5^oC. (*) $P < 0.05$…. ……...77
Figure 3.1.2.3 Simvastatin concentration dependence of the frequency of the CH_2 antisymmetric stretching mode for DMPC liposomes at 10^oC. (*) $P < 0.05$……78

Figure 3.1.2.4 Simvastatin concentration dependence of the frequency of the CH_2 antisymmetric stretching mode for DPPC liposomes at 29.5°C. (*) P < 0.05……78
Figure 3.1.2.5 Simvastatin concentration dependence of the frequency of the CH_2 symmetric stretching mode for DMPC liposomes at 35°C. (*) P < 0.05……80
Figure 3.1.2.6 Simvastatin concentration dependence of the frequency of the CH_2 symmetric stretching mode for DPPC liposomes at 54°C. (*) P < 0.05……80
Figure 3.1.2.7 Simvastatin concentration dependence of the frequency of the CH_2 antisymmetric stretching mode for DMPC liposomes at 35°C. (*) P < 0.05……81
Figure 3.1.2.8 Simvastatin concentration dependence of the frequency of the CH_2 antisymmetric stretching mode for DPPC liposomes at 54°C. (*) P < 0.05……81
Figure 3.1.2.9 Simvastatin concentration dependence of the bandwidth of the CH_2 symmetric stretching mode for DMPC liposomes at 10°C. (*) P < 0.05……83
Figure 3.1.2.10 Simvastatin concentration dependence of the bandwidth of the CH_2 symmetric stretching mode for DPPC liposomes at 29.5°C. (*) P < 0.05……83
Figure 3.1.2.11 Simvastatin concentration dependence of the bandwidth of the CH_2 antisymmetric stretching mode for DMPC liposomes at 10°C. (*) P < 0.05……84
Figure 3.1.2.12 Simvastatin concentration dependence of the bandwidth of the CH_2 antisymmetric stretching mode for DPPC liposomes at 29.5°C. (*) P < 0.05……84
Figure 3.1.2.13 Simvastatin concentration dependence of the bandwidth of the CH_2 symmetric stretching mode for DMPC liposomes at 35°C. (*) P < 0.05……86

Figure 3.1.2.14 Simvastatin concentration dependence of the bandwidth of the CH_2 symmetric stretching mode for DPPC liposomes at 54°C. (*) P < 0.05……86
Figure 3.1.2.15 Simvastatin concentration dependence of the bandwidth of the CH_2 antisymmetric stretching mode for DMPC liposomes at 35°C. (*) P < 0.05……87
Figure 3.1.2.16 Simvastatin concentration dependence of the bandwidth of the CH_2 antisymmetric stretching mode for DPPC liposomes at 54°C. (*) P < 0.05……....87
Figure 3.1.2.17 Simvastatin concentration dependence of the frequency of the C=O stretching mode for DMPC liposomes at 10°C. (*) P < 0.05……...89
Figure 3.1.2.18 Simvastatin concentration dependence of the frequency of the C=O stretching mode for DPPC liposomes at 29.5°C. (*) P < 0.05……..89
Figure 3.1.2.19 Simvastatin concentration dependence of the frequency of the C=O stretching mode for DMPC liposomes at 35°C. (*) P < 0.05……...91
Figure 3.1.2.20 Simvastatin concentration dependence of the frequency of the C=O stretching mode for DPPC liposomes at 54°C. (*) P < 0.05……....91
Figure 3.1.2.21 Simvastatin concentration dependence of the frequency of the PO_2^- antisymmetric double stretching mode for DMPC liposomes at 10°C. (*) P < 0.05……..93
Figure 3.1.2.22 Simvastatin concentration dependence of the frequency of the PO_2^- antisymmetric double stretching mode for DPPC liposomes at 29.5°C. (*) P < 0.05……..93
Figure 3.1.2.23 Simvastatin concentration dependence of the frequency of the PO_2^- antisymmetric double stretching mode for DMPC liposomes at 35°C. (*) P < 0.05……..95
Figure 3.1.2.24 Simvastatin concentration dependence of the frequency of the PO_2^- antisymmetric double stretching mode for DPPC liposomes at 54°C. (*) P < 0.05……95

Figure 3.2.1 DSC thermogram of DMPC liposomes (Kiselev *et a*l., 2001)…..97
Figure 3.2.2 DSC thermogram of DPPC liposomes (Mavramoustakos *et al*., 1997)……..98
Figure 3.2.3 DSC thermogram of DMPC liposomes in the presence and absence of different simvastatin concentrations in terms of mol%.....100
Figure 3.2.4 DSC thermogram of DPPC liposomes in the presence and absence of different simvastatin concentrations in terms of mol%.....101

CHAPTER 1

INTRODUCTION

1.1 Scope and Aim of This Study

Biological membranes have vital functions for the continuity of life. Plasma membrane or cell membrane completely surrounds the cell. And it separates the cell from the external world. Compartmentalization, providing a selectively permeable barrier, transporting solutes, responding to external signals, intercellular interaction, energy transduction and being a locus for biochemical activities are major functions of plasma membrane (Karp, 1999). Understanding the molecular organization of biological membranes is important to determine their structure and function.

Biophysical studies dealing with biomembranes are mainly based on the organization, structure and dynamics of the lipid matrix. Order-disorder phase transition or thermotropic mesomorphism is the most frequently studied property of the biological membranes by physical techniques like spectroscopic methods which provide information about molecular motion and molecular moieties. In recent years, there has been a great development in the field of spectroscopic instrumentation. As a result, it becomes possible to apply spectroscopic techniques to the researches of membrane structure and function. Especially non-perturbing techniques, such as Fourier Transform Infrared (FTIR) spectroscopy and Differential Scanning Calorimetry (DSC) provide significant and detailed information about changes in the phase transition behaviour, mobility and structure of individual molecular moieties (Lopez-Garcia *et al*., 1993; Daniels, 1973).

Investigating the phase transition behaviour of membrane lipids is important in understanding the membrane structure, stability and function in real biological systems. Moreover, it is often necessary to study the structure of artificial membranes before undertaking the study of natural membranes because of the huge complexities of real biological systems (Mantsch and Casal, 1984). Among the phospholipids, phosphatidylcholines (PCs), popularly called lecithins, are one of the most common constituents of biological membranes. Model membranes composed of phosphatidylcholines are the most widely studied (Tien and Ottova, 2000).

Cholesterol is a major precursor for the synthesis of many biologically important molecules like bile acids and steroid hormones in the body (Mathews *et al*., 2000). It is also one of the components of the cell membrane and determines the physico-chemical properties of the membrane (Lodish, 2004). Cholesterol synthesis occurs in all types of cells but mainly in liver cells (Evans and Rees, 2002). An early and rate-limiting step of the synthesis is catalyzed by HMG CoA reductase (Hamelin and Turgeon, 1998).

Another name of the statin drugs is HMG CoA reductase inhibitors and they stop the cholesterol synthesis at the rate-limiting step in the mevalonate pathway (Päivä, 2005). As a result of this inhibition the blood plasma levels of LDL-cholesterol and triglycerides decrease while the level of HDL-cholesterol increases (Schachter, 2004). Thus, cholesterol metabolism is regulated. Due to these properties statins are widely used in the treatment of hyperlipidemic patients (Wierzbicki *et al*., 2003).

Simvastatin is one of the members of the statin drugs. It is known that the long term use of simvastatin reduces the risks of mortality caused by coronary heart disease, atherosclerosis dependent myocardial infarction and ischemia attack (Lutgens and Daemen, 2004). Despite its vital effects, it is reported that

simvastatin has pleitropic effects on many different tissues (Almuti *et al*., 2006). In the nervous system, it causes peripheral neuropathy and memory problems (Jeppesen *et al*., 1999; King *et al*., 2003). On the other hand, it can be used in the treatment of central nervous system diseases (e.g. Alzheimer, Parkinson) (Almuti *et al*., 2006). In addition, myalgia, rhabdomyolysis and myopathy are major adverse effects of simvastatin on the muscular system (Rosenson, 2004; Carvalho *et al*., 2004; Evans and Rees, 2002). Simvastatin is widely used because of its high efficacy.

In this study we report our findings on the effect of simvastatin on lipid organization and fluidity of model membranes which was accomplished by monitoring the thermotropic phase transition profiles of DMPC and DPPC with different physical techniques. To our knowledge this is the first study to report the interactions of simvastatin with phospholipid membranes. One of the most important findings of this study is that simvastatin decreases membrane fluidity and induces phase separation. The reason why we have chosen to study simvastatin-model membrane interactions is to understand the molecular mechanism of simvastatin interactions. In the literature, there are many researches about the simvastatin effects on the biological systems but these studies were performed at the organ or tissue level. Moreover, to understand all effects of simvastatin very well, molecular mechanisms of its interactions should be known. Biological membranes are very important because of their major functions and simvastatin has significant effects on the tissue membranes but how simvastatin acts on the biological membranes at the molecular level is unknown. At the molecular level the purpose of this study is to investigate the location of simvastatin in the model membrane; its effects on the main and pre-transition profiles, order and dynamics with respect to its interaction with membrane headgroup and acyl chain with different simvastatin to lipid ratios for a temperature range of 20-70^{o}C by using different non-perturbing

biophysical techniques; namely, Fourier Transform Infrared (FTIR) spectroscopy, and Differential Scanning Calorimetry (DSC).

The last part of this study has been devoted to investigate the acyl chain length effect on the simvastatin-model membrane interactions by using the same techniques with DMPC and DPPC lipids. This part is also so important because in the literature it is known that effects of many drugs, enzymes, proteins like cyclosporin A (Söderlund *et al*., 1999), human plasma lecithin:cholesterol acyltransferase (Pownall *et al*., 1985), melittin (Ohki, 2005) on the biological systems depend on the acyl chain length of phospholipids.

Structurally biological membranes are very complex because they have various types of lipids in different ratios. Including proteins and presence of lipid asymmetry between the inner and outer leaflets of the bilayer are also other factors making the structure of biological membranes so complex. As a result, to understand the effects of simvastatin on the real biological membranes and systems at the molecular level clearly, we want to investigate the interactions of cholesterol reducing agent simvastatin with phospholipid model membranes having a simpler structure.

1.2 Biological Membranes

Plasma membrane or the cell membrane is the structure which separates the cell from the external world. Membranes have various functions. Their one major function is compartmentalization. Because of compartmentalization many chemical activities proceed without any disturbance from the outside and their regulation can be done independently. Also membranes provide a

selectively permeable barrier from one side to the other side of the cell. Moreover, membranes provide the communication between the compartments that they separate. Transportation is another major function of the cell membrane. They have the required mechanism in their structure for the physical transportation of substances from one side to the other side. Membranes have receptors in their structure. These receptors form a complementary structure with specific molecules known as ligands. Thus, membranes have an important role in signal transduction. Energy transduction, taking part in intercellular interaction and providing a suitable space for biochemical activities are some other main funtions of the cell membrane. (Karp, 1999).

All biological membranes are lipid-protein assemblies and the components are held together by noncovalent bonds. Membranes also contain short chains of carbohydrates. In 1972, S. J. Singer and G. Nicolson proposed *fluid-mosaic model* to explain the chemical structure of biological membranes. Figure 1.2.1 shows fluid-mosaic model of a cell membrane. According to this model, lipid bilayer mainly serves as a structural framework for the membrane. The lipid molecules are present in a fluid state and they can move laterally within the plane of the membrane. The proteins occur as a mosaic of discontinuous particles that penetrate deeply into, and even completely through, the lipid sheet. The most important property of the fluid mosaic model is presenting cellular membranes as dynamic structures in which the components are mobile and capable of coming together to engage in various types of transient or semipermanent interactions. The proteins of the membrane perform some specific functions, however, lipid bilayer provides a barrier preventing the indiscriminate movements of water-soluble materials into and out of the cell. The ratio of lipid to protein varies considerably depending on the type of cellular membrane, the type of organism and the type of cell (Karp, 1999; Mathews *et al*., 2000).

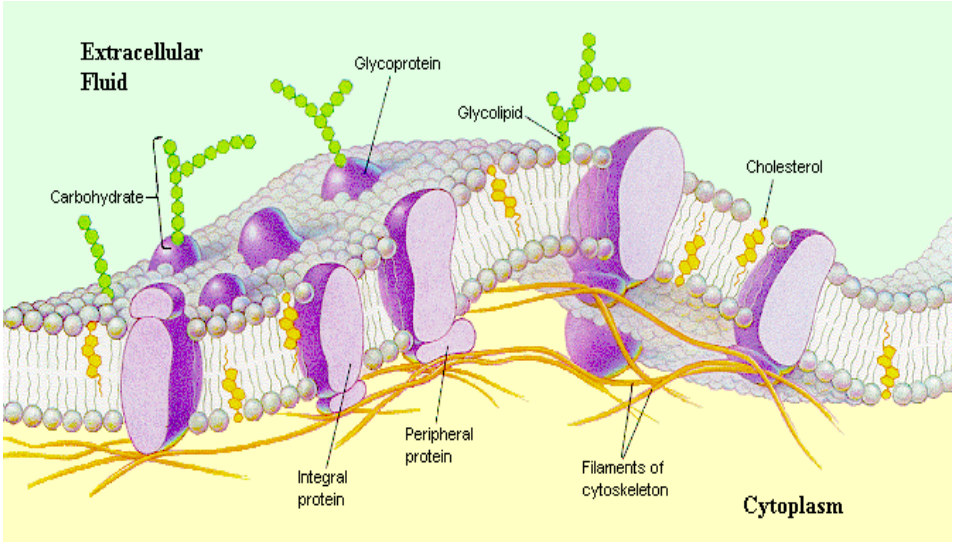

Figure 1.2.1 Fluid-mosaic model of a cell membrane.

Membranes contain various types of lipids, all of which are amphipathic which means that they contain both hydrophilic and hydrophobic regions. There are three main types of membrane lipids which are phosphoglycerides, sphingolipids, and cholesterol. Most membrane lipids have a phosphate group which makes them phospholipids. Most membrane phospholipids are built on a glycerol backbone so they are known as phosphoglycerides. Figure 1.2.2 shows the chemical structure of a phospholipid. Unlike triglycerides, which have three fatty acids, membrane glycerides are diglycerides. Only two of the hydroxyl groups of their glycerol are esterified to fatty acids, however, the third is esterified to a phosphate group. The molecule, which has the phosphate group and the two fatty acyl chains, is called phosphatidic acid. Nevertheless, phosphatidic acid is almost absent in most membranes. Instead, membrane phosphoglycerides have an additional group linked to the phosphate, most commonly either choline (forming phosphatidylcholine), ethanolamine (forming phosphatidylethanolamine), serine (forming phosphatidylserine), or inositol (forming phosphatidylinositol). Each of these groups is small and

hydrophilic and, together with the charged phosphate to which it is attached, forms a highly water-soluble domain at one end of the molecule, called the head group. In contrast the fatty acyl chains are long, unbranched, hydrophobic hydrocarbons. If a membrane fatty acid lack double bonds then it is fully saturated. If it has one double bond then it is monounsaturated. If it has more than one double bond then it is polyunsaturated. Phosphoglycerides generally contain one unsaturated and one saturated fatty acyl chain (Karp, 1999; Tien and Ottova, 2000).

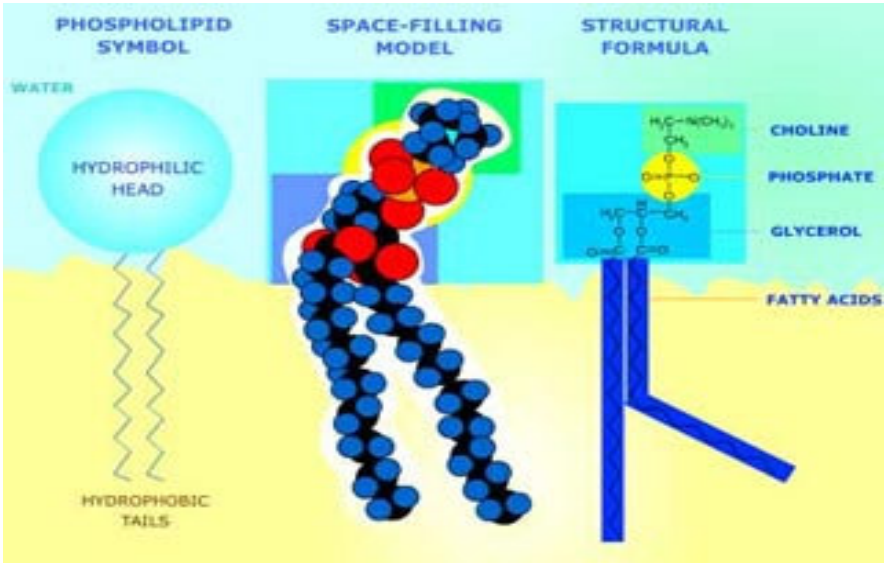

Figure 1.2.2 Chemical structure of a phospholipid.

Amphipathic phospholipids, like other amphiphilic molecules, are subject to two conflicting forces: the hydrophilic head is attracted to water, while the hydrophobic hydrocarbon moiety avoids water and seeks to aggregate with other hydrophobic molecules (like-dissolves-like). This dichotomy is elegantly resolved by the formation of a lipid bilayer in an aqueous environment (Tien and Ottova, 2000).

1.3 Molecular Motions in Lipid Bilayers

There are various types of molecular motions in lipid bilayers. A phospholipid molecule has three kinds of movements in a membrane. Figure 1.3.1 shows movements of a phospholipid molecule within membranes. One of these movements is *flip-flop* motion or transverse diffusion. In this type of motion phospholipids move from one leaflet to another at a very slow rate. The half-life of a phospholipid molecule staying within one layer, as opposed to moving across to the other layer, is measured in hours to days. Such a slow rate is expected because for flip-flop to occur, the hydrophilic head group of the lipid must pass through the internal hydrophobic sheet of the membrane, which is thermodynamically unfavorable (Karp, 1999; Mathews *et al.*, 2000). In other words, there is a large activation energy barrier for the movement of polar head group through hydrophobic interior (Smith *et al.*, 1983).

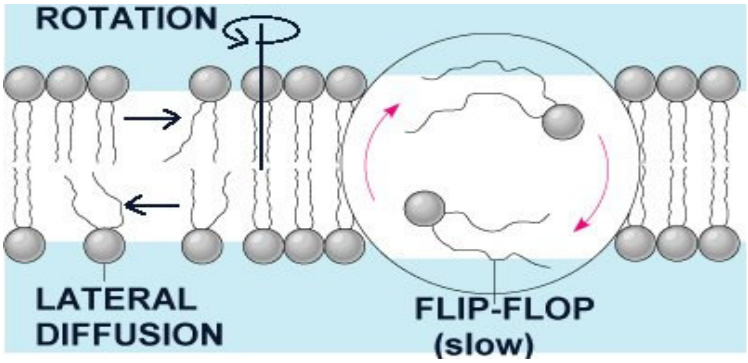

Figure 1.3.1 Movements of a phospholipid molecule within membranes.

Rotation is another type of motion of phospholipid molecules. Axial rotation of lipids along their long axis perpendicular to the plane of the membrane occurs every 0.1-100 ns. In lateral diffusion, phospholipid molecules move rapidly in the plane of the membrane. A lipid molecule exchange places with

neighbouring molecules in the same monolayer. Segmental motion of acyl chains causes an increased disorder toward the center of the membrane (Becker *et al*., 1996). Due to the bond rotation potential carbon-carbon bonds can only occur in three rotational states which are trans (t), gauche minus (g^-) and gauche plus (g^+). Gauche conformers have a higher free energy than trans conformers due to steric hinderence. The average conformation for a free chain is determined by the energy difference between trans and gauche isomers and cooperative interactions between nearest neighbours. All-trans conformation of a poly methylene chain is the lowest potential energy conformation. In this conformation saturated acyl chains are longest, thinnest and most closely packed. However, a single gauche conformer in an acyl chain causes a big difference in the properties of the neighbouring acyl chains (Seelig and Seelig, 1974; Jain, 1988).

The lipid bilayer consists of two distinct leaflets, and there is no reason to assume that the lipid composition of the two halves should be identical. In fact, a large body of evidence indicates that the lipids of the plasma membrane are distributed in a highly asymmetric pattern. The lipid bilayer can be thought of as composed of two more-or-less stable, independent monolayers having different physical and chemical properties (Karp, 1999). Not only individual lipids distributed very asymmetrically, but the distribution also varies considerably among cell types. The consequences of such differences in phospholipid composition are numerous. Fluidity may be different on one side of the membrane or the other. The difference in charged groups on the two surfaces contributes to the membrane potential. Distribution of membrane proteins is also asymmetric. Presence of asymmetry in the distribution of lipids and proteins between the inner and outer leaflets of the bilayer makes the real biological membranes so complex (Mathews *et al*., 2000).

1.4 Liposomes as Model Membranes

If a small amount of phosphatidylcholine is suspended in an aqueous solution, which is then subjected to mechanical agitation, the phospholipid molecules become assembled spontaneously to form the walls of fluid-filled spherical vesicles, called liposomes. The walls of these liposomes consist of a single continuous lipid bilayer that is organized in the same manner as that of the lipid bilayer of a natural membrane. Liposomes have proven invaluable in membrane research (Karp, 1999). Many things can be learned about biomembranes by studying liposomes. In other words, we can have a better knowledge of structural-functional relationship of lipids, proteins, carbohydrates, pigments, and their complexes, mechanisms of transport, energy transduction, signal processing, and our common senses such as vision, olfaction, hearing, gustation, and touching sensations (Tien and Ottova, 2000). Membrane proteins can be inserted into liposomes and their function studied in a much simpler environment than that of a natural membrane (Karp, 1999). A liposome may contain one or more lipid bilayer. Typically, several of these vesicles will form one inside the other in diminishing size, creating a multilamellar structure of concentric phospholipid shells separated by layers of water. Liposomes can be prepared from a wide range of natural and synthetic lipids among which phospholipids are most commonly used. These phospholipids can be neutral, or positively charged phospholipids (such as phosphatidylcholine, phosphatidylethanolamine, etc.). Cholesterol is frequently used in liposome formulations to increase the stability. Moreover, liposomes can be prepared in sizes varying from 20 nm to 100 μm or more in diameter, according to the desired purpose. Procedures and raw materials for formulating liposomes must be considered with care to avoid adverse effects on liposome stability (Tien and Ottova, 2000).

Liposomes having more than one bilayer are called multilamellar vesicles (MLV) or multivesicular vesicles (MVV). Figure 1.4.1 shows the structure of a liposome and the types of liposomes. There are also small unilamellar vesicles (SUV) which have diameters between 20-50 nm. The large unilamellar vesicles (LUV) are prepared from SUVs by applying different techniques like reverse-phase evaporation method and detergent dialysis (removal) method (Ostro, 1983; Rosoff, 1996; Tien and Ottova, 2000). Real biological membranes are in the form of unilamellar liposomes of approximately 900 nm in diameter. Liposomes can be used besides models of biomembranes, as drug carriers and be loaded with a great variety of molecules, such as proteins, nucleotides, small drug molecules, and even plasmids. Liposomes are extremely adaptable, and due to the diversity of their composition, they can be utilized for a large number of applications (Rosoff, 1996; Tien and Ottova, 2000).

a)

b)

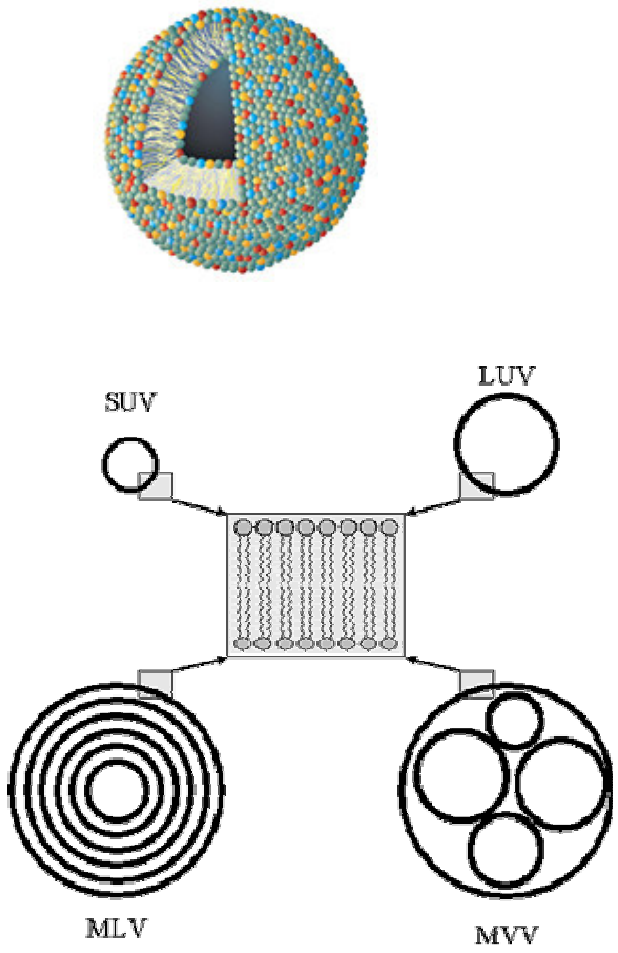

Figure 1.4.1 a) The structure of a liposome, b) The types of liposomes.

1.5 Thermotropic Phase Transitions in Lipid Bilayers

The internal temperature of most organisms (other than birds and mammals) fluctuates with the temperature of the external environment. Since it is essential for many activities that the membranes of a cell remain in a fluid state. Fluidity allows for interactions to take place within the membrane. For example, membrane fluidity makes it possible for clusters of membrane proteins to assemble at particular sites within the membrane and form specialized structures, such as intercellular junctions, light-capturing complexes, and

synapses. Because of membrane fluidity, molecules that interact can come together, carry out the necessary reaction, and move apart. Fluidity also plays a role in membrane assembly. Many of the most basic cellular processes, including cell movement, cell growth, cell division, formation of intercellular junctions, secretion, and endocytosis, depend on the movement of membrane components and would probably not be possible if memranes were rigid, nonfluid structures (Karp, 1999).

The phase transition in lipid bilayers can be described as a cooperative melting of the acyl chains. Shorter chains melt at lower temperatures and longer chains melt at higher temperatures (Phillips *et al*., 1970). The physical state of the lipid of a membrane is described by its fluidity (or viscosity). As with many other substances, lipids can exist in a crystalline solid phase or a liquid phase of varying viscosity depending on the temperature. For example, a simple artificial bilayer made of phosphatidylcholine and phosphatidylethanolamine, whose fatty acids are largely unsaturated. If the temperature of the bilayer is kept relatively warm (e.g., 37^{o}C), the lipid exists in a relatively fluid state. At this temperature, the lipid bilayer is best described as a two-dimensional liquid crystal. As in a crystal, the molecules still retain a specified orientation; in this case, the long axes of the molecules remain essentially parallel, yet individual phospholipids can rotate around their axes or move laterally within the plane of the bilayer. If the temperature is slowly lowered, a point is reached where the bilayer distinctly changes. The lipid is converted from its normal liquidlike state to a frozen crystalline gel in which the movement of the phospholipids is greatly restricted. The temperature at which this change occurs is called the transition temperature (Karp, 1999).

The molecular organization of phospholipids in the bilayer are found in four different states which are; crystalline gel, gel, rippled gel and liquid crystalline. Thus, there are three phase transitions, namely, solid (gel) phase transition,

rippled gel phase transition and liquid crystalline phase transition between these four states as the temperature increases. The transition from gel phase to liquid crystalline phase in a phospholipid bilayer is a highly cooperative transition from order to disorder, involving a lateral expansion and a decrease in thickness and density. Within the transition range, two-dimensional domains of liquid and gel phase exist. Below and above this range, the membrane exists in gel and liquid phases, respectively (Jain *et al*., 1975).

The transition temperature of a membrane or lipid bilayer can be measured calorimetrically. The membrane suspension is placed in a calorimeter, an instrument that measures the energy required to raise the temperature of the specimen. As in the case of any substance undergoing a transition from a solid to a liquid state, energy is absorbed by the system in order to break the intermolecular restraints without causing a corresponding increase in the temperature of the substance. The transition in phase is seen as a sharp peak in the thermogram (Karp, 1999).

Temperatures, at which the phase transitions of phospholipids occur, are the following: i) The main phase transition temperature (T_m): Transition from rippled gel phase to liquid crystalline phase, ii) The pretransition temperature (T_p): Transition from gel phase to rippled gel phase which occurs 5-10^oC below T_m, iii) The sub-transition temperature (T_s): Transition from crystalline gel phase to gel phase (Silver, 1985; Datta, 1987). It is known that the DMPC and DPPC liposomes undergo three following phase transitions (Fuldner, 1981; Ruocco and Shipley, 1982; Janiak *et al*., 1979; Silver, 1985)

$$L_c \xrightarrow{T_{sub}(18\text{-}20^oC)} L_\beta \xrightarrow{T_{pre}(35^oC)} P_\beta \xrightarrow{T_m(41^oC)} L_\alpha$$

where L_c, L_β, P_β, and L_α corresponds to crystalline gel, gel, rippled gel and liquid crystalline bilayer structures, respectively (Jain, 1988). Figure 1.5.1

shows the lamellar bilayer phases. Above the main phase transition temperature, the lipids are in liquid-crystalline state. The alkane chains become highly flexible near the middle of the bilayer due to the rotational motions about C-C bonds. If the rotation is 120^{o}, it leads to transient gauche isomer (or kink) formation. The possibility of kink formation increases toward the methyl end of the alkane chains (Heller, 1993).

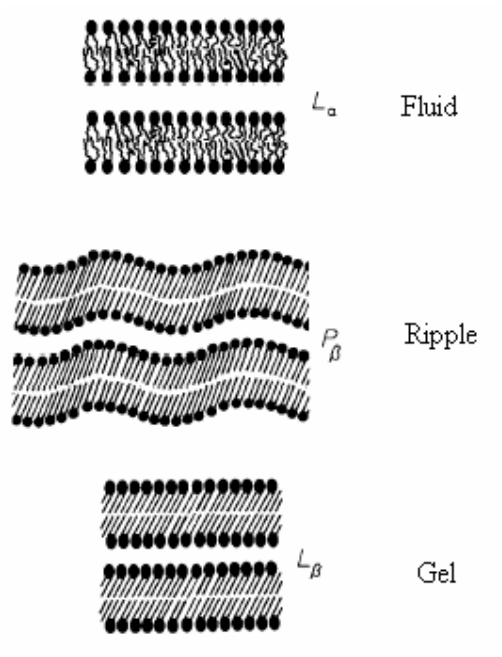

Figure 1.5.1 Schematic illustration of the lamellar bilayer phases.

In the bilayer, at sufficiently low temperatures, there is a little translational motion of lipid molecules. And their properties resemble those of hydrocarbon crystals in many ways. As the temperature increases, the properties of bilayers demonstrate abrupt changes at one or more temperatures. A small sudden increase in the phase transition curve corresponds to the pretransition peak associated with the tilting of the hydrocarbon chains. And a sudden larger increase corresponds to the main transition peak of the hydrated phospholipids

from gel phase to the liquid crystalline phase, which is associated with complete melting of hydrocarbon chains (Severcan and Cannistraro, 1988).

The transition temperature of a particular bilayer depends on the particular lipids of which it is constructed. The most important determinant is the degree to which the fatty acyl chains of the phospholipids are unsaturated, that is, contain double bonds (specifically *cis* double bonds). The ability of the molecules to be packed together determines transition temperature and fluidity. Another factor that influences bilayer fluidity is fatty acid chain length (Karp, 1999).

1.6 Statins and Simvastatin

Cholesterol is essential to life in many ways like being a regulator of homeostasis, a precursor to the corticosteroids (e.g., cortisol, aldosterone) and sex hormones (e.g., progesterone, testosterone), and a critical factor in the maintenance of cell membrane integrity. However, high levels of this lipophilic substance lead to atherosclerosis, a predisposing factor to the development of coronary artery disease. Atherosclerosis involves an accumulation of cholesterol esters and other blood lipids and lipoproteins in macrophage cells found in the intima of arteries. Lipid-engorged macrophage cells become foam cells, and foam cell infiltration progresses to fatty streaks in the arterial wall. Plaque formation, thrombosis, and vessel occlusion can follow, leading to coronary artery diseases. This type of diseases involves one or more specific cardiovascular pathologies, including myocardial infarction, ischemia, and angina (Roche, 2005).

In addition to free cholesterol and its esters, triglycerides (long-chain fatty acid esters of the polyalcohol glycerol) and lipoproteins (macromolecular substances that solubilize blood lipids) are found in the bloodstream. High

levels of triglycerides and the lipid-rich lipoproteins that promote the formation of atherosclerotic plaques (low density lipoproteins [LDL] and very low density lipoproteints [VLDL]) are also a significant health risk. Patients with elevated levels of triglycerides and "bad cholesterol" are at risk for myocardial infarction and/or cerebral vascular accident (stroke) (Roche, 2005).

The hydroxymethylglutaryl coenzyme A (HMG-CoA) reductase catalyzes the conversion of hydroxymethylglutaryl (HMG) to mevalonate, an early and rate limiting step in cholesterol synthesis (Brown and Goldstein, 1980). Figure 1.6.1 shows the mammalian mevalonate pathway. Pharmacological inhibition of the HMG-CoA reductase causes a decrease in cholesterol synthesis which leads to upregulation of low-density lipoprotein (LDL) receptors, thus increasing the rate of removal of LDL from plasma. HMG-CoA reductase is the target for a new class of highly effective inhibitors of cholesterol synthesis, namely lovastatin, simvastatin, pravastatin, fluvastatin and atorvastatin (Todd and Goa, 1990; Tsujita and Watanabe, 1989; Henwood and Heel, 1988; Connolly *et al*., 1993; Plosker and Wagstaff, 1996; Davignon, 1997). Figure 1.6.2 shows inhibition of HMG CoA reductase by statins. The chemical structures of lovastatin, simvastatin and pravastatin are closely related but the physico-chemical properties of lovastatin and simvastatin differ from those of pravastatin (Roth *et al*., 1991). Figure 1.6.3 shows the chemical structures of the hydroxymethylglutaryl coenzyme A (HMG-CoA) reductase inhibitors. Fluvastatin represents the first entirely synthetic HMG-CoA reductase inhibitor and shares physico-chemical characteristics with pravastatin as well as with lovastatin and simvastatin (Plosker and Wagstaff, 1996). On the other hand, the chiral Ca^{2+} salt of a pentasubstituted pyrrole, atorvastatin, presents a distinct chemical structure (Davignon, 1997). Lovastatin, simvastatin and pravastatin are structurally very similar. In fact, lovastatin is derived from a fungal source and simvastatin and pravastatin are chemical modifications of lovastatin (Todd

and Goa, 1990; Tsujita and Watanabe, 1989; Henwood and Heel, 1988; Hamelin and Turgeon, 1998).

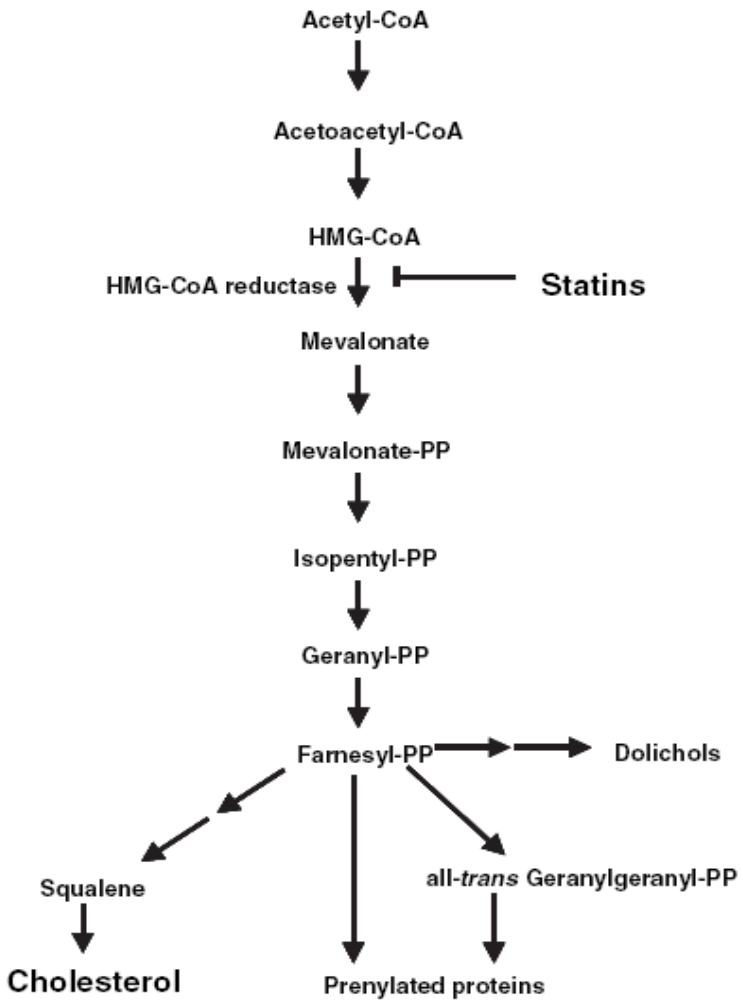

Figure 1.6.1 The mammalian mevalonate pathway.

When the open hydroxy forms of these drugs are compared, lovastatin and simvastatin differ from pravastatin in that they possess a methyl instead of a hydroxyl moiety at position 6. Furthermore, simvastatin differs from the other two as it possesses an additional methyl group at position 2 on the butanoate

lateral chain. While pravastatin is administered as the readily active open hydroxy-acid form, lovastatin and simvastatin are administered as inactive lactones, which must be metabolized to their corresponding open hydroxy-acid forms in order to inhibit HMG-CoA reductase (Todd and Goa, 1990; Tsujita and Watanabe, 1989; Henwood and Heel, 1988; Hamelin and Turgeon, 1998).

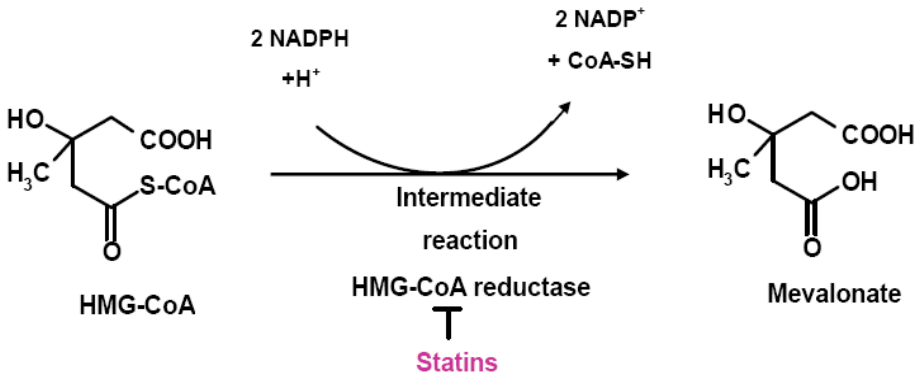

Figure 1.6.2 Inhibition of HMG CoA reductase by statins.

On the other hand, fluvastatin is the product of synthetic drug design and its structure is distinct from the described molecules. However, it shares the dihydroxy heptanoic acid function with pravastatin and is, just like this latter agent, administered as an active β-hydroxy acid form (Plosker and Wagstaff, 1996). Whether lactone prodrugs or active open hydroxy acids, all four HMG-CoA reductase inhibitors are provided with a bicyclic ring system which is together with the side-chain mandatory for anchoring into the active site of the HMG-CoA reductase. The described structural characteristics are closely related to the physico-chemical properties of HMG-CoA reductase inhibitors. Thus, the lactone prodrugs, lovastatin and simvastatin, are almost three orders of magnitude more lipophilic than their corresponding active open hydroxy-acid forms which in turn, are approximately 100 times more lipophilic than pravastatin (Serajuddin *et al*., 1991). Fluvastatin appears to have intermediate

physico-chemical characteristics because it is approximately twice as hydrophilic as lovastatin but 40 times more lipophilic than pravastatin (Lindahl *et al*., 1996; Appel and Dingemanse, 1996). The differences in lipophilicity are reflected in the potential of these various substances to cross cellular membranes nonselectively by passive diffusion, and explain why pravastatin does not easily cross cellular membranes whereas lovastatin and simvastatin do (Serajuddin *et al*., 1991; Hamelin and Turgeon, 1998).

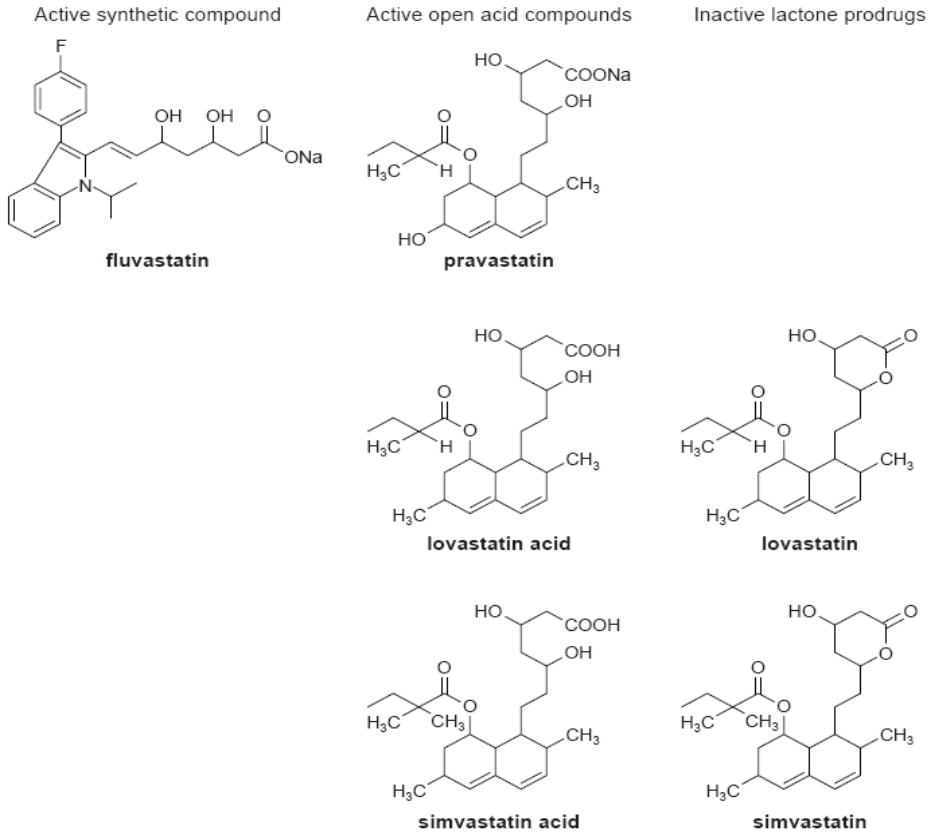

Figure 1.6.3 The chemical structures of the hydroxymethylglutaryl coenzyme A (HMG-CoA) reductase inhibitors.

Fluvastatin was characterized as a high permeability drug despite its relatively high hydrogen bond number. It was therefore suggested that this molecule, due

to its amphiphilic character, might form intra-molecular hydrogen bonds, thereby increasing its apparent lipophilicity and cell membrane permeability (Lindahl *et al*., 1996). However, fluvastatin, like pravastatin, does not cross the blood–brain barrier to any significant extent in contrast to the more lipophilic lactone compounds, lovastatin and simvastatin (Guillot *et al*., 1993; Hamelin and Turgeon, 1998).

Competitive inhibition of HMG-CoA reductase by the statins decreases hepatocyte cholesterol synthesis. The associated reduction in intracellular cholesterol concentration induces LDL-receptor expression on the hepatocyte cell surface, which results in increased extraction of LDL-C from the blood and decreased circulating LDL-C concentrations (Hobbs *et al*., 1992). Statins also have beneficial effects on other lipid parameters, including increases in high-density lipoprotein cholesterol (HDL-C) concentration and decreases in triglyceride concentration (Maron *et al*., 2000). Secondary mechanisms by which statins may reduce levels of atherogenic lipoproteins include inhibition of hepatic synthesis of apolipoprotein B100 and a reduction in the synthesis and secretion of triglyceride-rich lipoproteins (Ginsberg *et al*., 1987; Grundy, 1998). In addition, statins may exert beneficial cardiovascular effects independent of their lipid-modifying properties (Liao, 2002). These pleiotropic properties may be explained by inhibition of synthesis of nonsteroidal isoprenoid compounds, which are also produced from mevalonic acid, and include improvement of endothelial cell function, modification of inflammatory responses, and reduction of smooth muscle cell proliferation and cholesterol accumulation (Liao, 2002; Corsini *et al*., 1999). Large-scale clinical trials have demonstrated that the statins substantially reduce cardiovascular-related morbidity and mortality in patients with and without existing coronary heart disease (Scandinavian Simvastatin Survival Study Group, 1994; Shepherd *et al*., 1995; Sacks *et al*., 1996; Downs *et al*., 1998; The Long-term Intervention with Pravastatin in Ischemic Disease (LIPID) Study Group, 1998;

Heart Protection Study Collaborative Group, 2002; Shepherd *et al*., 2002; Sever, 2003). Statins have also been shown to slow the progression or even promote regression of coronary atherosclerosis, resulting in fewer new lesions and total occlusions compared with untreated hypercholesterolaemic patients (Christians *et al*., 1998; Vaughan *et al*., 1999; Smilde *et al*., 2001). This has been suggested to be a consequence of the shrinkage of the lipid core of the atherosclerotic plaque, avoiding plaque rupture that would otherwise trigger intramural haemorrhage and intraluminal thrombosis (Christians *et al*., 1998; Schachter, 2004).

The pleiotropic effects of a pharmacologic agent are actions other than those for which the agent was specifically developed. These effects may be undesirable, neutral or beneficial. The pleiotropic effects are either related or unrelated to the primary mechanism of action of the drug, and they are usually unanticipated. Many recent studies reported that the effects of statins extend beyond their cholesterol-lowering capacity (Takemoto *et al*., 2001; Werner *et al*., 2002) and most of their multiple activities are mediated by the ability to block the synthesis of isoprenoid products. Understanding the pleiotropic effects of statins is important to optimize their use in treatment and prevention of cardiovascular disease (Tchapda, 2005).

Statins affect many metabolic pathways and organ systems and they may positively impact multiple disease states independent of LDL-C reduction (Almuti *et al*., 2006). In recent years, understanding of the pathophysiology of atherosclerosis has evolved tremendously. It is no longer sufficient to consider it simply a lipid deposition disease. Inflammation (Ross, 1999; Ridker *et al*., 1999; Albert *et al*., 2001), endothelial dysfunction (Ross, 1999; Laufs *et al*., 1998), plaque instability (Van der Wal *et al*., 1994; Davies *et al*., 1993), thrombosis and smooth muscle proliferation may also impact the development and progression of atherosclerosis. And statins may ameliorate these processes.

Clinical trials have suggested an anti-inflammatory role for statins (Kleemann *et al*., 2003; Ridker *et al*., 1999; Albert *et al*., 2001; Ridker *et al*., 2005; Nissen *et al*., 2005; Ridker and JUPITER study group., 2004). Endothelial dysfunction is considered an early marker of atherosclerosis (Laufs *et al*., 1998). Several factors including diabetes mellitus, hypertension, cigarette smoking contribute to endothelial dysfunction (Ross, 1999; Harker *et al*., 1976). As a result of this dysfunction, many properties of the endothelium including its adhesiveness and permeability are altered. An appropriate balance between nitric oxide (NO), a vasodilator, and endothelin-1 (ET-1), a vasoconstrictor, is struck when the endothelium is functioning normally (von Haehling *et al*., 2003). Endothelial dysfunction may manifest as an imbalance between these two mediators. Statins may help correct this imbalance by enhancing the activity of endothelial NO synthase (eNOS) and thus increasing the production of NO (Laufs *et al*., 1998). They may also reduce the synthesis of ET-1 (Puddu *et al*., 2001; Hernandez-Perera *et al*., 1998). Furthermore, O'Driscoll et al. observed an augmentation in the NO-mediated vasodilator effects of the endothelium after only 4 weeks of therapy with simvastatin. This effect appeared to be independent of simvastatin's lipid-lowering effects (O'Driscoll *et al*., 1997). Atherosclerotic plaques are considered to be unstable when certain conditions are present. These include the presence of large numbers of macrophages and increased neo-vascularization of the intima in the area of the plaque (Van der Wal *et al*., 1994; Davies *et al*., 1993; Moreno *et al*., 1994; Willerson *et al*., 1986). Statins interfere with several functions of macrophages including their adhesion to the endothelium, trans-migration into tissue, the secretion of pro-inflammatory cytokines and the production of free radicals (Ross, 1999). Patients with atherosclerosis have an increased thrombotic potential due, in part, to increases in the production of thromboxane A2 (TXA2), which promotes platelet aggregation and vascular contraction, and due to alterations in the makeup of the platelet membrane (Notarbartolo *et al*., 1995; Mazeaud *et al*., 1992; Lacoste *et al*., 1995). Statins exert anti-thrombotic effects by

inhibiting the production of TXA2 (Notarbartolo *et al*., 1995; Almuti *et al*., 2006).

The pathogenesis of atherosclerosis involves, in part, the proliferation of smooth muscle cells in the intimal layer of blood vessels (Ross, 1993). Certain growth factors such as basic fibroblast growth factor (Negre-Aminou *et al*., 1997; Xu *et al*., 2002) and platelet-derived growth factor (Negre-Aminou *et al*., 1997) promote smooth muscle cell proliferation. Conversely, endothelial-derived NO has inhibitory effects on smooth muscle cell proliferation. Statins interfere with these processes by blocking the effects of the growth factors (Xu *et al*., 2002) while at the same time promoting NO production (Laufs *et al*., 1998). Oxidation of low-density lipoprotein (LDL) is considered an important step in the pathogenesis of atherosclerotic lesions. Oxidized LDL (Ox-LDL) is thought to attract monocytes into the vessel wall where they contribute to fatty streak formation and lesion expansion (Berliner *et al*., 1990). Rikitake et al. studied the anti-oxidant effects of fluvastatin both in vitro and in an animal model (Rikitake *et al*., 2001). Fluvastatin decreased the susceptibility of LDL-C to oxidation, and it prevented increases in the production of superoxide, a free radical partly responsible for the impaired endothelium-derived relaxation in hypercholesterolemic patients (Ohara *et al*., 1993; Ohara *et al*., 1995). Congestive heart failure is a syndrome that involves endothelial dysfunction, inflammation and neuro-hormonal imbalance in addition to impairment of cardiac function (Torre-Amione, 1999; Schrier and Abraham, 1999). Given their reported anti-inflammatory effects and their salutary effects on the endothelium, many investigators have studied the possible benefits of statins in congestive heart failure (Node *et al*., 2003; Horwich *et al*., 2004; Nakagami *et al*., 2003; Fuller *et al*., 1998; Almuti *et al*., 2006).

The potential to ameliorate the impact of diabetes on renal function (Usui *et al*., 2003) and to slow the progression to end stage renal disease among the

most promosing roles for statins in the field of nephrology. Statins may also benefit patients with chronic glomerulonephritis such as IgA nephropathy (Nakamura *et al*., 2002). Statins have also been reported to attenuate renal injury after an ischemic event (Yokota *et al*., 2003; Joyce *et al*., 2001). Furthermore, pre-medication with statins prior to the use of radiographic contrast agents may have protective effects on renal function (Attallah *et al*., 2004; Almuti *et al*., 2006).

Statins have shown promise in the prevention of ischemic stroke in patients with coronary artery disease (White *et al*., 2000; Schwartz *et al*., 2001). Furthermore, some of the beneficial central nervous system effects of statins may be due to their augmentation of NO production as NO may improve central nervous system collateral blood flow, enhance cerebral vasodilator responses and prevent apoptosis (Laufs *et al*., 2000; Kureishi *et al*., 2000; Dimmeler *et al*., 1999). In Alzheimer's disease, elevated central nervous system cholesterol levels are thought to accelerate the cleavage of amyloid precursor protein to beta-amyloid (Fassbender *et al*., 2002; Locatelli *et al*., 2002), a compound considered cytotoxic to oligodendrocytes and neurons. In a double-blinded, placebo-controlled study, the administration of simvastatin for a 6-month period to normo-cholesterolemic patients with mild Alzheimer's disease was found to decrease central nervous system beta-amyloid levels (Simons *et al*., 2002). In addition, a recently completed study of 63 patients with mild-to-moderate Alzheimer's disease suggested that statin use slowed cognitive decline and improved some of the depressive symptoms associated with the disease (Sparks *et al*., 2004). Overall, statin use in individuals ≥50 years old has been associated with about a 70% decrease in clinically diagnosed dementia (Jick *et al*., 2000; Almuti *et al*., 2006).

Statins may have beneficial effects on autoimmune diseases such as rheumatoid arthritis, diabetes mellitus, psoriasis and inflammatory bowel disease (Leung *et al*., 2003). Modulation of T lymphocyte proliferation, differentiation and activation appears to be the primary mechanism. In a murine model of inflammatory arthritis, simvastatin suppressed both developing and clinically evident cases of the disease (Leung *et al*., 2003). The immunomodulatory effects of statins may also be beneficial for recipients of solid organ transplants (Kobashigawa *et al*., 1995; Mehra *et al*., 2002). Statin use may decrease mortality in patients with bacterial-induced sepsis (Pruefer *et al*., 2002). Statins also exert activity against the α toxin released by *Staphylococcus aureus* in septic patients (Adamo *et al*., 1989; Buerke *et al*., 2002; Sibelius *et al*., 2000). There is some evidence that statins may decrease the incidence of colon cancer (Sacks *et al*., 1996; Pedersen *et al*., 1996) and potentially ameliorate some of the effects of inflammatory bowel disease (Sasaki *et al*., 2003). The evidence supporting a beneficial effect of statins in osteoporosis is equivocal (Bauer *et al*., 2004). Many in vivo and in vitro animal studies have suggested such benefits (Song *et al*., 2003; Mundy *et al*., 1999) and human observational studies have also indicated as such (Chan *et al*., 2000; Meier *et al*., 2000). Statin use decreases the incidence of choroidal neo-vascularization, which has been associated with a large proportion of severe vision loss among patients with age-related macular degeneration (Wilson *et al*., 2004). Emerging evidence suggests a benefit for short-term statin administration peri-operatively in patients undergoing non-cardiac vascular surgery (Durazzo *et al*., 2004; Almuti *et al*., 2006).

On the other hand, muscle problems are the most common reported adverse effects of statins. Perhaps the most feared adverse effects of statins is rhabdomyolysis, a condition in which there is severe breakdown of muscle tissue that may be toxic to the kidneys and result in kidney failure or death (Golomb, 2004). Cognitive problems also accur with statins and may also have

more impact in elderly patientns. Two randomized trials that were designed to assess cognitive effects of statins have shown worsening in cognitive function (Muldoon *et al*., 2002, 2000). In addition, several case reports (King *et al*., 2003, 2001; Orsi *et al*., 2001) and one large case series (involving 60 patients) (Wagstaff *et al*., 2003) have reported deleterious cognitive effects of statins on memory and cognitive function. A large variety of other adverse effects have been reported with statins, including (but not limited to) gastrointestinal and neurological effects, psychiatric problems, immune effects (e.g., lupus-like syndrome), erectile dysfunction and gynecomastia (breast enlargement in men), rash and skin problems, and sleep problems (Golomb, 2004). Moreover, animal studies and pre-marketing clinical trials of statins have given signals of hepato-toxicity, primarily minor elevations in serum levels of alanine aminotransferase (ALT) and aspartate aminotransferase (AST) enzymes (Tolman, 2002; Vasudevan *et al*., 2005).

1.6.1 Simvastatin-Membrane Interactions

Çalışkan et al. in 2000 reported a reduction in the cholesterol to phospholipid ratio in erythrocyte membranes after four weeks of simvastatin therapy, but their dose was suprapharmacologic and similar alterations may require a long time in humans (Çalışkan *et al*., 2000). In addition, Kirsch et al. in 2003 showed that simvastatin directly and/or indirectly exert various effects on membrane cholesterol homeostasis in the central nervous system. Kirsch also stated that lovastatin and pravastatin but not simvastatin significantly reduced cholesterol levels in the exofacial plasma membrane leaflet of synaptosomal cells. Such a result is interesting because both lovastatin and simvastatin are lipophilic and their chemical structures are similar. And these changes were accompanied by modified membrane bulk fluidity (Kirsch *et al*., 2003).

Moreover, Djaldetti et al. in 2006 explained an increase in the phagocytic capacity of the macrophages due to the simvastatin-induced increase in the membrane fluidity. Djaldetti also stated that alterations in membrane bilayer lipid composition and particularly its cholesterol content may affect phagocytic cell function either by changes in membrane rigidity, or by redistribution of the cholesterol in the cell membrane (Djaldetti *et al.*, 2006). Furthermore, related about the membrane fluidity and neutrophil functions Spika et al in 1996 stated that diminished membrane fluidity due to increased membrane stability decreased neutrophil functions, such as phagocytosis and chemotaxis (Spika *et al*., 1996).

Vevera et al. in 2005 demonstrated that a significant decrease in serum cholesterol and a nonsignificant decrease in membrane cholesterol concentration after 2 months of simvastatin therapy. Membrane fluidity is directly related with membrane cholesterol level. If the cholesterol level is decreased in the membrane then membrane fluidity is increased (Vevera *et al*., 2005).

In addition, Rabini et al. in 1993 reported an initial decrease and an elevation after 4 months in the membrane dynamics caused by simvastatin. In the same study Rabini et al. also demonstrated an initial increase in cholesterol concentration and in cholesterol/phospholipid molar ratio, with a significant decrease only after 4 months (Rabini et al., 1993). Furthermore, Koter et al. in 2002 reported a decrease in the fluidity of erythrocyte membranes at the depth of the fifth carbon atom in the fatty acid chains of phospholipids in hypercholesterolemic patients relative to the control group. And there are no statistically significant differences between the healthy donors and patients with hypercholesterolemia with respect to fluidity in the hydrophobic region of the erythrocyte membrane. In this study, Koter studied with atorvastatin which is one type of statin drugs and fluidity of plasma membranes was determined

by a spin label study (Koter *et al*., 2002). However, Koter et al. in 2003, using electron paramagnetic resonance (EPR) spectroscopy, reported that simvastatin increases lipid fluidity in erythrocyte plasma membranes (Koter *et al*., 2003).

1.7 Absorption Spectroscopy

Molecules absorb light. The wavelengths that are absorbed and the efficiency of absorption depend on both the structure and the environment of the molecule, making absorption spectroscopy a useful tool for characterizing both small and large macromolecules (Freifelder, 1982). The total energy of a molecule is given by the sum of energies of every different motion that the molecule has. Then, the formula of total energy:

$$E_{total} = E_{transition} + E_{rotation} + E_{vibraion} + E_{electronic} + E_{electron\ spin\ orientation} + E_{nuclear\ spin\ orientation} \quad (1.7.1)$$

In a solution, a molecule can translate, rotate and vibrate. The energies associated with each of these motions are quantized (Campbell, 1984).

Light, in its wave aspect, consists of mutually perpendicular electric and magnetic fields, which oscillate sinusoidally as they are propagated through space (Figure 1.7.1). The energy of the wave is:

$$E = h.c/\lambda = h.\nu \quad (1.7.2)$$

in which “h” is Planck’s constant, “c” is the velocity of light, “λ” is the wavelength, and “ν” is the frequency. When such a wave encounters a molecule, it can be either scattered (i.e., its direction of propagation changes) or absorbed (i.e., its energy is transferred to the molecule) (Freifelder, 1982).

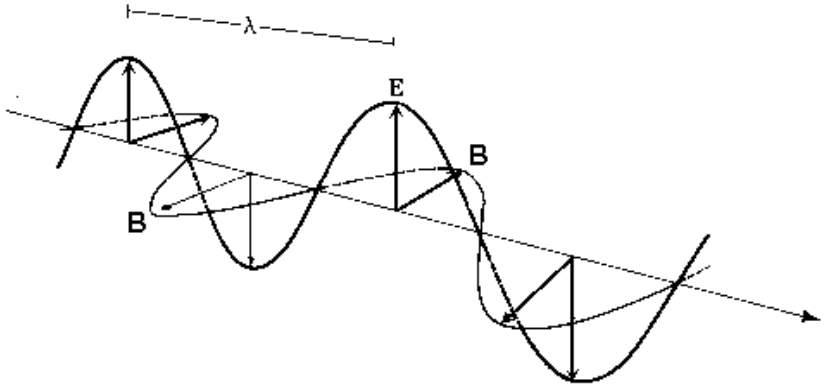

Figure 1.7.1 Propagation of an electromagnetic wave through space.

The relative probability of the occurrence of each process is a property of the particular molecule encountered. If the electromagnetic energy of the light is absorbed, the molecule is said to be excited or in an excited state. A molecule or part of a molecule that can be excited by absorption is called a chromophore. This excitation energy is usually converted into heat (kinetic energy) by the collision of the excited moecule with another molecule (e.g., a solvent molecule). With some molecules it is reemitted as fluorescence. In both cases, the intensity of the light transmitted by a collection of chromophores is less than the intensity of the incident light (Freifelder, 1982).

An excited molecule can possess any one of a set of discrete amounts (quanta) of energy described by the laws of quantum mechanics. These amounts are called the energy levels of the molecule. The major energy levels are determined by the possible spatial distributions of the electrons and are called electronic energy levels; on these are superimposed vibrational levels, which indicate the various modes of vibration of the molecule (e.g., the stretching and bending of various covalent bonds). There are even smaller subdivisions called rotational levels, but they are of little importance in absorption spectroscopy. All these energy levels are usually described by an energy-level diagram

(Figure 1.7.2). The lowest electronic level is called the ground state and all others are excited states (Freifelder, 1982).

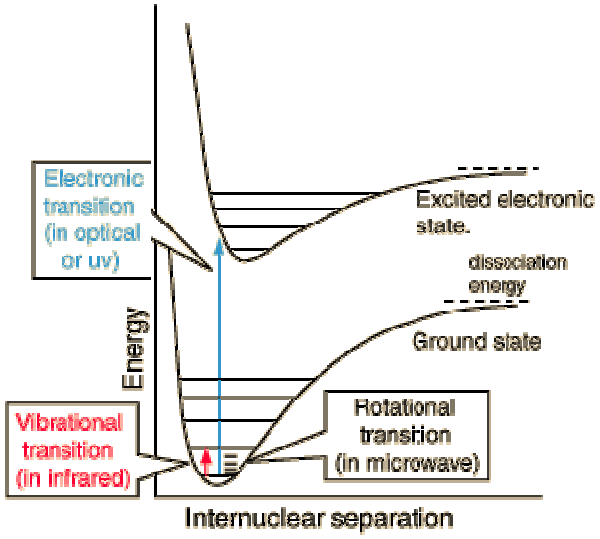

Figure 1.7.2 Typical energy-level diagram showing the ground state and the first excited state. Vibrational levels are shown as horizontal lines and rotational levels are also shown in between the two vibrational levels in the ground state. A possible electronic transition between the first vibrational level of the ground state and the second vibrational level of the first excited state is indicated by the long arrow. A vibrational transition within the ground state is indicated by the short arrow.

The absorption of energy is most probable only if the amount absorbed corresponds to the difference between energy levels. This can be expressed by stating that light of wavelength can be absorbed only if

$$\lambda = \frac{hc}{E_2 - \mathrm{E}_1} \tag{1.7.3}$$

in which E_1 is the energy level of the molecule before absorption and E_2 is an energy level reached by absorption. A change between energy levels is called a

transition. Mechanically, a transition between electronic energy levels represents the energy required to move an electron from one orbit to another. Transitions are represented by vertical arrows in the energy-level diagram. A plot of the probability of absorption versus wavelength is called an absorption spectrum and absorption spectroscopy refers to the gathering and analysis of absorption data (Freifelder, 1982).

1.7.1 Infrared Spectroscopy

Infrared spectroscopy is certainly one of the most important analytical techniques available to today's scientists. One of the great advantages of infrared spectroscopy is that virtually any sample in virtually any state may be studied. Liquids, solutions, pastes, powders, films, fibres, gases and surfaces can all be examined with a judicious choice of sampling technique. As a consequence of the improved instrumentation, a variety of new sensitive techniques have now been developed in order to examine formerly intractable samples (Stuart, 2004). Transitions between vibrational levels of the ground state of a molecule result from the absorption of light in the infrared (IR) region: from 10^3 nm to 10^5 nm (Figure 1.7.1.1). These vibrational levels and, hence, infrared spectra are generated by the characteristic motions (bond stretching, bond bending, and more complex motions) of various functional groups (e.g., methyl, carbonyl, amide, etc.). Figure 1.7.1.2 shows types of normal vibrations for CO_2 molecule. The value of infrared spectral analysis comes from the fact that the modes of vibration of each group are very sensitive to changes in chemical structure, conformation, and environment. Infrared spectroscopy is thought of as being different principally from visible and ultraviolet spectroscopy because it has a somewhat different technology and because it is used to examine chemical groups not accessible to ultraviolet and visible-light absorption spectroscopy (Freifelder, 1982).

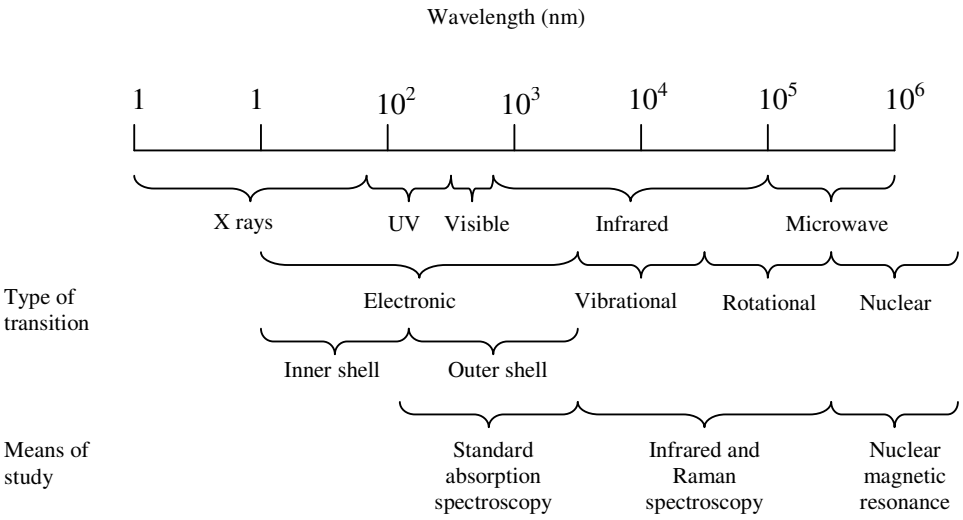

Figure 1.7.1.1 The part of the electromagnetic spectrum that is relevant to physical biochemistry.

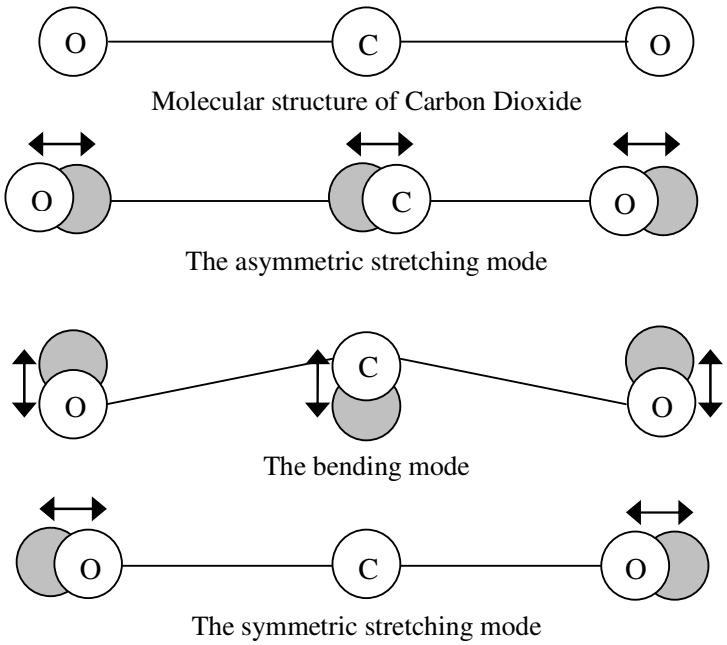

Figure 1.7.1.2 Types of normal vibrations for CO_2 molecule.

Infrared spectroscopy is a technique based on the vibrations of the atoms of a molecule. An infrared spectrum is commonly obtained by passing infrared radiation through a sample and determining what fraction of the incident radiation is absorbed at a particular energy. For a molecule to show infrared absorptions it must possess a specific feature, i.e. an electric dipole moment of the molecule must change during the vibration. This is the selection rule for infrared spectroscopy. Because of the difference in electronegativity between carbon and oxygen, the carbonyl group is permanently polarized. Stretching this bond will increase the dipole moment and, hence, C=O stretching is an intense absorption. Wavenumbers of some characteristic infrared absorption bands are given in Table 1.7.1.1. A molecule can only absorb radiation when the incoming infrared radiation is of the same frequency as one of the fundamental modes of vibration of the molecule. This means that the vibrational motion of a small part of the molecule is increased while the rest of the molecule is left unaffected (Stuart, 2004).

1.7.2 Instrumentation of Fourier-Transform Infrared Spectrometer

Fourier-transform infrared (FTIR) spectroscopy is based on the idea of the interference of radiation between two beams to yield an interferogram (Griffiths and de Haseth, 1986). The latter is a signal produced as a function of the change of pathlength between the two beams. The two domains of distance and frequency are interconvertible by the mathematical method of Fourier-transformation. The basic components of an FTIR spectrometer are shown schematically in Figure 1.7.2.1. The radiation emerging from the source is passed through an interferometer to the sample before reaching a detector. Upon amplification of the signal, in which high-frequency contributions have been eliminated by a filter, the data are converted to digital form by an analog-to-digital converter and transferred to the computer for Fourier-transformation (Stuart, 2004).

Table 1.7.1.1. Band assignments of some characteristic infrared absorbtion bands according to their wavenumbers in cm^{-1} (Stuart, 2004).

Wavenumber (cm^{-1})	Assignment	Wavenumber (cm^{-1})	Assignment
3010	=C-H stretching	1085	PO_2^- symmetric stretching
2956	CH_3 asymmetric stretching	1070	CO-O-C symmetric stretching
2920	CH_2 antisymmetric stretching	1047	C-O-P stretching
2870	CH_3 symmetric stretching	972	$(CH_3)_3N^+$ asymmetric stretching
2850	CH_2 symmetric stretching	820	P-O asymmetric stretching
1730	C=O stretching	730,720,718	CH_2 rocking
1485	$(CH_3)_3N^+$ asymmetric bending	1350-1250	O-H bending
1473,1472, 1468,1463	CH_2 scissoring	1560	CO_2^- asymmetric stretching
1460	CH_3 asymmetric bending	1415	CO_2^- symmetric stretching
1405	$(CH_3)_3N^+$ symmetric bending	1615	NH_2 bending
1378	CH_3 symmetric bending	1640-1610, 1550-1485	NH_3^+ bending
1400-1200	CH_2 wagging band progression	1160,1100	NH_3^+ rocking
1228	PO_2^- antisymmetric stretching	1602,1450,760 700	Benzene ring vibrations
1170	CO-O-C asymmetric stretching	1600,1450	Benzene ring vibrations

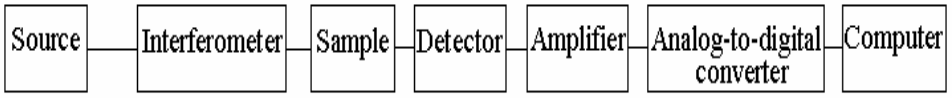

Figure 1.7.2.1 Basic components of an FTIR spectrometer.

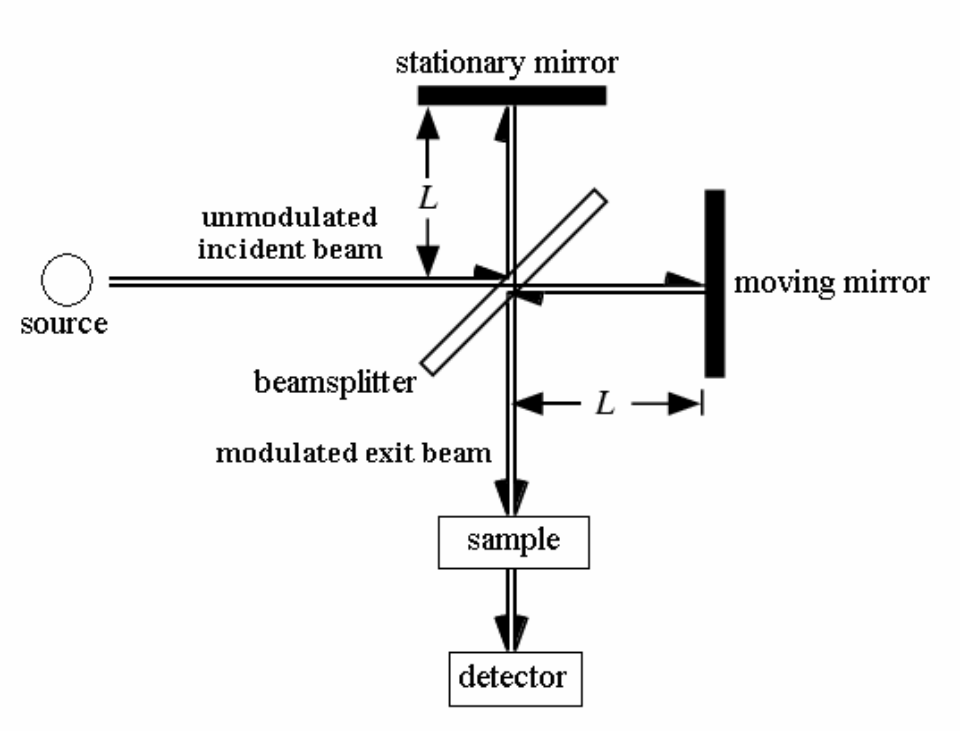

Figure 1.7.2.2 Schematic of a Michelson interferometer.

The most common interferometer used in FTIR spectrometry is a Michelson interferometer (Figure 1.7.2.2), which consists of two perpendicularly plane mirrors, one of which can travel in a direction perpendicular to the plane. A semi-reflecting film, the beamsplitter, bisects the planes of these two mirrors. The beamsplitter material has to be chosen according to the region to be examined. FTIR spectrometers use a Globar or Nernst source for the mid-infrared region. If the far-infrared region is to be examined, then a high-

pressure mercury lamp can be used. For the near-infrared, tungsten-halogen lamps are used as sources. The moving mirror is a crucial component of the interferometer. It has to be accurately aligned and must be capable of scanning two distances so that the path difference corresponds to a known value. A number of factors associated with the moving mirror need to be considered when evaluating an infrared spectrum. The interferogram is an analogue signal at the detector that has to be digitized in order that the Fourier-transformation into a conventional spectrum can be carried out (Stuart, 2004).

1.7.3 Infrared Spectroscopy in Membrane Research

Infrared spectroscopy can provide valuable structural information about lipids, which are important molecular components of membranes. The infrared spectra of phospholipids can be divided into the spectral regions that originate from the molecular vibrations of the hydrocarbon tail, the interface region and the head group (Watts and De Pont, 1986; Lewis and McElhaney, 2002). The hydrocarbon tail gives rises to acyl chain modes. The most intense vibrations in the infrared spectra of lipid systems are the CH_2 stretching vibrations and these give rise to bands in the 3100 to 2800 cm^{-1} region. In certain phospholipid membranes that contain unsaturated acyl chains, the typical lamellar liquid crystalline phase converts to a micellar non-lamellar phase upon heating (Jackson and Mantsch, 1993). Such a thermally induced transition involves a major structural rearrangement. Temperature studies of the infrared spectra of phospholipids provide a sensitive means of studying such transitions in lipids. Spectral modes arising from the head group and interfacial region also provide valuable information (Mushayakarara and Levin, 1982). Useful infrared bands for studying the interfacial region of lipid assemblies are the ester group vibrations, particularly the C=O stretching bands in the 1750-1700 cm^{-1} region. Quantitative infrared analysis can be carried out on blood serum to determine the relative amounts of lipid present (Bhandara *et al.*, 1994). Triglycerides,

phospholipids and cholesterylesters are the classes of lipid that occur in blood serum and such compounds occur naturally in concentrations that make infrared analysis attractive (Stuart, 2004).

1.7.4 Advantages of Fourier Transform Infrared Spectroscopy

1) FTIR spectroscopy is a rapid and sensitive analytical method with an easy use of sampling techniques (Stuart, 2004).
2) The main advantage of FTIR spectrometer, a rapid-scanning instrument, is the ability to increase the signal-to-noise ratio (SNR) by signal-averaging, leading to an increase of signal-to-noise proportional to the square root of the time (Stuart, 2004).
3) Due to being a non-perturbing technique it is possible to apply FTIR spectroscopy directly to biological samples. In other words, it does not involve introduction of exogenous probes or potentially harmful preparative procedures (Mantsch, 1984).
4) Infrared spectroscopy, in principle, operates on a time-scale that has the potential to sample directly the fastest conformational alterations that occur in biological membranes, namely acyl chain trans-gauche isomerizations (Mendelsohn *et al*., 1989).
5) Now it is possible to determine frequency and bandwidth values with uncertainties of better than ± 0.05 cm^{-1} (Mantsch, 1984).
6) Digital subtraction, which is point-by-point subtraction of two different spectra by a software programme, is also produce good difference spectra. It is very useful in obtaining infrared spectra in aqueous solutions (Campbell and Dwek, 1984).

1.8 Differential Scanning Calorimetry

Differential scanning calorimetry (DSC) is a technique commonly used for determining the thermal properties of a variety of materials including biologically relevant systems. The main applications of DSC include determination of the effect of composition, hydration, pH, and solvent, on the phase-transition temperatures and enthalpies of biological membranes and pharmaceuticals; thermal characterization of complex processes, such as the denaturation of proteins; and specific heat measurements in the glass-transition of polymers (Ceckler and Cunningham, 1997).

The DSC contains a sample cell and a reference cell that are maintained at the same temperature. As an experiment proceeds, the sample and reference cells are raised in temperature in a controlled manner such that the two cells always are maintained at the same temperature. The power supplied to heat each cell is monitored during this process. When a phase transition occurs in the sample cell, there is a difference in the power needed to heat the two cells. The power required to maintain both cells at the same temperature is measured and converted to give an output of heat capacity versus temperature. The heat capacity versus temperature curve is analyzed to determine the transition temperature, T_m, and the calorimetric enthalpy of transition, ΔH_{cal} (Ohline *et al*., 2001).

For first order phase transitions such as the bilayer gel to liquid-crystalline transition, the transition temperature, T_m, is where the heat capacity, C_p, reaches its maximum value. The value of the calorimetric enthalpy (ΔH_{cal}) for the phase transition is determined by integrating the area under the peak.

$$\Delta H_{cal} = \int C_p \, dT \qquad (1.8.1)$$

From these values, the entropy of the phase transition is determined:

$$\Delta S = \Delta H_{cal} / T_m \quad (1.8.2)$$

Comparison of ΔH_{cal}, ΔS and T_m shows the effect of a structural modification (e.g. chain length) on the thermodynamics of the phase transition. However, unlike a simple organic compound's crystal to liquid melting transition, the phase transition in bilayers involves more than just the initial and final states. In fact, intermediate "states" are formed during the transition, and a "non-two-state" model is necessary for phospolipids in liposomes (Mason, 1998; Microcal, Inc., 2002; Sturtevant *et al*., 1987) . These intermediate states result from the formation of domains (e.g. disordered, mobile areas within the gel phase) before the phase transition temperature, and are due to lateral movement of the phospholipids within the bilayer. The asymmetric shape of the DSC peak reflects the fact that a non-two-state transition is occurring (Ohline *et al*., 2001).

1.8.1 Instrumentation of Differential Scanning Calorimetry

A typical differential scanning calorimeter consists of two sealed pans: a sample pan and a reference pan (which is generally an empty sample pan). These pans are often covered by or composed of aluminum, which acts as a radiation shield (Dean, 1995). The two pans are heated, or cooled, uniformly while the heat flow difference between the two is monitored. This can be done at a constant temperature (isothermally), but is more commonly done by changing the temperature at a constant rate, a mode of operation also called temperature scanning (Dean, 1995).

During the determination, the instrument detects differences in the heat flow between the sample and reference. This information is sent to an output device, most often a computer, resulting in a plot of the differential heat flow between the reference and sample cell as a function of temperature. When there are no thermodynamic physical or chemical processes occurring, the heat flow difference between the sample and reference varies only slightly with temperature, and shows up as a flat, or very shallow base line on the plot. However, an exothermic or endothermic process within the sample results in a significant deviation in the difference between the two heat flows. The result is a peak in the DSC curve. Generally, the differential heat flow is calculated by subtracting the sample heat flow from the reference heat flow. When following this convention, exothermic processes will show up as positive peaks (above the baseline) while peaks resulting from endothermic processes are negative (below the baseline) (Dean, 1995). Figure 1.8.1.1 shows instrumentation of a DSC.

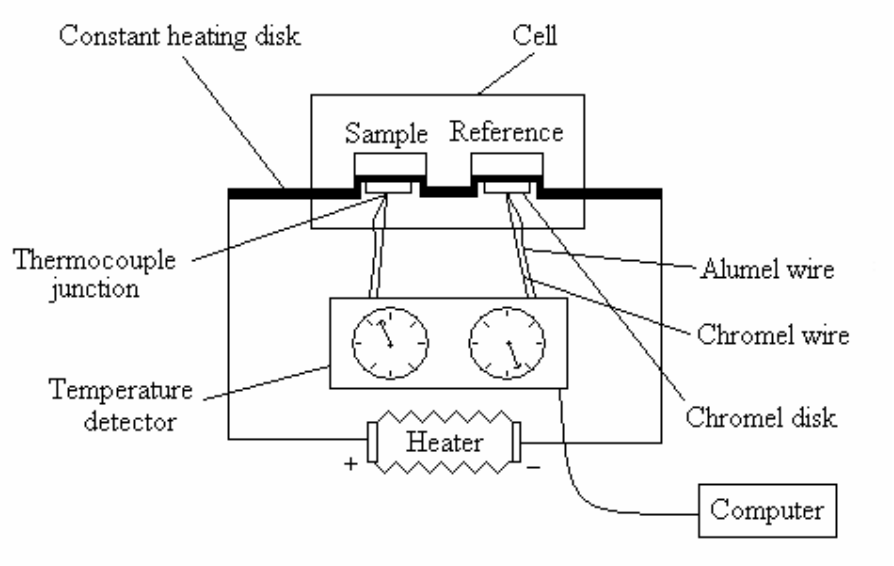

Figure 1.8.1.1 Schematic illustration of a DSC.

The sample (in a condensed form such as powder, liquid, or crystal) is generally placed in an aluminum sample pan, which is then placed in the sample cell. The reference consists of a matched empty aluminum sample pan that is placed in the reference cell of the instrument. The sample pans are designed to have a very high thermal conductivity. Sample sizes generally range from 0.1 to 100 mg. The instrument cells are often airtight to shield the sample and reference from external thermal perturbations. This also allows experiments to be performed under variable pressures and atmospheres (Dean, 1995).

1.8.2 Differential Scanning Calorimetry in Membrane Research

Differential scanning calorimetry is a sensitive and non-invasive technique (Kazancı *et al*., 2001). It is used to characterize phase transitions with respect to such thermodynamic parameters as transition temperature, enthalpy of transition, entropy of transition, and glass transition temperature (Koyama *et al*., 1999). DSC has a wide usage in drug industry like investigating the stability, physical and chemical properties of drugs (Schneider *et al*., 1999). Protein-protein, protein-ligand interactions and protein domain organization studies also involve usage of DSC tehnique (Weber and Salemme, 2003). Determination of thermal stability and reversibility (Anton *et al*., 2000), measurement of heat capacity (C_p) for the calculation of reaction enthalpies, purity determination of chemicals, and chemical half-life determinations (Mayor *et al*, 2000) are some other applications of DSC. Differential scanning calorimetry is a classic method, but application to biological systems is a recent event. The DSC should be ideally suited to investigate protein denaturation in membranes and intact cells. DSC has been used to study phase transitions in lipid bilayers and membranes corroborating the results obtained with low-angle X-ray diffraction studies. The phase transitions observed in the DSC can be correlated with changes in biological properties (Tien and Ottova, 2000).

The gel to liquid-crystalline phase transition is highly "cooperative." In cooperative transitions, well before the transition temperature is reached from below, the molecules begin to reorganize and to move in consort with each other. In other words, the molecules cooperate with each other in gaining new motional freedom; when one molecule picks up motional energy then other nearby molecules find it easier to add motional energy. As the temperature approaches the transition temperature, T_m, the distance range of this cooperation increases. Near the phase transition temperature, you can picture islands of lipids in a more mobile phase intermixed with the less mobile gel phase. The number of molecules on average in these disordered "islands" is called the cooperative unit. In these islands the motions of the molecules are highly correlated. These correlated interactions aid in the sudden change of order at the phase transition temperature. The larger the cooperative unit, the narrower the phase transition temperature range. The gel to liquid-crystalline phase transition is first-order with some of the characteristics of second-order transitions. First-order phase transitions have a change in enthalpy and volume at the phase transition temperature. In other words, in first-order transitions there is an abrupt change in the properties of the system at the phase transition temperature. In this respect, a first order phase transition is "completely correlated," that is completely cooperative. In a first order phase transition all the molecules undergo the phase transition together, subject only to the availability of thermal energy. A pure first-order transition has an infinitely sharp transition. Second-order transitions do not have enthalpy and volume changes at the transition temperature. For second order phase transitions, the formation of cooperative, correlated motions with limited range broadens the transition by pre-transition effects (i.e. the domains anticipate the transition or "start the transition" early). In the DSC of synthetic phospholipids the limited cooperativity of the transition results in a small peak at a lower temperature than the main melting peak, called the pre-transition, as well as a broadening of

the main melting transition (Chapman, 1975; Szoka and Papahadjopoulos, 1980; Koyama *et al*., 1999; Ohline *et al*., 2001).

CHAPTER 2

MATERIALS AND METHODS

2.1 Reagents

Simvastatin (2,2-dimethyl-,1,2,3,7,8,8a-hexahydro-3,7-dimethyl-8-[2-(tetrahydro-4-hydroxy-6-oxo-2*H*-pyran-2-yl)-ethyl]-1-naphthalenyl ester, [1*S*-[1α,3α,7β,8β(2*S**,4*S**),-8aβ]]) was purchased from Calbiochem (Merck), Darmstadt, Germany. 1,2-Dimyristoyl-*sn*-glycero-3-phosphocholine (DMPC) and 1,2-Dipalmitoyl-*sn*-glycero-3-phosphocholine (DPPC) were purchased from Sigma, St. Louis, MO, USA. All reagents were used without further purification.

2.2 Phosphate Buffer Preparation

A concentration of 10 mM phosphate buffer with pH 7.4 was prepared by using Na_2HPO_4 powder with a molecular weight of 141.96 g. First, 0.2839 g of Na_2HPO_4 powder was added to 150 ml double distilled water. Second, obtained solution was stirred up until the powder was completely dissolved. Third, pH value was adjusted to 7.4 at 25 ^{o}C either by adding hydrogen chloride HCl or sodium hydroxide NaOH. During the pH adjustment solution was stirred up. Finally, sufficient double distilled water was added to bring the volume up to 200 ml.

2.3 Simvastatin Stock Solution Preparation

Simvastatin stock solution was prepared by dissolving 5 mg simvastatin powder with a molecular weight of 418.6 g in 1 mL pure ethanol and treating with 0.813 mL of 1 N NaOH in a glass tube. Later, the pH of the solution was adjusted to 7.2 by adding small quantities of 1 N HCl . Thus, the inactive form of simvastatin was converted to the active open ring structure form by a reaction with NaOH.

2.4 Preparation of Model Membranes

DMPC and DPPC multilamellar liposomes were prepared according to the procedure reported by Toyran and Severcan (2003). To prepare simvastatin containing liposomes desired amount of simvastatin was taken from the stock solution and put in an eppendorf tube. The excess ethanol was evaporated by nitrogen stream and then desired amount of DMPC or DPPC was added and dissolved with chloroform in the same eppendorf tube. Again the excess chloroform was evaporated by nitrogen stream and the remaining solvent in the eppendorf tube was removed by spin vacuum drying for 2 hours. The dry thin films were then hydrated by adding phosphate buffer, pH 7.4 with the desired amount of hydration. Multilamellar liposomes were formed by vortexing the mixture for 20 minutes at 20^{o}C above the T_m of DMPC (~43^{o}C) and the T_m of DPPC (~62^{o}C). Pure DMPC or DPPC multilamellar liposomes were prepared by following the same procedure only without using the simvastatin stock solution.

2.5 Sample Preparation for the FTIR Experiments

5 mg of DMPC or DPPC was used to prepare thin films. Obtained dry thin films were hydrated by adding 25 µL of 10 mM phosphate buffer, pH 7.4.

Infrared spectra were recorded on a Perkin Elmer Spectrum 100 FT-IR spectrometer. 20 µL of liposome samples were placed between water insoluble CaF_2 windows with 12 µm sample thickness. Interferograms were averaged for 20 scans at 2 cm^{-1} resolution. Temperature of samples was regulated by Graseby Specac temperature controller unit. Samples were scanned between 24-70°C with 2°C intervals but above the 60°C interval was increased to 5°C. Samples were incubated for 5 minutes at each temperature before the spectrum acquisition.

2.5.1 Infrared Spectral Regions Used in This Study

In model membrane studies the structural changes caused by a drug can be easily detected and understood by analysing infrared absorption bands because any change occurred in the molecular structure directly affects the vibrational modes of the molecule. Hence, by examining some parameters which belong to the infrared absorption bands like frequency and bandwith, it is possible to monitor many changes in the structure of the lipid assemblies.

In this study, there are mainly four absorption bands taken into consideration. Two of them are caused by carbon-hydrogen stretching vibrations and known as antisymmetric and symmetric CH_2 stretching modes in the spectral region of 3100-2800 cm^{-1}. The CH_2 antisymmetric stretching located at 2920 cm^{-1} and CH_2 symmetric stretching located at 2851 cm^{-1} are strong lipid bands which are sensitive to conformational changes. And they respond to any difference occurred in the trans/gauche ratio in acyl chains (Lee and Chapman, 1986). Moreover, conformational changes can also be detected by examining asymmetric CH_3 at 2956 cm^{-1} and symmetric CH_3 at 2872 cm^{-1} bands which are stretching modes of the terminal methyl group. Frequencies of the CH_2 stretching modes reflect conformational disorder and they increase when

gauche bonds in the fatty acyl chains start to increase (Lopez-Garcia *et al*., 1993; Dluhy *et al*., 1983; Severcan, 1997).

Also one absorption band is C=O stretching in 1750-1700 cm^{-1} region which reflects the ester group vibrations. This band is very useful for probing the interfacial region because in the structure of DMPC and DPPC ester groups are located between polar and nonpolar interfaces. And any change in the structure of lipid molecule can be monitored by analysing this sensitive interfacial region. Examining C=O stretching band gives information about the strength of hydrogen bonding. In diacyl lipids there are two bands because of two ester carbonyl groups in the molecule. One band around 1742 cm^{-1} with a trans conformation in the C-C bond and the other one around 1728 cm^{-1} (Mendelsohn and Mantsch, 1986). However, only a broad band contour is found in hydrated samples and its mid-point is around 1735 cm^{-1}.

The other absorption band is PO_2^- antisymmetric double stretching in the 1260-1200 cm^{-1} region. Moreover, in the 1380-1180 cm^{-1} region there are series of bands which belong to the polymethylene chains. Nonetheless, it is difficult to observe this CH_2 wagging band progression in the spectra of phospholipids because of overlapping with the strong PO_2^- antisymmetric double stretching band. Furthermore, there is a weak CH_2 rocking-twisting band in the 1150-700 cm^{-1} region. However, it is not possible to monitor this band because CaF_2 windows used in this study are not transparent to the region lower than 1000 cm^{-1}.

The O-H stretching bands due to buffer appear in the regions of 3400-3200 cm^{-1} and 1800-1500 cm^{-1}. However, the region of 3400-3200 cm^{-1} overlaps with the region of C-H stretching band and the region of 1800-1500 cm^{-1} overlaps with the region of C=O stretching band. Therefore, spectrum of the buffer without simvastatin and lipids was taken at different temperatures and it

was subtracted from the spectra of liposomes at corresponding temperatures. Subtraction process was done manually by using Perkin Elmer software programme. Figures 2.5.1.1 and 2.5.1.2 show the infrared spectra of DMPC and DPPC liposomes respectively before and after water subtraction. Moreover, molecules in the air interfere with the spectra of samples. To prevent this interfering, spectrum of the air was recorded as a background spectrum and subtracted automatically from the spectra of samples by using the same software programme of FTIR spectroscopy. Figure 2.5.1.3 shows the infrared spectrum of air.

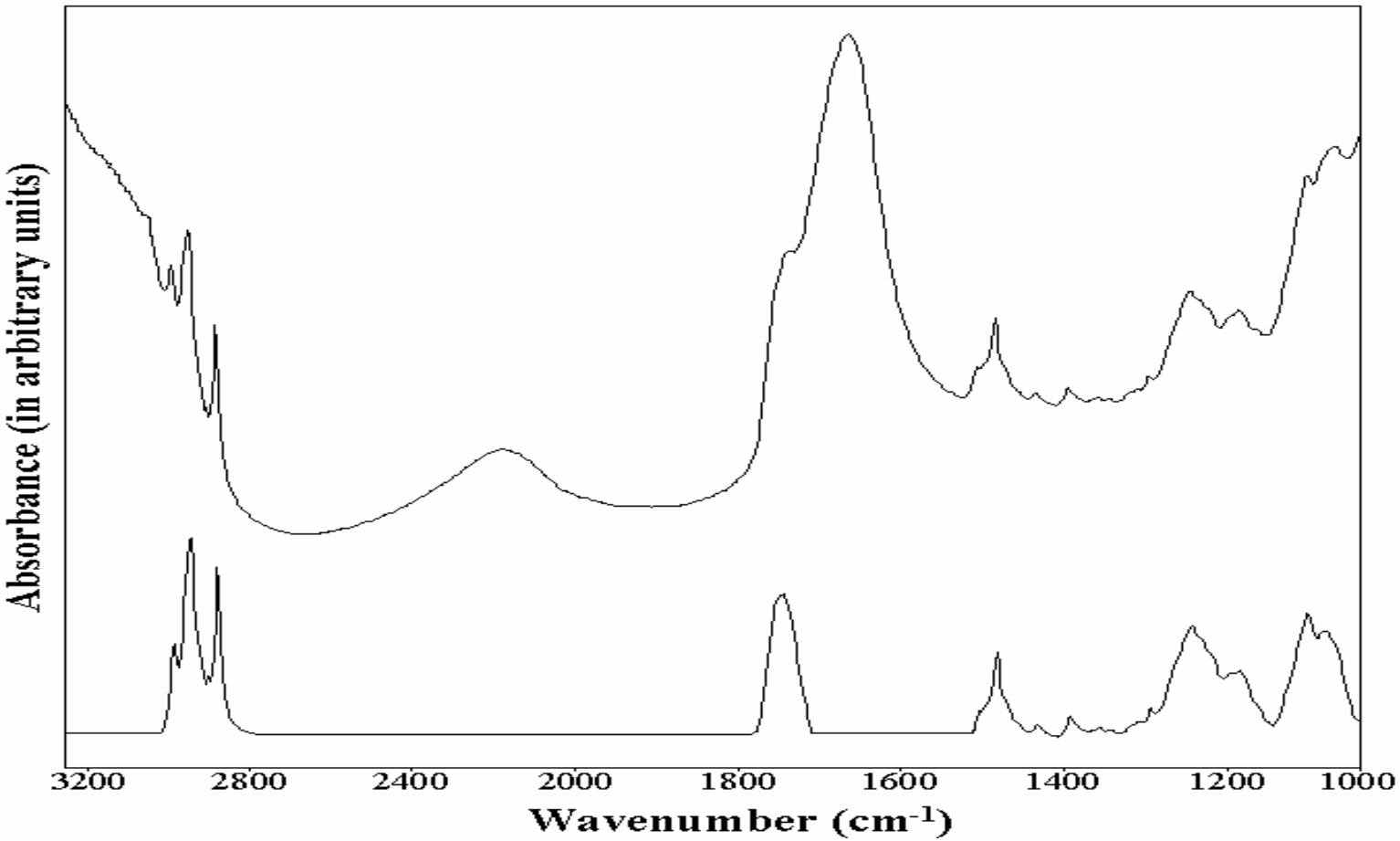

Figure 2.5.1.1 FTIR spectrum of DMPC liposomes. Upper spectrum shows the liposomes before water bands were subtracted and the spectrum below shows the liposomes after subtraction.

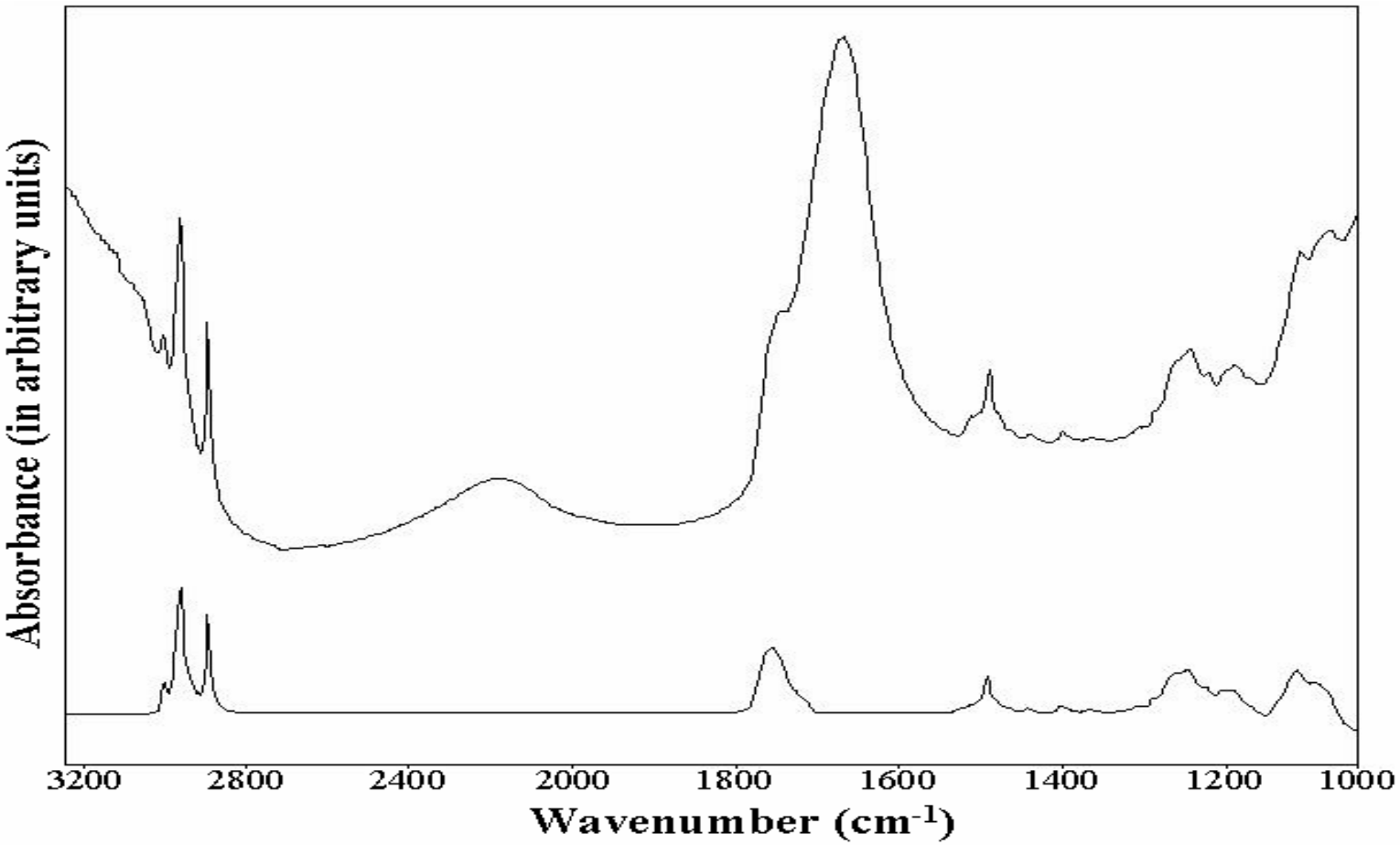

Figure 2.5.1.2 FTIR spectrum of DPPC liposomes. Upper spectrum shows the liposomes before water bands were subtracted and the spectrum below shows the liposomes after subtraction.

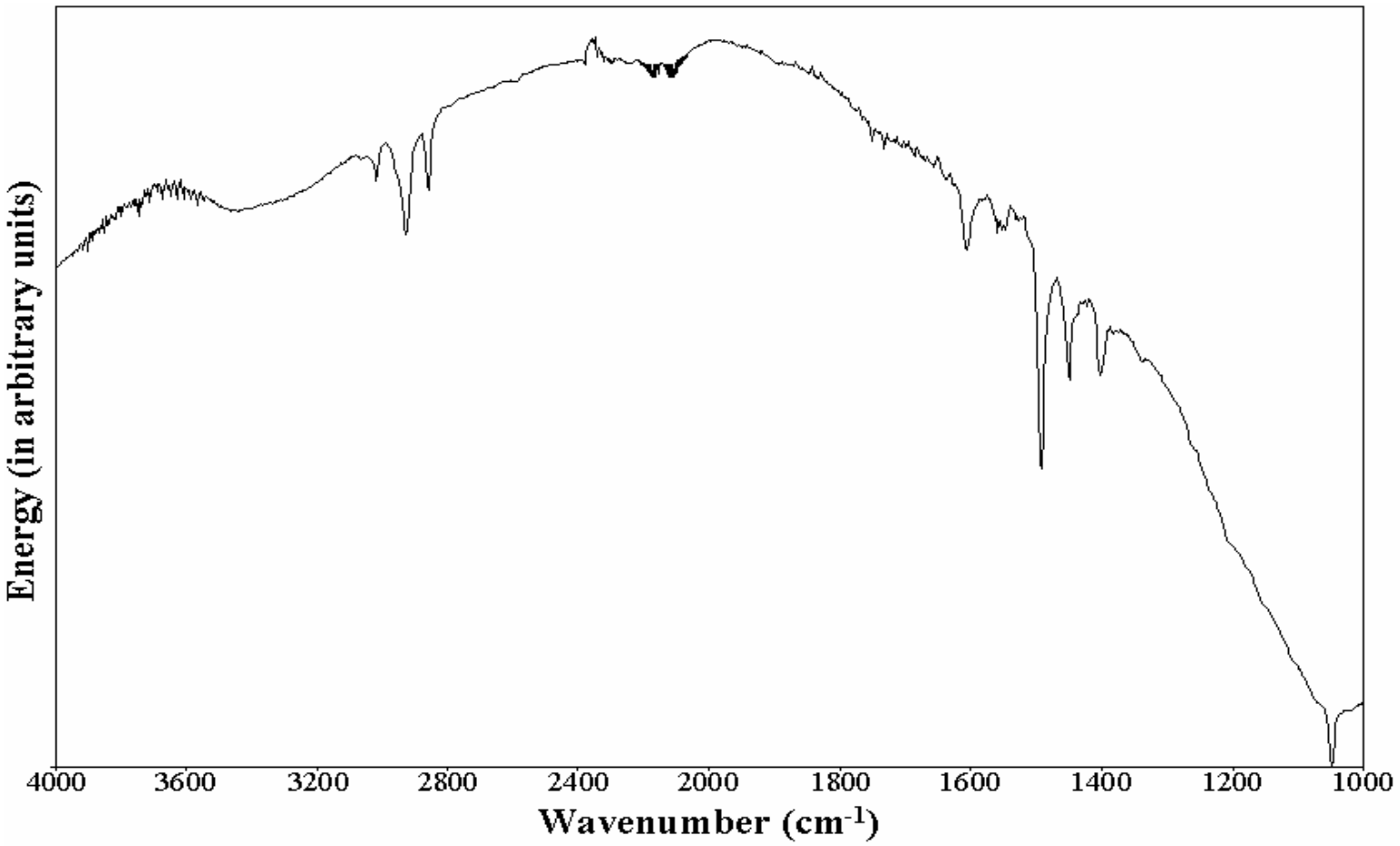

Figure 2.5.1.3 Infrared spectrum of air.

2.6 Sample Preparation for the DSC Experiments

2 mg of DMPC or DPPC was used to prepare thin films. Obtained dry thin films were hydrated by adding 50 µL of 10 mM phosphate buffer, pH 7.4. Liposome preparation was done as described before. 50 µL of liposome samples were placed in high volume pans and these pans were sealed by a special sample encapsulating press. An empty pan was used as a refence pan during the experiment. Heating rate was chosen as 1^{o}C/min. DMPC liposome samples were heated between 0-50^{o}C and DPPC liposome samples were heated between 20-70^{o}C . Experiments were carried out with TA DSC Q100.

2.6.1 Thermogram Analysis

Differential Scanning Calorimetry is generally used to determine the main phase transition temperature and transition enthalpy change in model membrane studies (Bach *et al*., 2001; Tahir *et al*., 1999; Momo *et al*., 2002; Severcan *et al*., 2005; Korkmaz and Severcan, 2005). If there is an interaction between the drug and model membrane it is reflected to the phase transition profile of the liposome. Therefore, it becomes possible to monitor such an interaction on the thermogram analysis directly. Moreover, DSC is used for estimation of purity and identification of materials (Daniels, 1973).

In this study, liposomes which are made from DMPC or DPPC lipids were used. Each lipid has its own characteristic main phase transition temperature and transition enthalpy change. For DMPC, the main phase transition temperature is 22.80^{o}C with an enthalpy change of 7.90 cal/g and the pretransition temperature is 14.60^{o}C (Kiselev *et al*., 2001). For DPPC, the main phase transition temperature is 41.20^{o}C with an enthalpy change of 12.50 cal/g and the pretransition temperature is 35.20^{o}C with an enthalpy change of 1.60 cal/g (Mavramoustakos *et al*., 1997). Calibration of the instrument, different

heating rates applied to samples and the usage of different pan types during the experiment may cause some slight variations from the data given above (Koyama *et al*., 2000). On the DSC thermogram, the main phase transition of a lipid appears as a sharp peak and occur within a very narrow temperature interval. Therefore, thermally induced phase transition occurs abruptly. Figures 2.6.1 and 2.6.2 show the phase transitions of DMPC and DPPC, respectively. The maximum point of the peak is taken as the main phase transition temperature of the lipid. Moreover, integrating the area under the peak gives the enthalpy of transition by an equation of:

$$\left(\frac{dq}{dt}\right)_{\mathrm{p}} = \frac{dH}{dt} \qquad (2.6.1.1)$$

The width of the peak measured from the half height in terms of temperature is also another useful parameter. The value of the width and the main phase transition temperature give information about the size and packing of cooperative units undergoing the transition. If the width is increased by the drug incorporated into the bilayer, then the cooperativity of the transition is reduced (Tahir *et al*., 1999). Variations in enthalpy values show the interstitial and substitutional impurities. Any change in the main phase transition temperature provides information about the fluidity of the system (Castelli *et al*., 2001). By analysing the mentioned parameters it is possible to understand if there is an interaction between DMPC or DPPC liposomes and simvastatin.

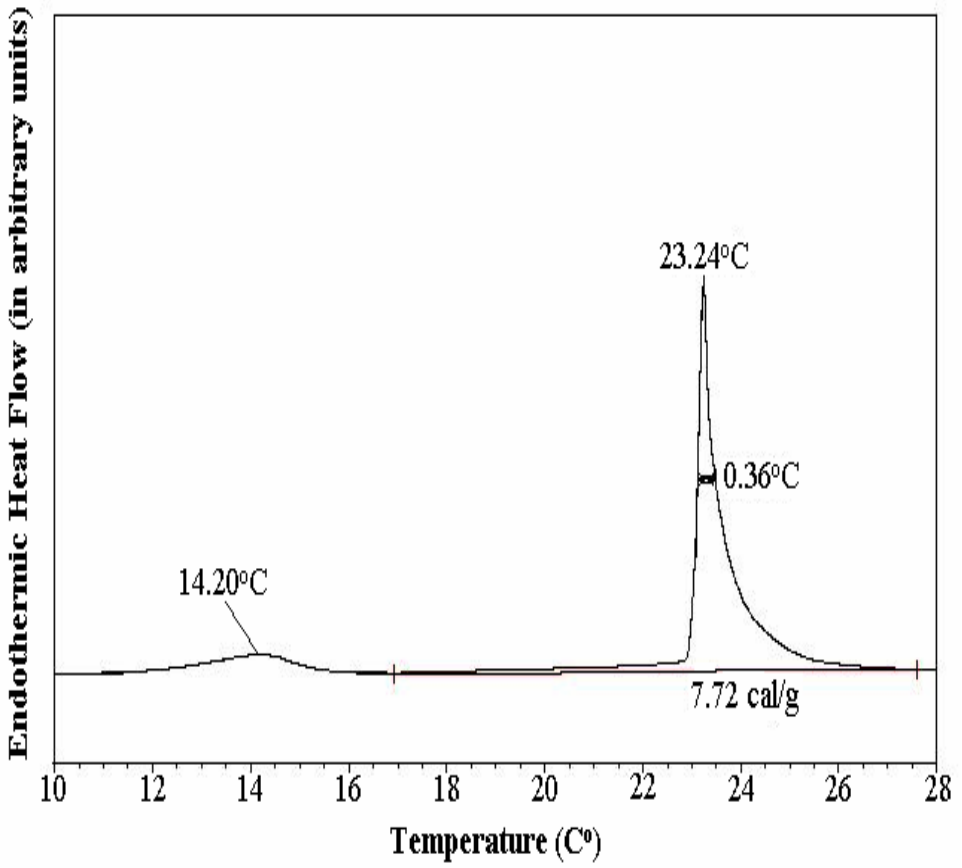

Figure 2.6.1 Phase Transition Thermogram of DMPC. The little peak on the left is the pretransition curve and the following one is the main transition curve. Three parameters namely the width, the main phase transition temperature and the transition enthalpy change used in the DSC analysis were indicated on the main transition curve.

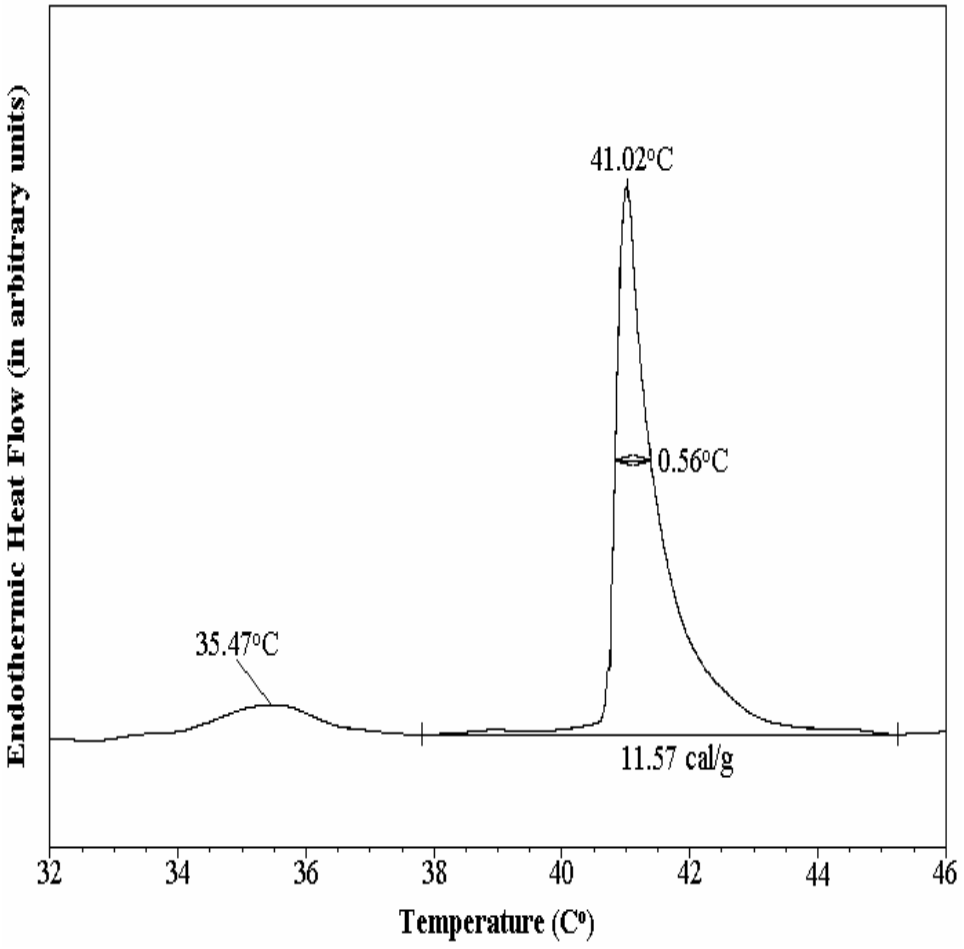

Figure 2.6.2 Phase Transition Thermogram of DPPC. The little peak on the left is the pretransition curve and the following one is the main transition curve. Three parameters namely the width, the main phase transition temperature and the transition enthalpy change used in the DSC analysis were indicated on the main transition curve.

CHAPTER 3

RESULTS

In this part of the study, interactions of DMPC or DPPC multilamellar bilayers with different simvastatin concentrations were discussed. Simvastatin concentrations used in the experiments were 1mol%, 6mol%, 12mol%, 18mol%, and 24mol%. Fourier Transform Infrared (FTIR) Spectroscopy and Differential Scanning Calorimetry (DSC) were used in this study to monitor and understand the interactions between model membranes and simvastatin.

3.1 FTIR Studies

FTIR studies can be separated into two parts. In the first part, temperature dependent FTIR studies for DPPC model membranes were carried out. The experiments were repeated twice and similar results were obtained. FTIR spectra of DPPC liposomes were analysed with respect to the CH_2 symmetric and antisymmetric, C=O stretching and PO_2^- antisymmetric bands. During the analyses of these infrared absorption bands, their wavenumber and bandwidth values were investigated. The variations on these parameters were measured and plotted on a graph as a function of temperature to interpret the results. Therefore, we can understand the simvastatin-induced structural changes on DPPC model membranes at the molecular level.

In the second part, FTIR studies were carried out to understand the effect of acyl chain length comparing the FTIR spectra of DMPC and DPPC lipids which have 12 and 14 methylene groups in their fatty acyl chains, respectively. Again the same absorption bands and parameters were used for the analyses of

FTIR spectra of DMPC or DPPC liposomes. The measured parameters were plotted on column graphes as a function of simvastatin concentrations. And these graphs were given for only two temperatures corresponding to the gel and liquid crystalline phase of the lipids. For DMPC liposomes the selected temperatures were 10^{o}C and 35^{o}C. For DPPC liposomes the selected temperatures were 29.5^{o}C and 54^{o}C. Every experiment at each temperature was repeated 5 times and the results were averaged. Later, Mann-Whitney U test was applied. Final results which were statistically significant were shown by an asterisk on the graphs.

3.1.1 Temperature Dependent FTIR Studies of DPPC Model Membranes

As mentioned in the previous section four infrared absorption bands were used for the analysis of FTIR results. These are CH_2 symmetric and antisymmetric, C=O stretching and PO_2^- antisymmetric bands. Figure 3.1.1.1 shows the infrared absorption spectra of pure DPPC multilamellar liposomes in the C-H stretching region at different temperatures. As it can be seen from the figure, peak height, wavenumber and bandwidth values changed as temperature increased.

Figure 3.1.1.2 shows the FTIR spectra of DPPC liposomes in the presence and absence of low and high simvastatin concentrations in the C-H stretching region at 41.4^{o}C. As it can be seen in the figure, for pure DPPC liposomes the CH_2 symmetric stretching mode has a peak at 2850 cm^{-1} and CH_2 antisymmetric stretching mode has a peak at 2920 cm^{-1}. Moreover, CH_3 asymmetric and symmetric stretching bands located at 2956 cm^{-1} and 2872 cm^{-1}, respectively.

Figure 3.1.1.3 shows the FTIR spectra of DPPC liposomes in the presence and absence of low and high simvastatin concentrations in the 1800-1000 cm^{-1}

region at 45.1°C. As it can be seen in the figure, for pure DPPC liposomes the C=O ester carbonyl stretching band located at 1735 cm^{-1} and the PO_2^- antisymmetric double stretching band located at 1230 cm^{-1}. The figures 3.1.1.2 and 3.1.1.3 showed that simvastatin changed the bandwidth, band frequency and band intensity values.

Moreover, we run FTIR spectra for DMPC or DPPC lipids and simvastatin in solution at the concentrations used in this study because simvastatin molecule also contain C-H and C=O stretching groups. As it can be seen from the figure 3.1.1.4, the contribution of simvastatin to the C-H and C=O stretching bands are negligible. Therefore, the C-H and C=O stretching bands in the spectra of simvastatin containing DMPC or DPPC liposomes mainly monitors the lipid functional groups.

Figure 3.1.1.5 shows the FTIR spectra of the pure DMPC and DPPC liposomes in their gel phases. As it can be seen in the figure, the bandwidth of the DMPC lipids is longer than that of the DPPC lipids at the CH_2 antisymmetric stretching mode. The bandwidth of the CH_2 symmetric and the CH_2 antisymmetric stretching modes gives information about the membrane fluidity or membrane stability. An increase in the bandwidth means an increase in the membrane fluidity or a decrease in the membrane stability. Thus, DPPC membranes are more stable than DMPC membranes with respect to their structures.

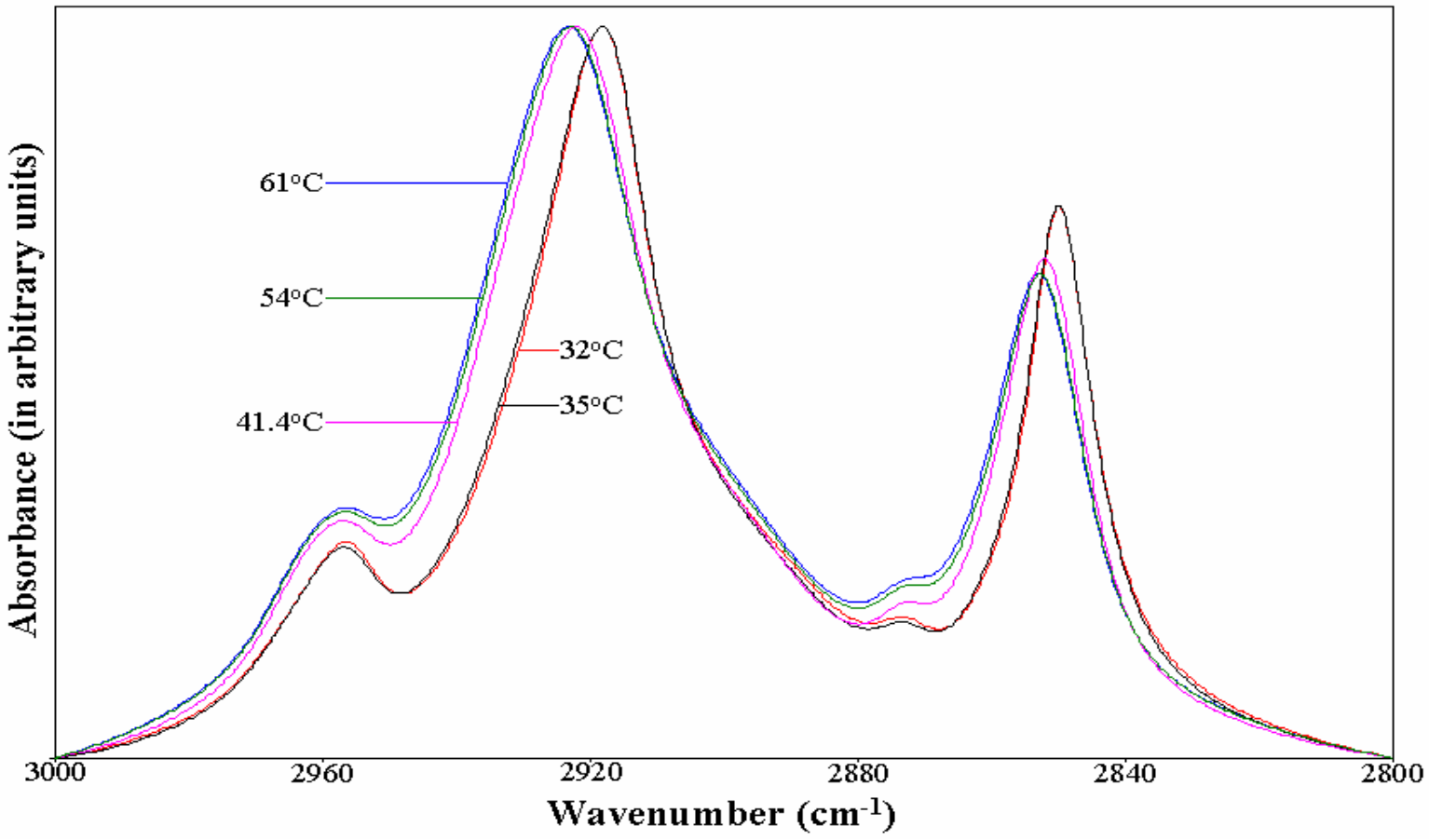

Figure 3.1.1.1 FTIR spectra of pure DPPC multilamellar liposomes in the C-H stretching region at different temperatures. The spectra were normalized with respect to the CH_2 antisymmetric stretching band located at 2920 cm^{-1}.

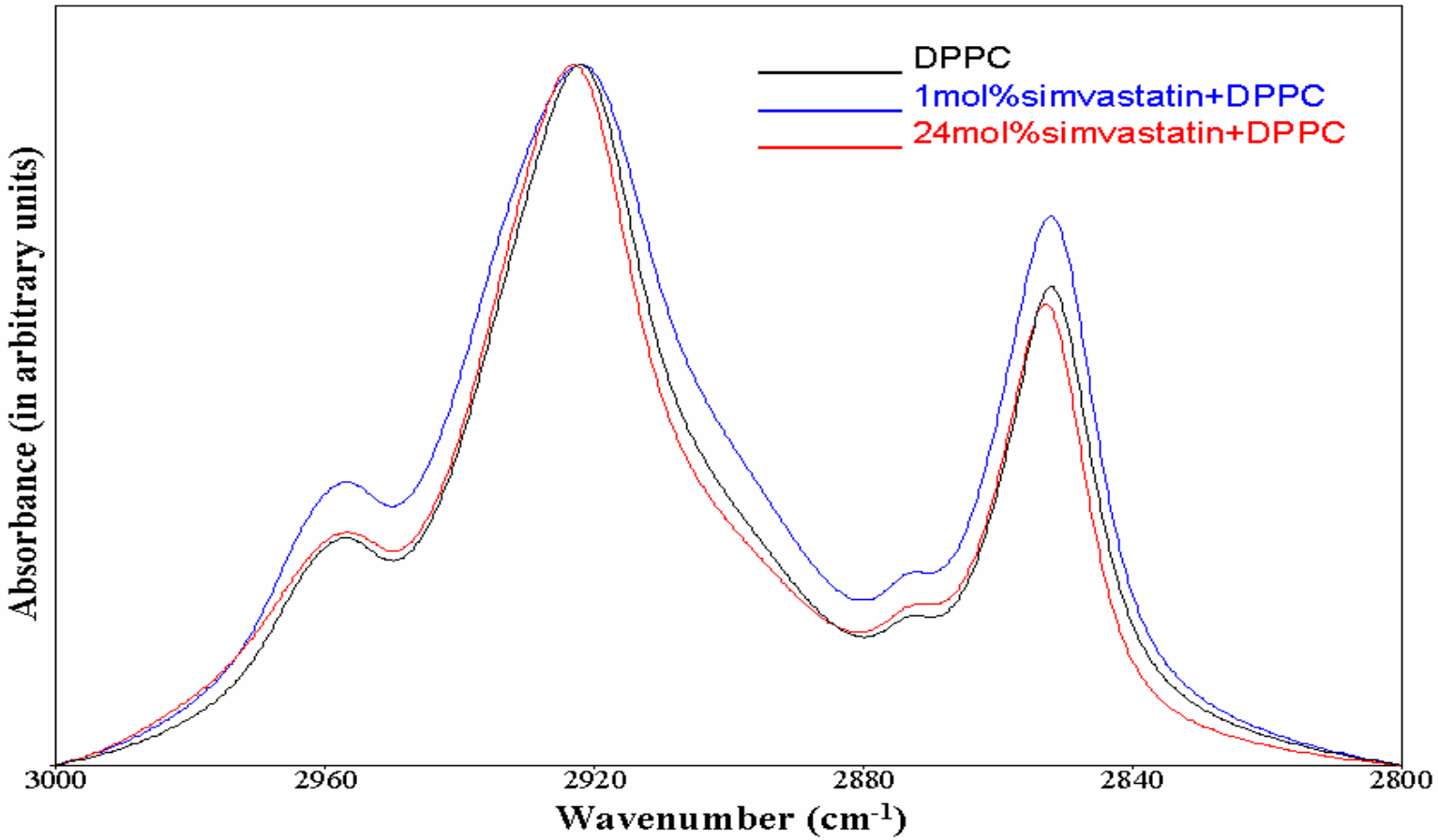

Figure 3.1.1.2 FTIR spectra of DPPC liposomes in the presence and absence of low and high simvastatin concentrations in the C-H stretching region at 41.4°C. The spectra were normalized with respect to the CH_2 antisymmetric stretching band located at 2920 cm^{-1}.

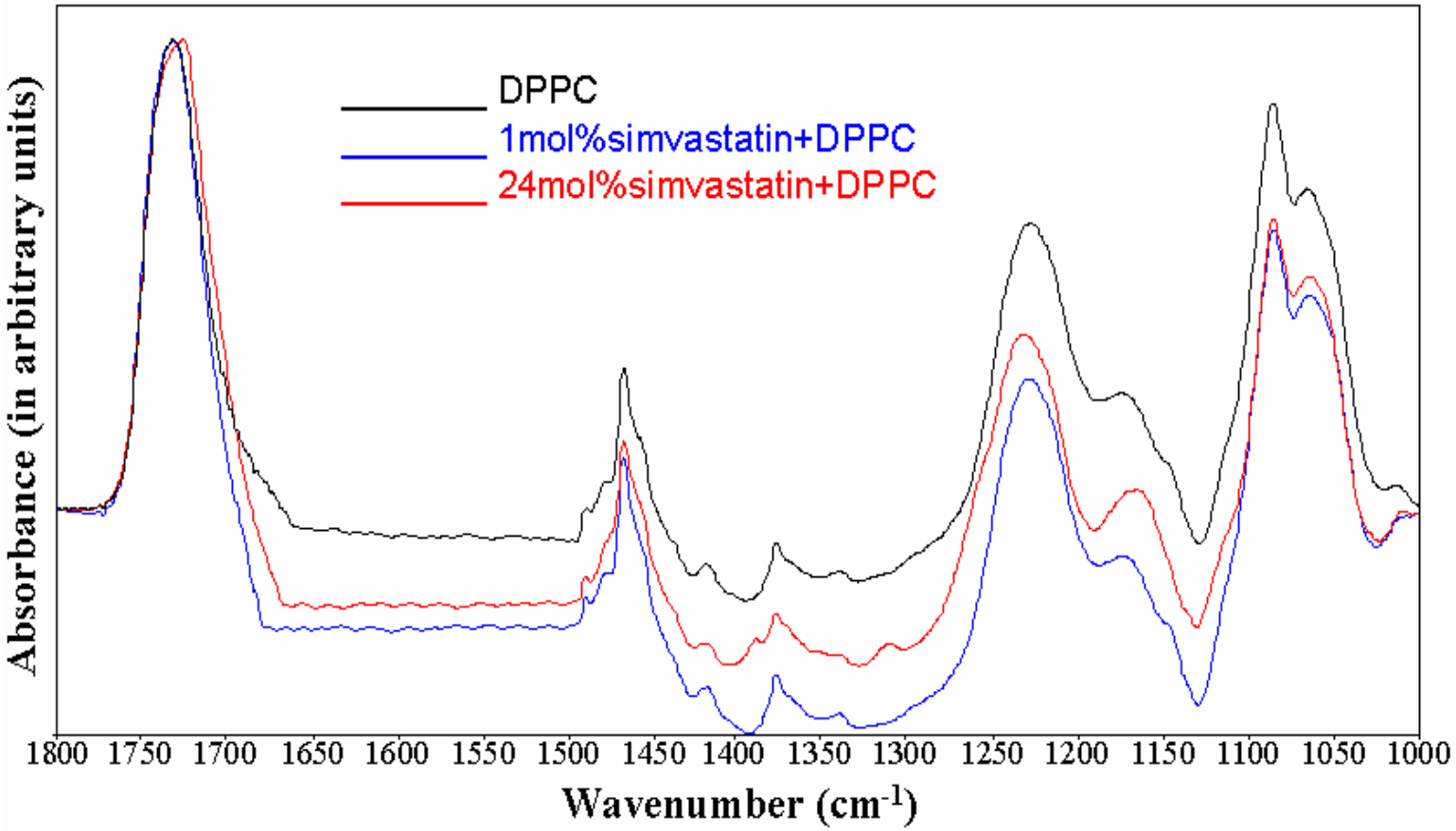

Figure 3.1.1.3 FTIR spectra of DPPC liposomes in the presence and absence of low and high simvastatin concentrations in the 1800-1000 cm^{-1} region at 45.1°C. The spectra were normalized with respect to the C=O stretching band located at 1735 cm^{-1}.

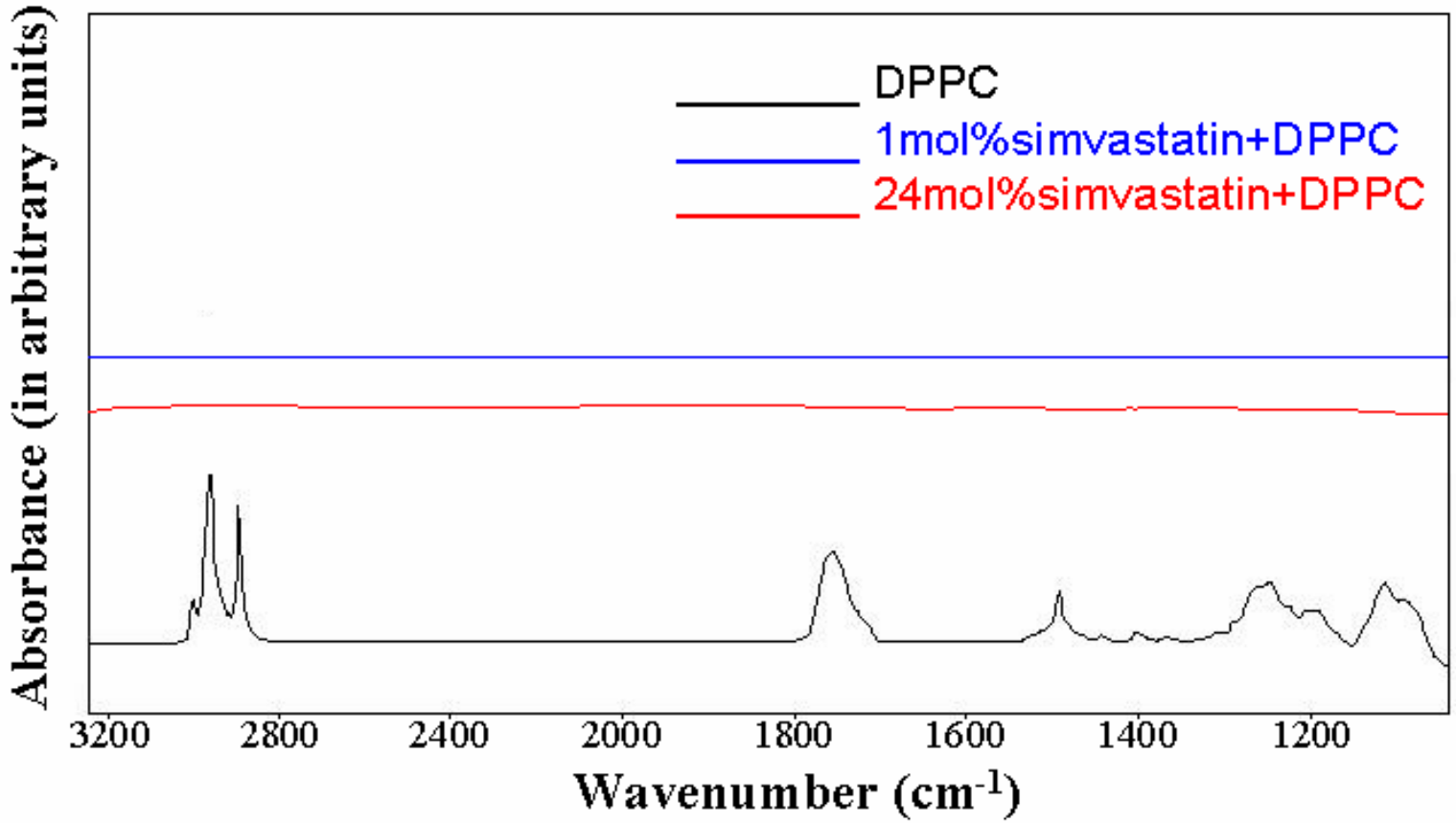

Figure 3.1.1.4 FTIR spectra of pure DPPC liposomes and simvastatin at low and high concentrations corresponding to 1 and 24 mol% in solution at room temperature.

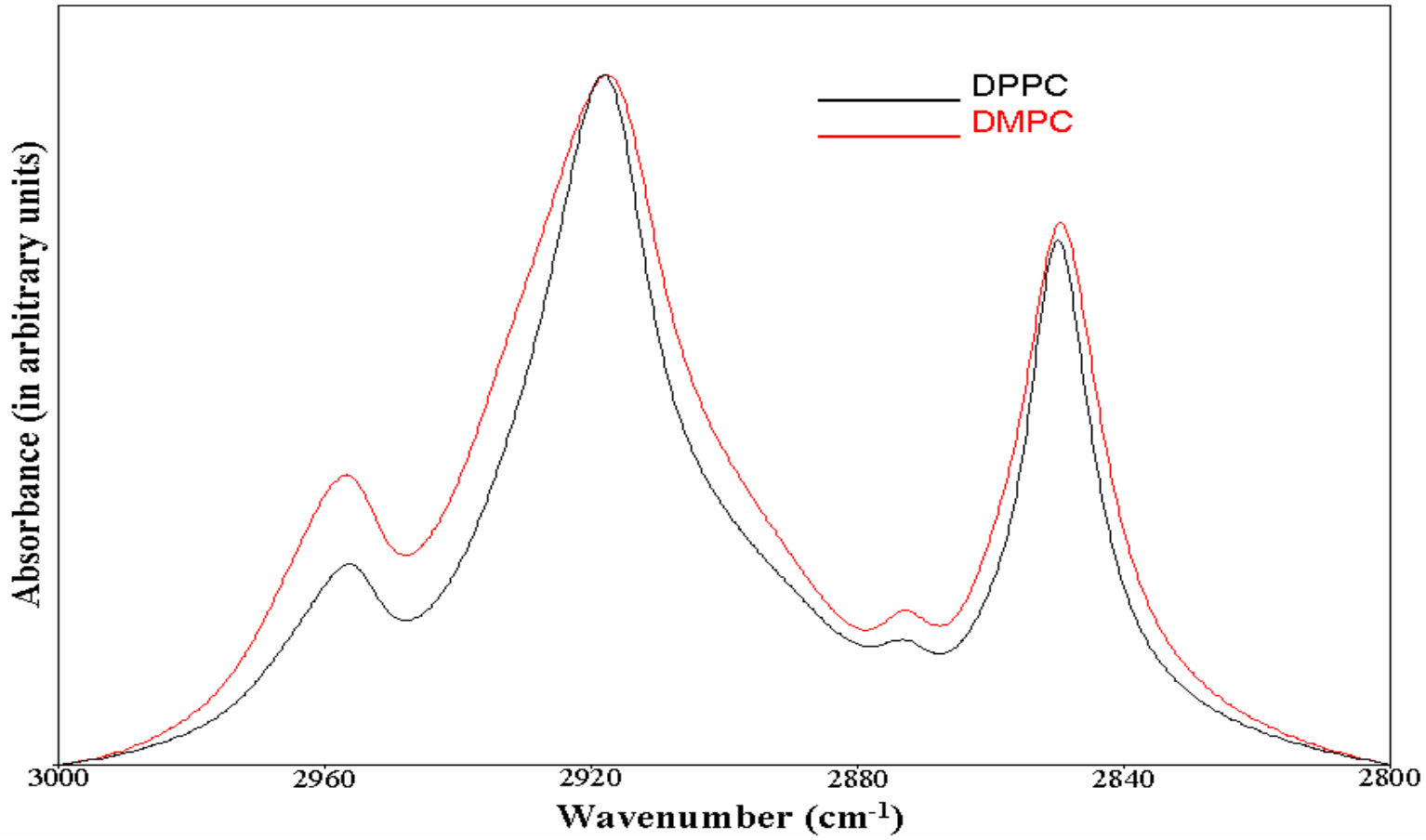

Figure 3.1.1.5 FTIR spectra of the pure DPPC and DMPC liposomes in their gel phases in the 3000-2800 cm^{-1} region. The spectra were normalized with respect to the CH_2 antisymmetric stretching band located at 2920 cm^{-1}.

Order-disorder state of the system and phase transition behaviour were studied by the analysis of C-H stretching mode as reported by Severcan (1997) and Toyran and Severcan (2003). Ordering state of the system is reflected in the spectrum as a decrease in the frequency of the C-H stretching mode. Figure 3.1.1.6 shows temperature dependence of the frequency of the CH_2 symmetric stretching mode of DPPC multilamellar liposomes in the presence and absence of different simvastatin concentrations. The frequency values were measured at centre of 80% of the height of the bandwidth of the peaks. As it can be seen in the figure, as simvastatin concentration increased the phase transition curve was broaden. The main phase transition temperature (T_m) of pure DPPC liposomes was around 41^oC and the pretransition temperature was around 35^oC. T_m value was shifted to lower values as simvastatin concentration increased. On the other hand, the pretransition temperature was completely eliminated by the addition of simvastatin. The same results were obtained for the CH_2 antisymmetric stretching mode which is shown in Figure 3.1.1.7. Furthermore, in both figures it was observed that simvastatin increased the frequency of oscillation, implying a decrease in the order of the system both in the gel and liquid crystalline phases. The degree of disordering effect increased by increasing the simvastatin concentration. Disordering effect of simvastatin in the gel phase was more profound than in the liquid crystalline phase.

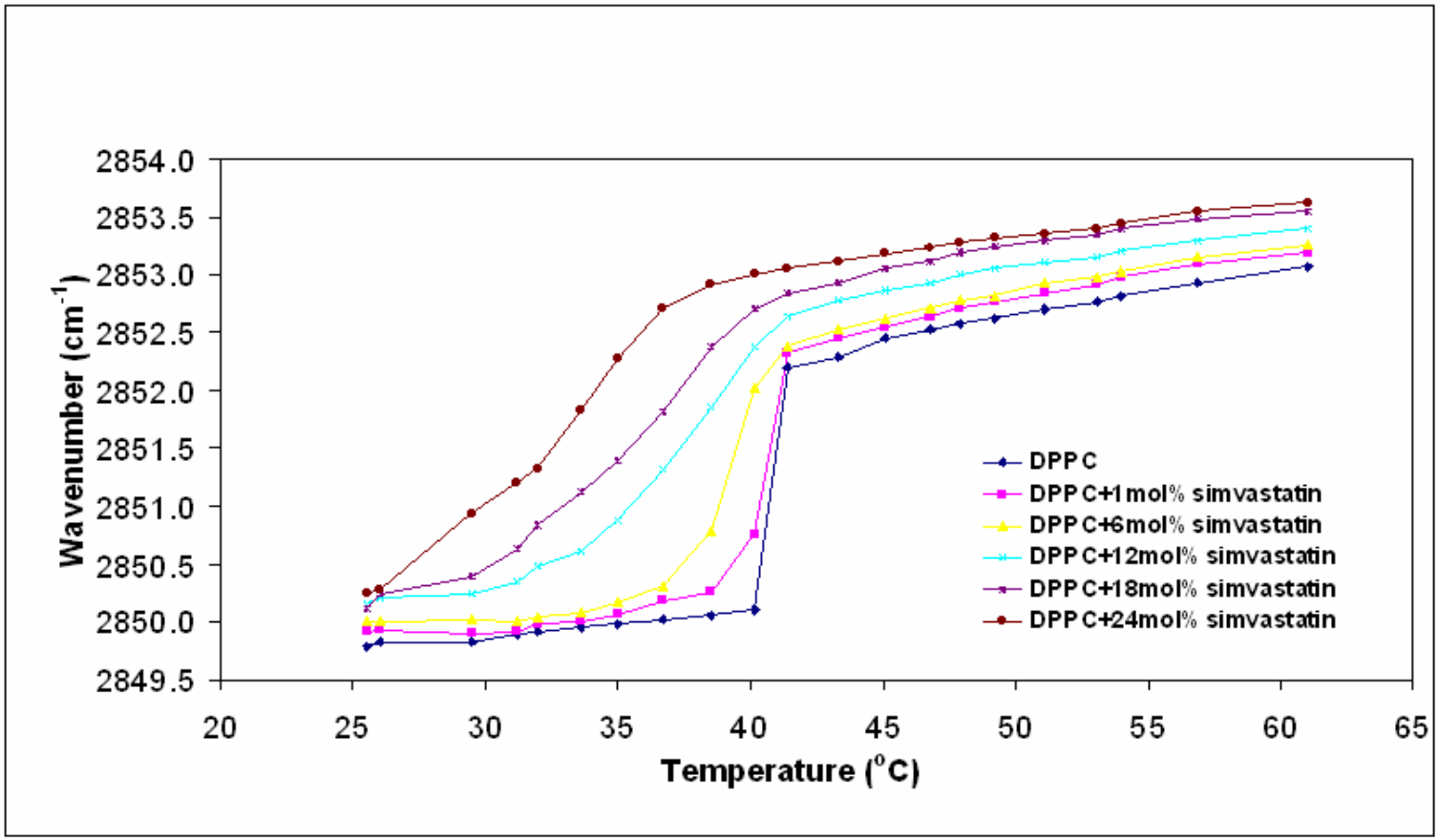

Figure 3.1.1.6 Temperature dependence of the frequency of the CH_2 symmetric stretching mode in the presence and absence of different simvastatin concentrations for DPPC liposomes.

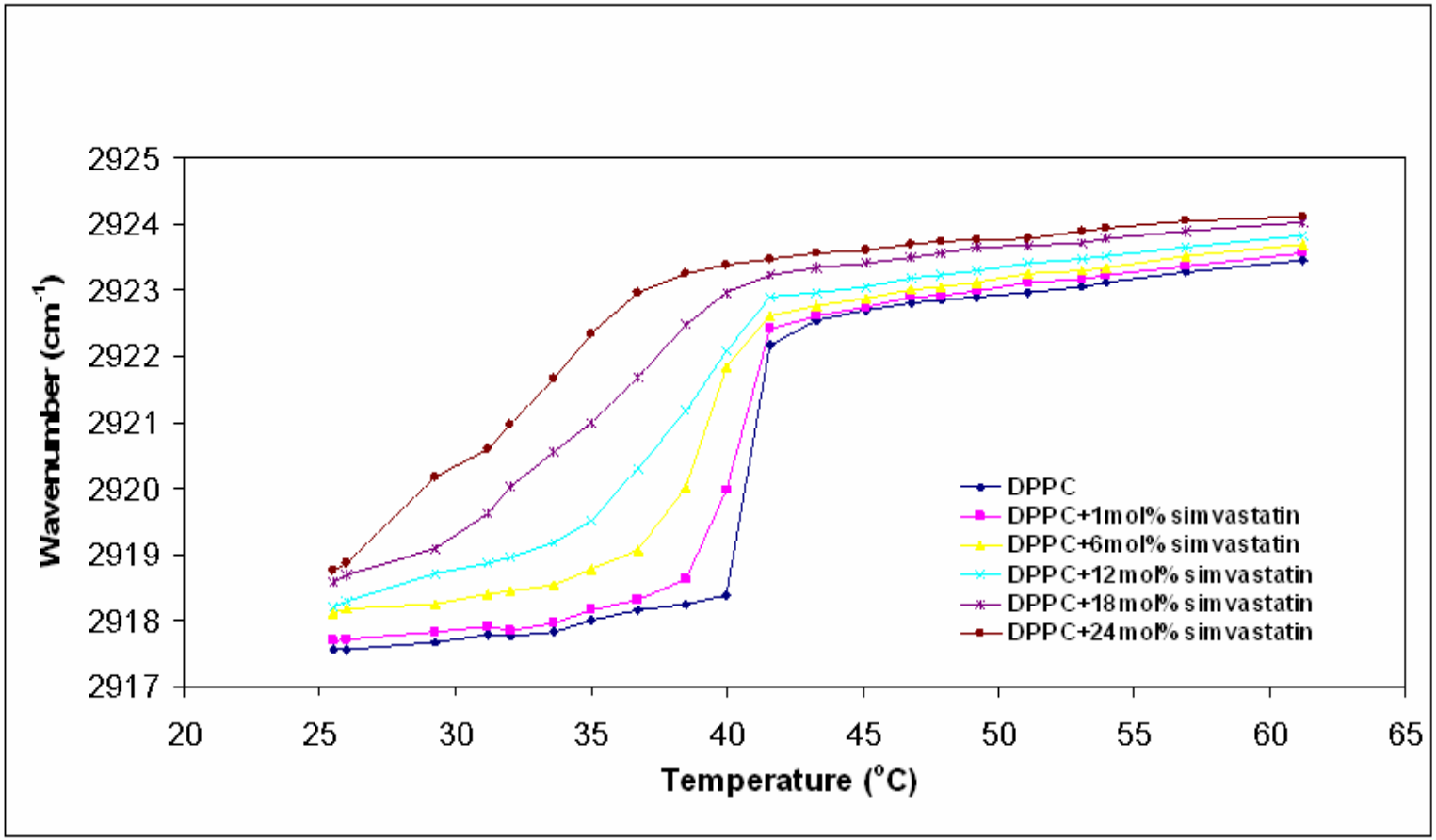

Figure 3.1.1.7 Temperature dependence of the frequency of the CH_2 antisymmetric stretching mode in the presence and absence of different simvastatin concentrations for DPPC liposomes.

Temperature dependence of the bandwidth of the CH_2 symmetric and antisymmetric stretching modes in the presence and absence of different simvastatin concentrations for DPPC liposomes were shown in Fig. 3.1.1.8 and Fig. 3.1.1.9, respectively. The widths were measured at 75% of height of the peaks. Bandwidth analysis gives information about the dynamics of the system. Bilayer permeability properties are related to the fluidity. And fluidity at a certain degree is required for normal and optimal activity of membrane associated proteins. The increment in bandwidth value is the indication of an increment in lipid dynamics (Yi and MacDonald, 1973; Toyran and Severcan, 2003). As it can be seen in both figures, dynamics of the system decreased as the simvastatin concentration increased. In other words, as the simvastatin concentration increased lipid fluidity decreased. Moreover, the degree of stabilizing effect directly proportional to the degree of simvastatin concentration. Furthermore, the broadening of the main phase transition profile were observed from the figures.

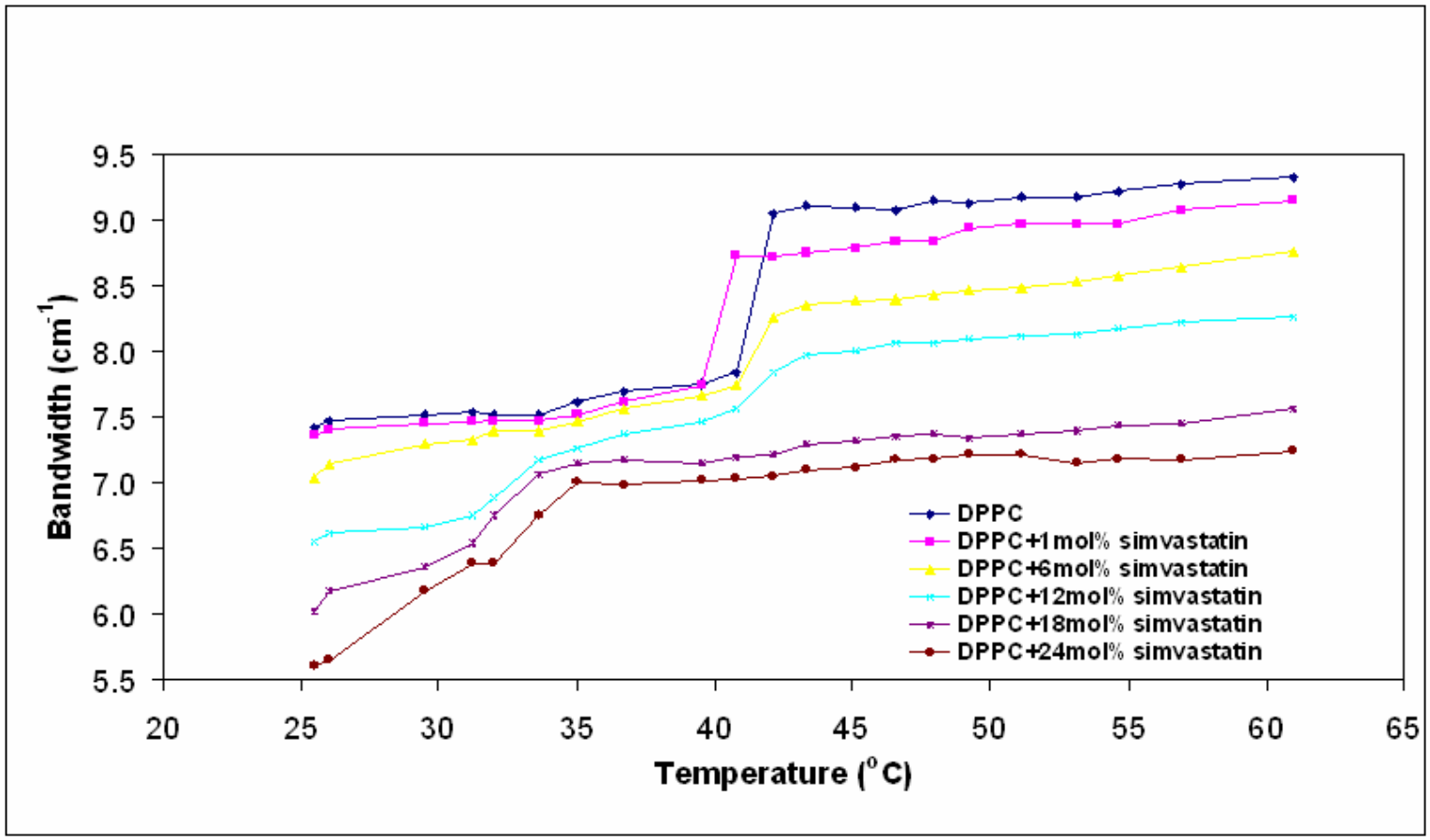

Figure 3.1.1.8 Temperature dependence of the bandwidth of the CH_2 symmetric stretching mode in the presence and absence of different simvastatin concentrations for DPPC liposomes.

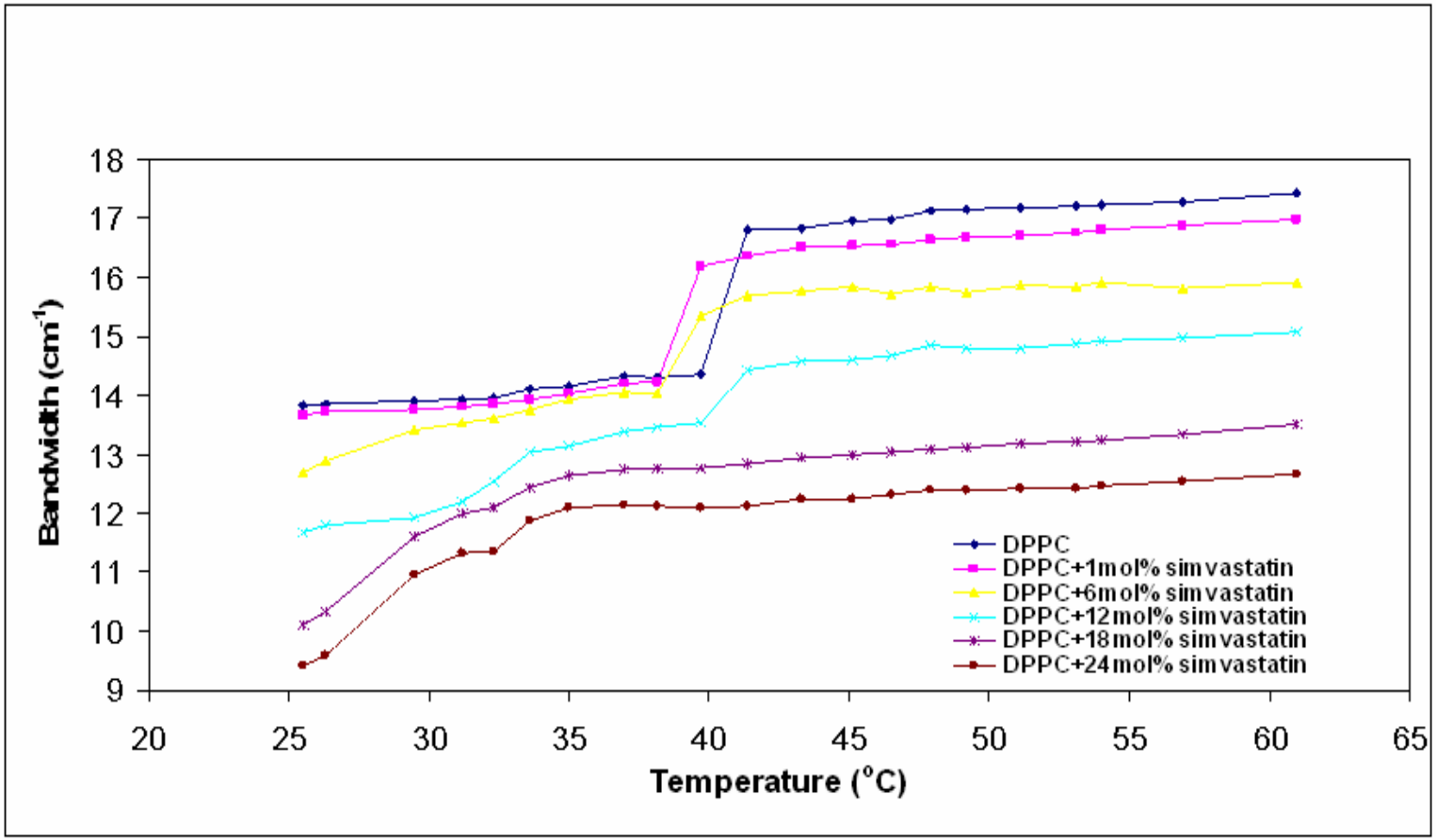

Figure 3.1.1.9 Temperature dependence of the bandwidth of the CH_2 antisymmetric stretching mode in the presence and absence of different simvastatin concentrations for DPPC liposomes.

In order to examine the interaction of simvastatin with glycerol backbone near the head group of phospholipids in interfacial region, the C=O stretching band frequency was analysed. Temperature dependence of the frequency of the C=O stretching mode in the presence and absence of different simvastatin concentrations for DPPC liposomes was shown in Figure 3.1.1.10. A decrease in the frequency of oscillation indicates strengthening of the existing hydrogen bonds of the glycerol skeleton closer to the head groups or the formation of new hydrogen bonds (Frengeli and Günthard, 1976). As it can be seen in the figure, the frequency of oscillation shifted to lower values as simvastatin concentration increased implying that either simvastatin strengths the existing hydrogen bonds of the glycerol skeleton closer to the head groups or new hydrogen bonds were formed. Formation of new hydrogen bonds occured between hydroxyl groups of simvastatin and either carbonyl groups of lipids or water molecules around.

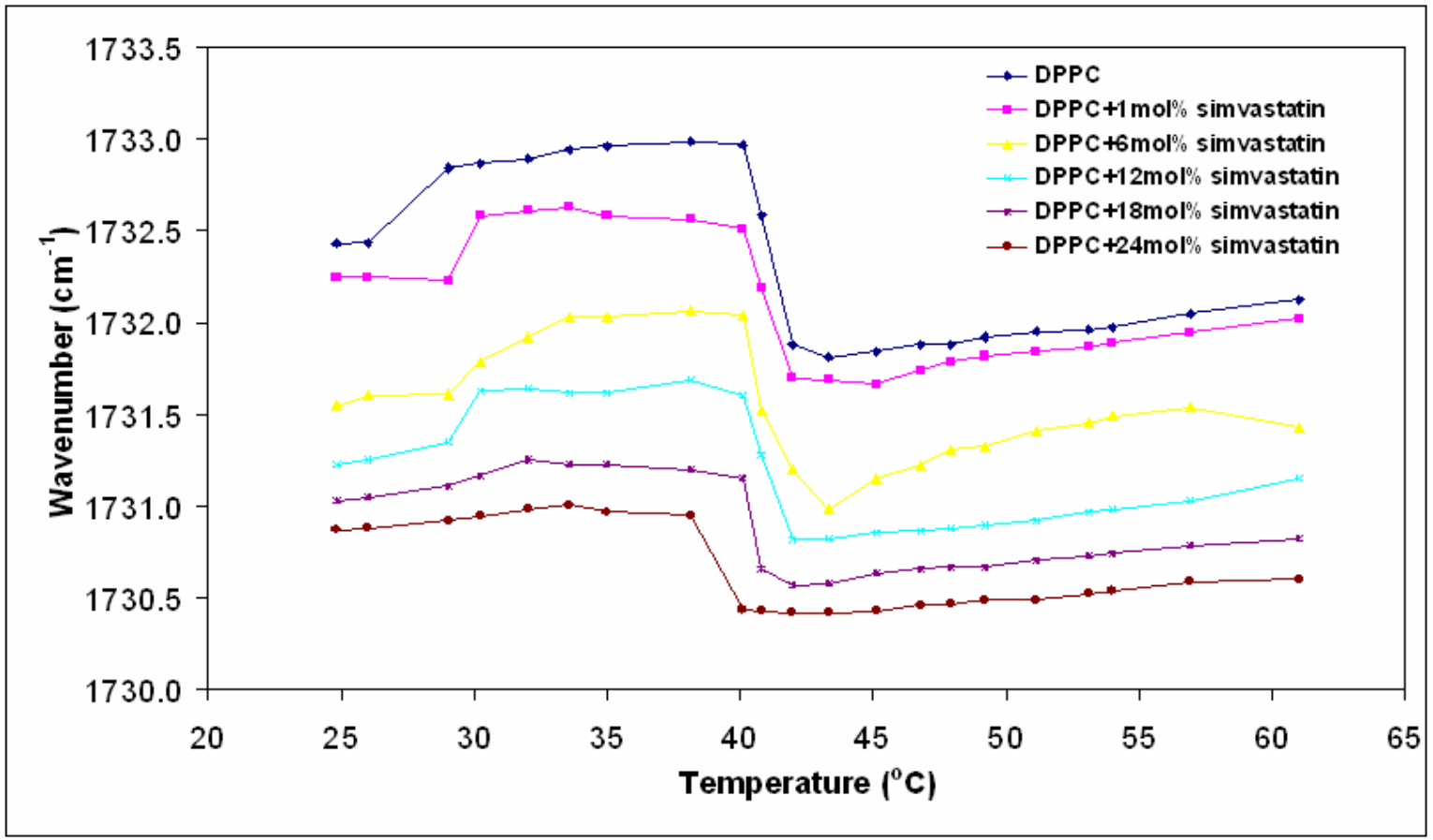

Figure 3.1.1.10 Temperature dependence of the frequency of the C=O stretching mode in the presence and absence of different simvastatin concentrations for DPPC liposomes.

The interaction between simvastatin and head group of DPPC multilamellar liposomes was monitored by analysing the PO_2^- antisymmetric double stretching band. Figure 3.1.1.11 shows the temperature dependence of the frequency of the PO_2^- antisymmetric stretching mode in the presence and absence of different simvastatin concentrations for DPPC liposomes. As it can be seen in the figure, the frequency of oscillation shifted to higher values as simvastatin concentration increased. In the figure it is clear that increasing simvastatin concentration caused an increase in the wavenumber of the PO_2^- antisymmetric double stretching band implying a dehydration around these functional groups in the polar part of the lipids (Toyran and Severcan, 2003). This dehydration effect in the gel phase was more profound than in the liquid crystalline phase for 1mol%, 6mol%, and 12mol% of simvastatin concentrations.

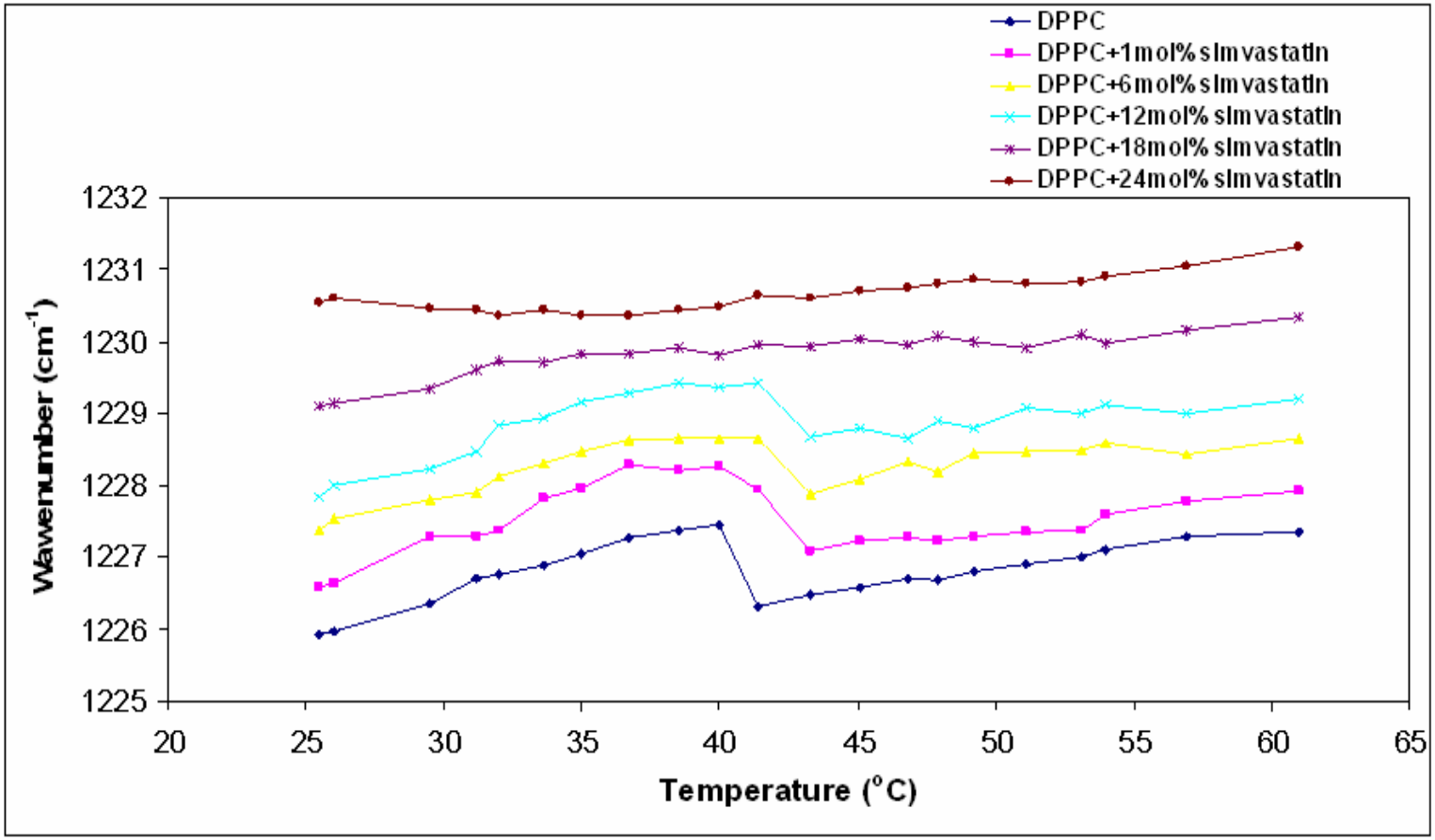

Figure 3.1.1.11 Temperature dependence of the frequency of the PO_2^- antisymmetric double stretching mode in the presence and absence of different simvastatin concentrations for DPPC liposomes.

3.1.2 FTIR Studies to Monitor the Acyl Chain Length Effect Between DMPC and DPPC Lipids

In this part, FTIR studies were carried out to monitor the effect of acyl chain length on the simvastatin-membrane interactions by using two different lipids with different chain length. These lipids are DMPC and DPPC which have molecular formulas of $C_{36}H_{72}NO_8P$ and $C_{40}H_{80}NO_8P$, respectively. There are two CH_2 difference between them. Again the same absorption bands and parameters were used for the analyses of FTIR spectra of DMPC or DPPC liposomes. For each lipid FTIR spectroscopy were performed at two different temperatures which monitors the gel and the liquid crystalline phase of the lipid membranes. For DMPC liposomes these temperatures are 10^{o}C and 35^{o}C, and for DPPC liposomes they are 29.5^{o}C and 54^{o}C, respectively. Every experiment at each temperature was repeated 5 times and results were averaged. Later, Mann-Whitney U test was applied to measured frequency and bandwidth values. Final results which are statistically significant were shown by an asterisk on the graphs.

Order-disorder state of the membranes was monitored by analysing the frequency values of the CH_2 symmetric and antisymmetric stretching bands in the presence and absence of different simvastatin concentrations (Severcan, 1997; Toyran and Severcan, 2003). Figures 3.1.2.1 and 3.1.2.2 show simvastatin dependence of the frequency of the CH_2 symmetric stretching modes of DMPC and DPPC liposomes respectively in their gel phase. As it can be seen in both figures, the frequency values of the samples increased as the simvastatin concentration increased, implying a decrease in the orders of DMPC and DPPC lipids in the gel phase. The same results were also observed for the CH_2 antisymmetric stretching bands. Figures 3.1.2.3 and 3.1.2.4 show simvastatin dependence of the frequency of the CH_2 antisymmetric stretching modes of DMPC and DPPC liposomes respectively in their gel phase which

have similar trend. As these results revealed that acyl chain length difference between DMPC and DPPC lipids has no effect on the order-disorder state of the model membranes in this study.

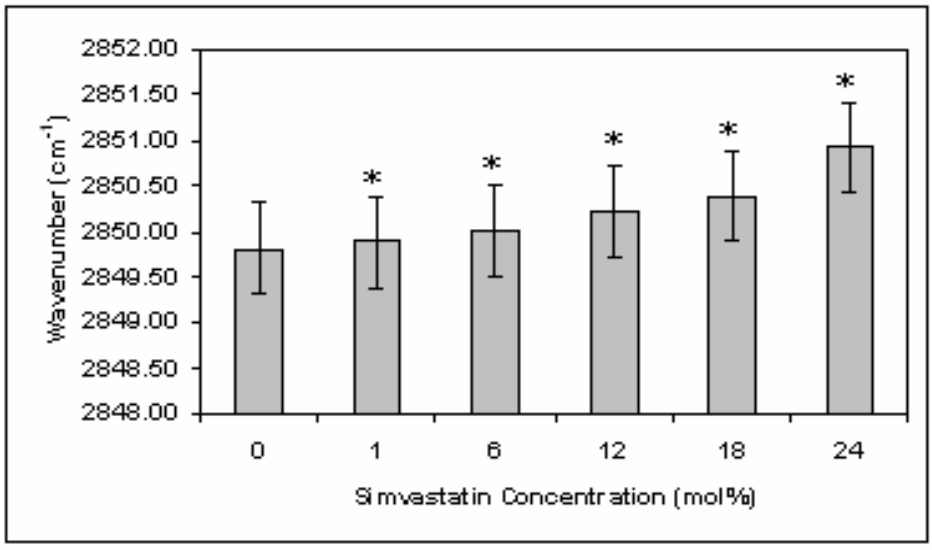

Figure 3.1.2.1 Simvastatin concentration dependence of the frequency of the CH_2 symmetric stretching mode for DMPC liposomes at 10°C. (*) P < 0.05.

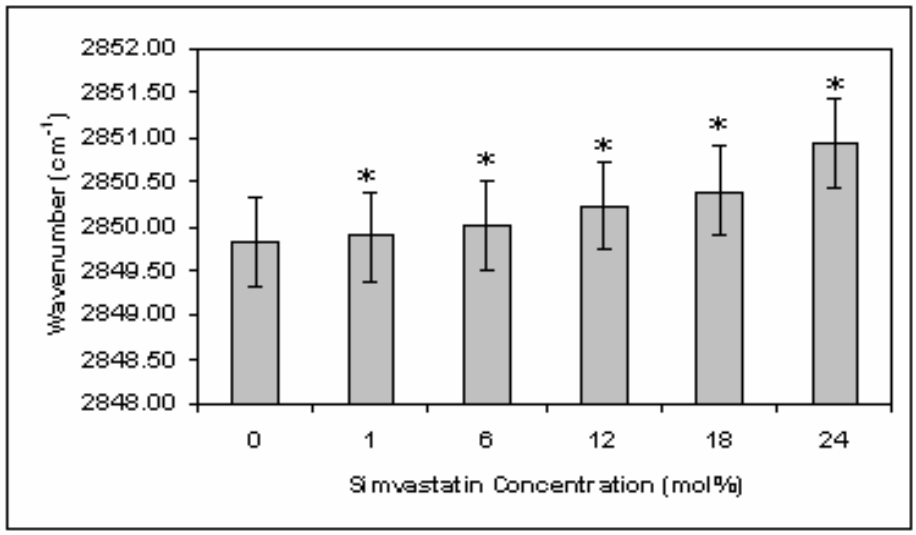

Figure 3.1.2.2 Simvastatin concentration dependence of the frequency of the CH_2 symmetric stretching mode for DPPC liposomes at 29.5°C. (*) P < 0.05.

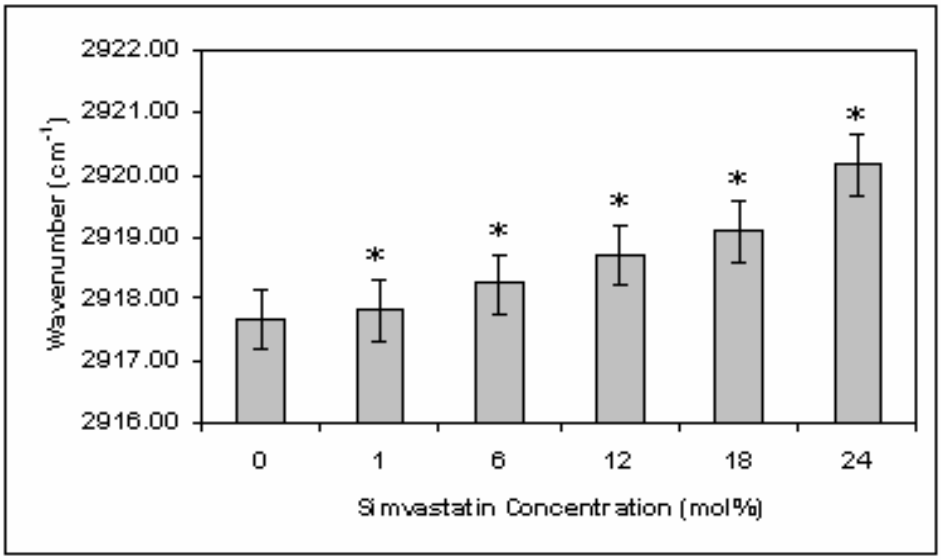

Figure 3.1.2.3 Simvastatin concentration dependence of the frequency of the CH_2 antisymmetric stretching mode for DMPC liposomes at 10°C. (*) P < 0.05.

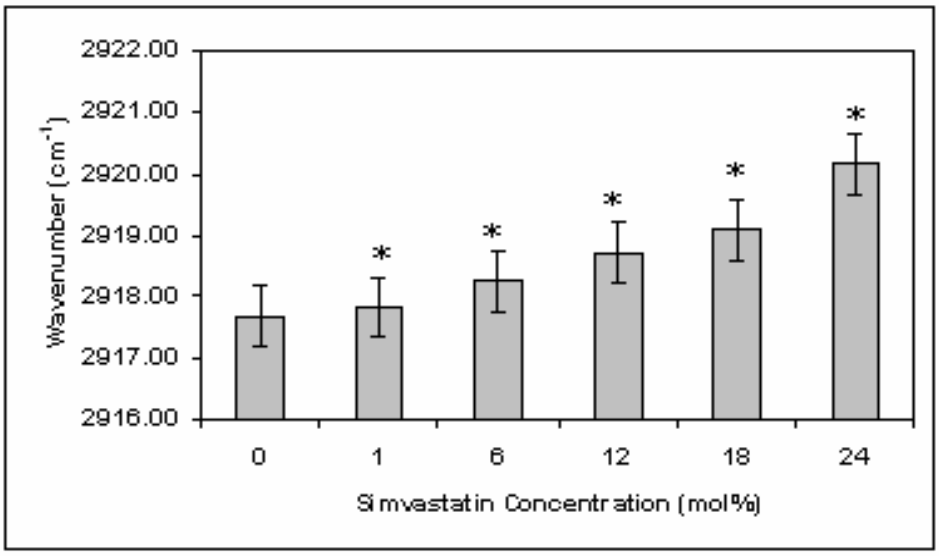

Figure 3.1.2.4 Simvastatin concentration dependence of the frequency of the CH_2 antisymmetric stretching mode for DPPC liposomes at 29.5°C. (*) P < 0.05.

Figures 3.1.2.5 and 3.1.2.6 show simvastatin dependence of the frequency of the CH_2 symmetric stretching modes of DMPC and DPPC liposomes respectively in their liquid crystalline phase. As it can be seen in both figures, the frequency values of the samples increased implying that orders of DMPC and DPPC lipids in the liquid crystalline phase decreased as the simvastatin concentration in the liposomes increased. The same results were also observed for the CH_2 antisymmetric stretching bands. Figures 3.1.2.7 and 3.1.2.8 show simvastatin dependence of the frequency of the CH_2 antisymmetric stretching modes of DMPC and DPPC liposomes respectively in their liquid crystalline phase. These figures were in the same trend for both DMPC and DPPC liposomes implying that acyl chain length difference between DMPC and DPPC lipids has no effect on the order-disorder state of the model membranes in this study.

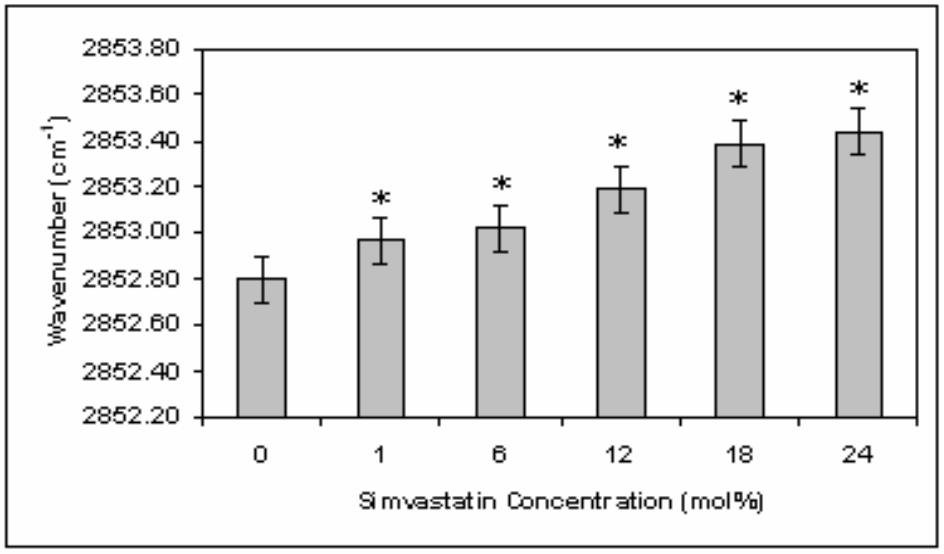

Figure 3.1.2.5 Simvastatin concentration dependence of the frequency of the CH_2 symmetric stretching mode for DMPC liposomes at 35°C. (*) P < 0.05.

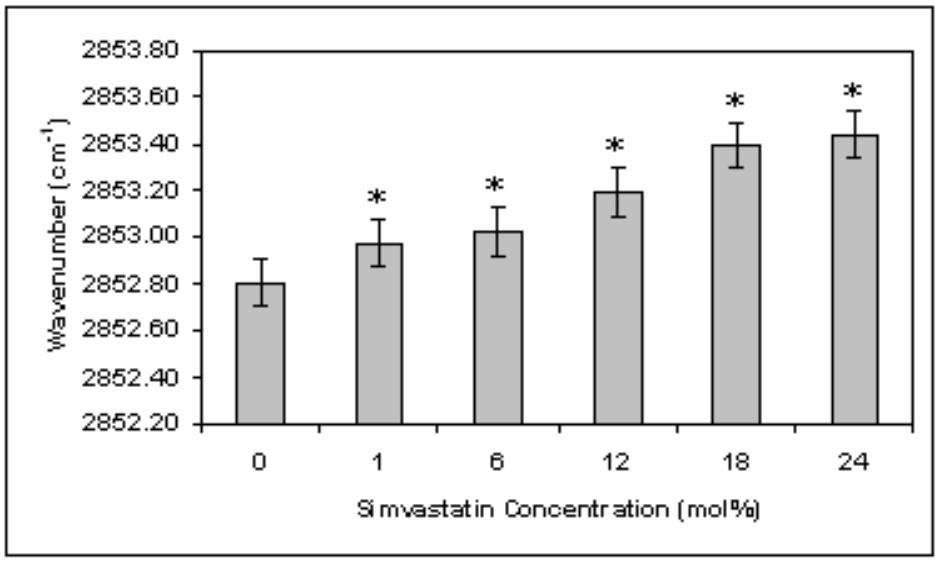

Figure 3.1.2.6 Simvastatin concentration dependence of the frequency of the CH_2 symmetric stretching mode for DPPC liposomes at 54°C. (*) P < 0.05.

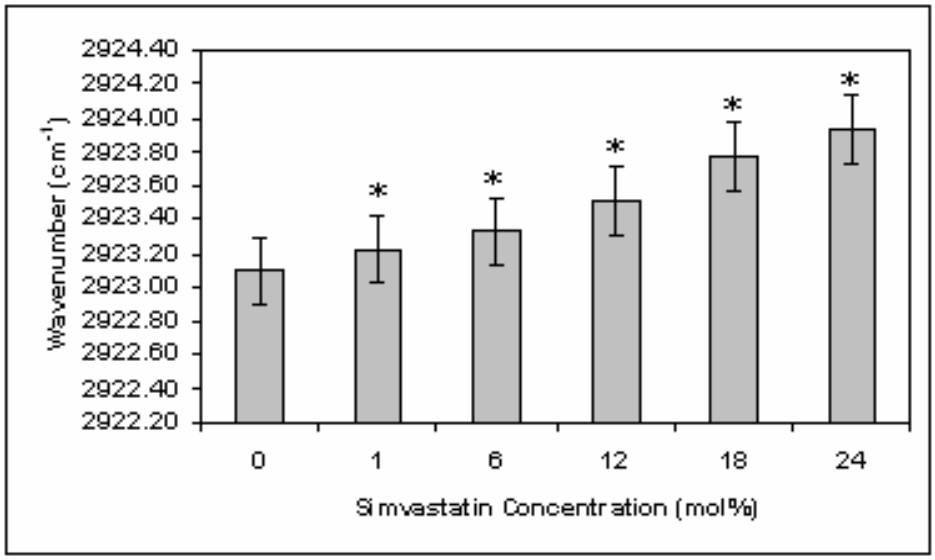

Figure 3.1.2.7 Simvastatin concentration dependence of the frequency of the CH_2 antisymmetric stretching mode for DMPC liposomes at 35°C. (*) P < 0.05.

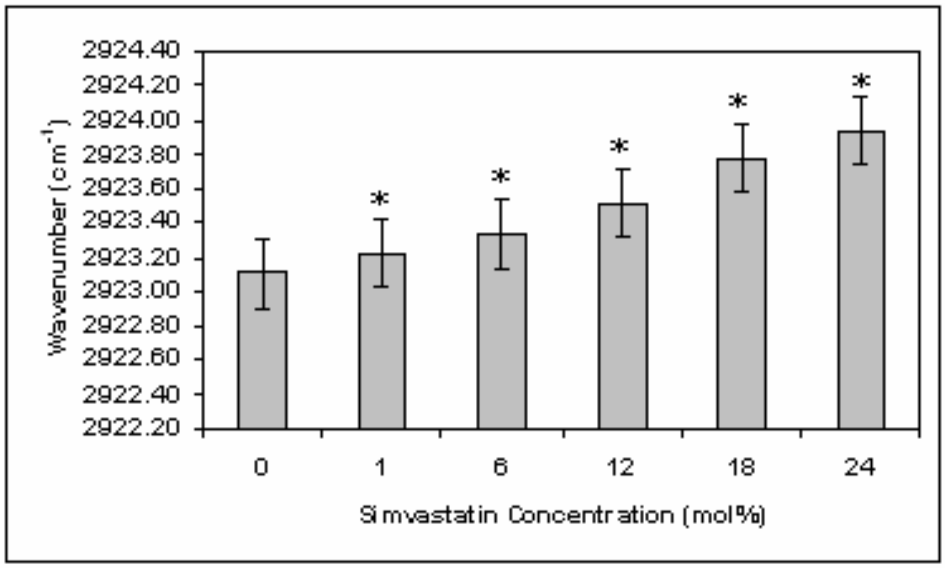

Figure 3.1.2.8 Simvastatin concentration dependence of the frequency of the CH_2 antisymmetric stretching mode for DPPC liposomes at 54°C. (*) P < 0.05.

Lipid dynamics or membrane fluidity of the DMPC or DPPC liposomes was monitored by analysing the bandwidth values of the CH_2 symmetric and antisymmetric stretching bands in the presence and absence of different simvastatin concentrations (Yi and MacDonald, 1973; Toyran and Severcan, 2003). Figures 3.1.2.9 and 3.1.2.10 show simvastatin dependence of the bandwidth of the CH_2 symmetric stretching modes of DMPC and DPPC liposomes respectively in their gel phase. As it can be seen in both figures, the bandwidth values of the samples decreased as the simvastatin concentration increased. The results imply that the dynamics of DMPC and DPPC liposomes decreased as the simvastatin concentration in the liposomes increased. The same results were also observed for the CH_2 antisymmetric stretching bands as seen from the figures 3.1.2.11 and 3.1.2.12 which show simvastatin dependence of the bandwidth of the CH_2 antisymmetric stretching modes of DMPC and DPPC liposomes respectively in their gel phase. As it can be seen from these figures, acyl chain length difference between DMPC and DPPC lipids has no effect on the lipid dynamics of the model membranes in this study.

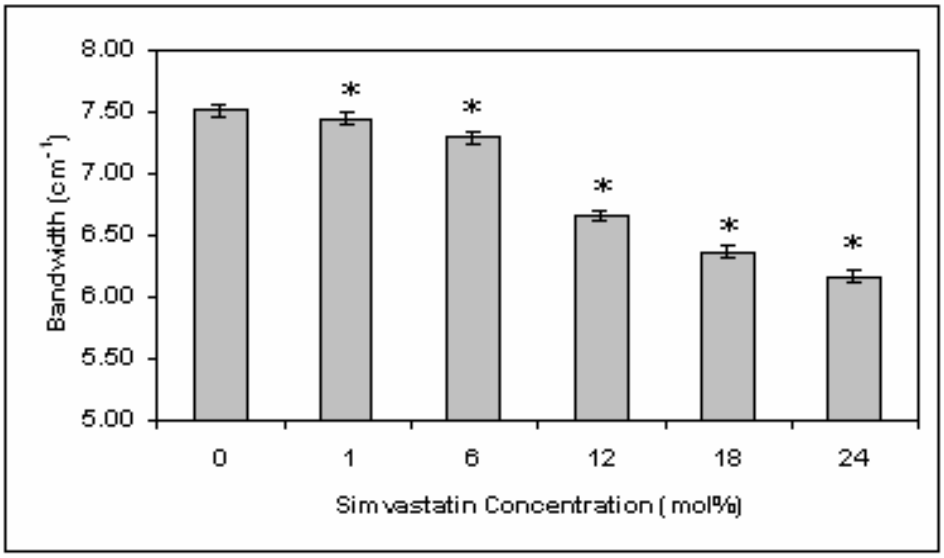

Figure 3.1.2.9 Simvastatin concentration dependence of the bandwidth of the CH_2 symmetric stretching mode for DMPC liposomes at 10°C. (*) P < 0.05.

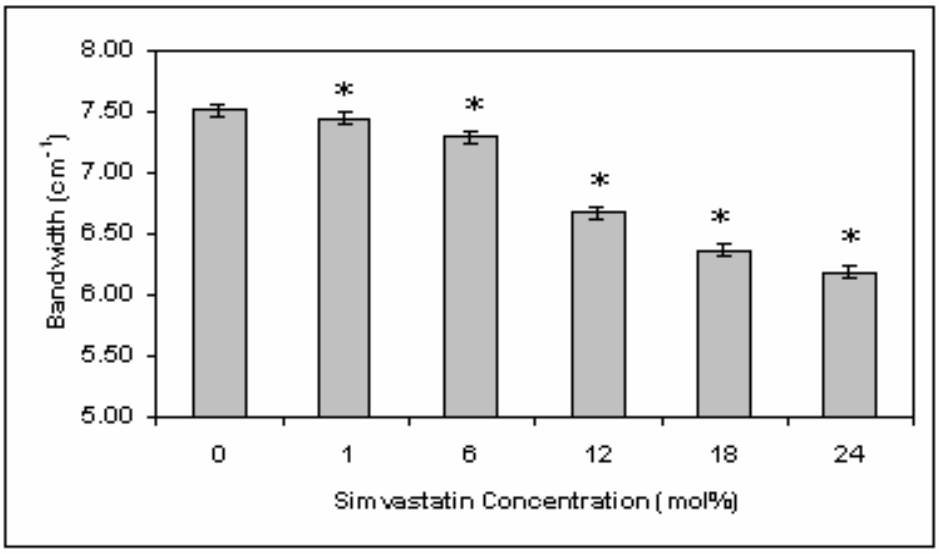

Figure 3.1.2.10 Simvastatin concentration dependence of the bandwidth of the CH_2 symmetric stretching mode for DPPC liposomes at 29.5°C. (*) P < 0.05.

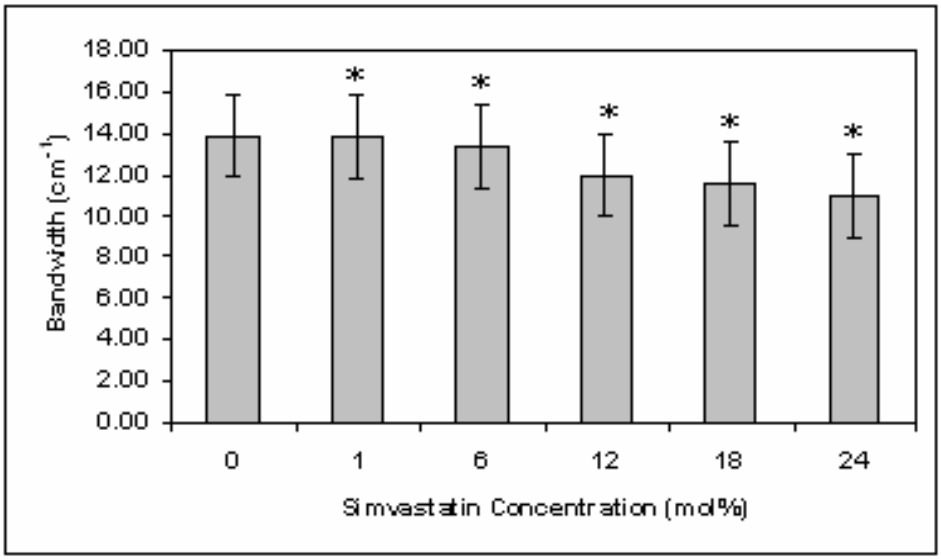

Figure 3.1.2.11 Simvastatin concentration dependence of the bandwidth of the CH_2 antisymmetric stretching mode for DMPC liposomes at 10°C. (*) P < 0.05.

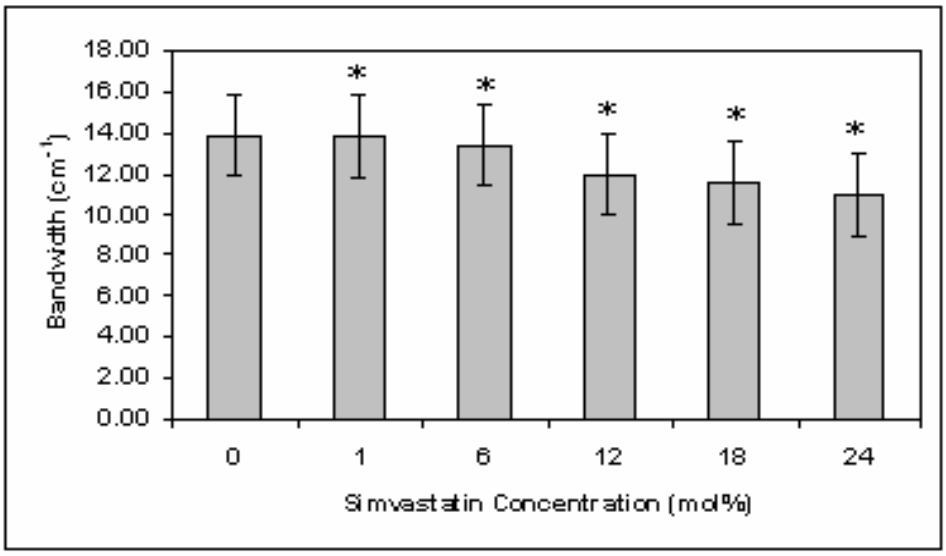

Figure 3.1.2.12 Simvastatin concentration dependence of the bandwidth of the CH_2 antisymmetric stretching mode for DPPC liposomes at 29.5°C. (*) P < 0.05.

Lipid dynamics or membrane fluidity of the DMPC or DPPC liposomes in the liquid crystalline phase was again monitored by analysing the bandwidth values of the CH_2 symmetric and antisymmetric stretching bands in the presence and absence of different simvastatin concentrations. Figures 3.1.2.13 and 3.1.2.14 show simvastatin dependence of the bandwidth of the CH_2 symmetric stretching modes of DMPC and DPPC liposomes respectively in their liquid crystalline phase. As it can be seen in both figures, the bandwidth values of the samples decreased as the simvastatin concentration increased. Therefore, dynamics of DMPC and DPPC lipids in the liquid crystalline phase decreased as the simvastatin concentration in the liposomes increased. The same results were also observed for the CH_2 antisymmetric stretching bands as depicted in the figures 3.1.2.15 and 3.1.2.16 which show simvastatin dependence of the bandwidth of the CH_2 antisymmetric stretching modes of DMPC and DPPC liposomes respectively in their liquid crystalline phase. The results revealed that acyl chain length difference between DMPC and DPPC lipids has no effect on the lipid dynamics of the model membranes in this study.

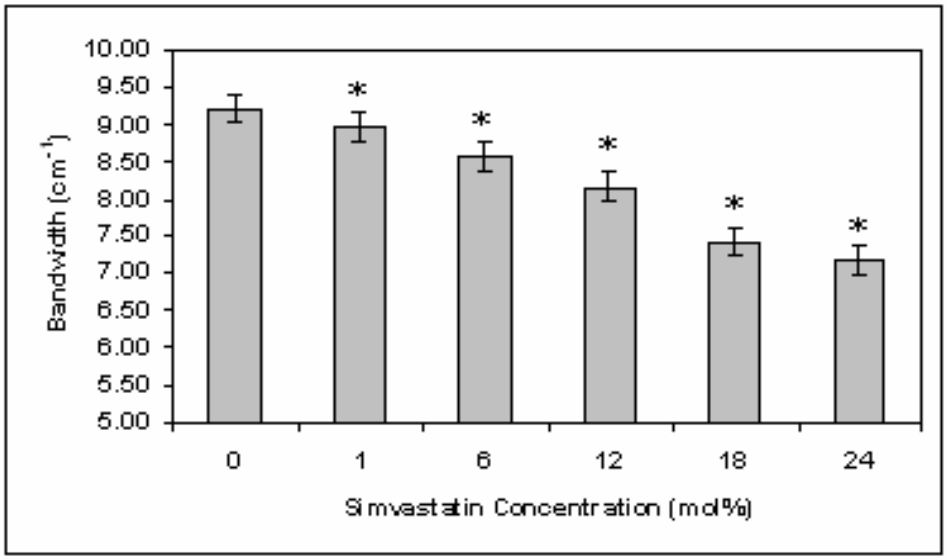

Figure 3.1.2.13 Simvastatin concentration dependence of the bandwidth of the CH_2 symmetric stretching mode for DMPC liposomes at 35°C. (*) P < 0.05.

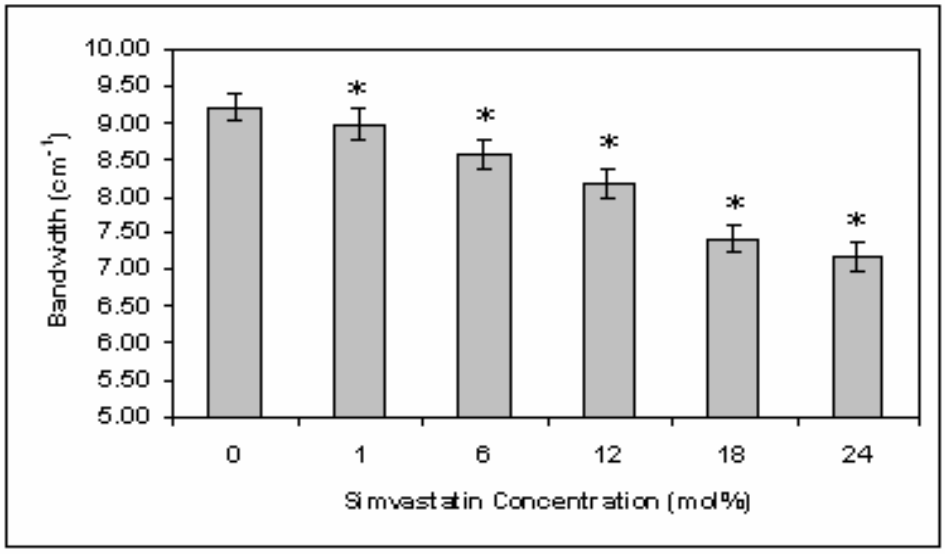

Figure 3.1.2.14 Simvastatin concentration dependence of the bandwidth of the CH_2 symmetric stretching mode for DPPC liposomes at 54°C. (*) P < 0.05.

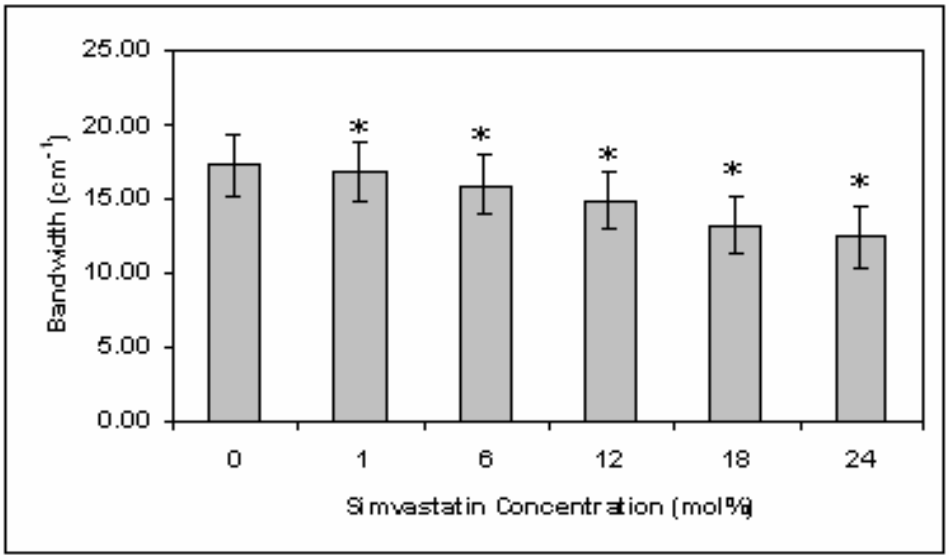

Figure 3.1.2.15 Simvastatin concentration dependence of the bandwidth of the CH_2 antisymmetric stretching mode for DMPC liposomes at 35°C. (*) P < 0.05.

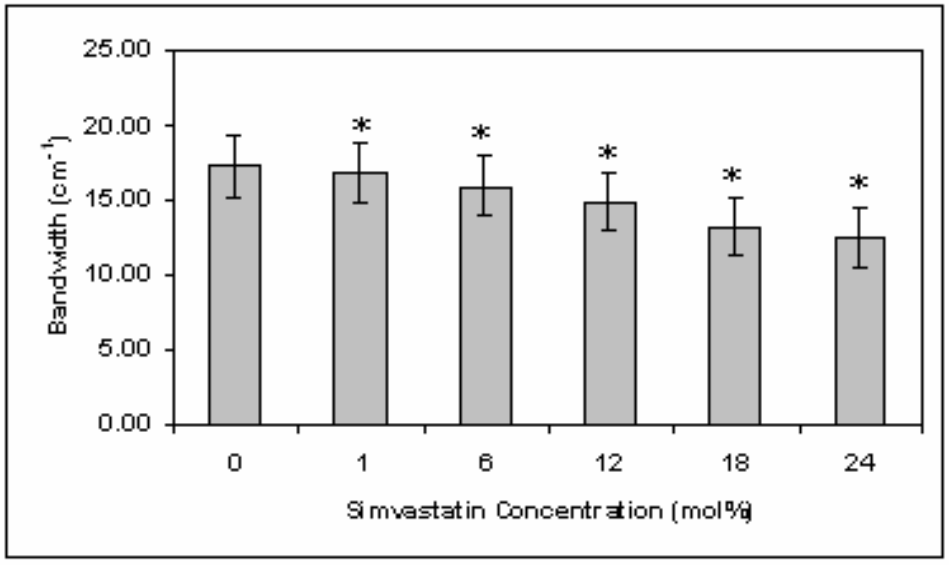

Figure 3.1.2.16 Simvastatin concentration dependence of the bandwidth of the CH_2 antisymmetric stretching mode for DPPC liposomes at 54°C. (*) P < 0.05.

The C=O stretching band frequency was analysed to examine the interaction of simvastatin with glycerol backbone near the head group of phospholipids in interfacial region in the presence and absence of different simvastatin concentrations. Figures 3.1.2.17 and 3.1.2.18 show simvastatin dependence of the frequency of the C=O stretching modes of DMPC and DPPC liposomes respectively in their gel phase. As it can be seen in both figures, the frequency values of the samples decreased as the simvastatin concentration increased. A decrease in the frequency of oscillation indicates strengthening of the existing hydrogen bonds of the glycerol skeleton closer to the head groups or the formation of new hydrogen bonds (Frengeli and Günthard, 1976). Therefore, simvastatin either strengths the existing hydrogen bonds of the glycerol skeleton closer to the head groups or causes new hydrogen bonding. Formation of new hydrogen bonds occur between hydroxyl groups of simvastatin and either carbonyl groups of lipids or water molecules around. Similar trend was obtained for DMPC and DPPC. Therefore, we can say that acyl chain length difference between DMPC and DPPC lipids has no effect on the hydrogen bonding at glycerol backbone near the head group of phospholipids in interfacial region in the gel phase in this study.

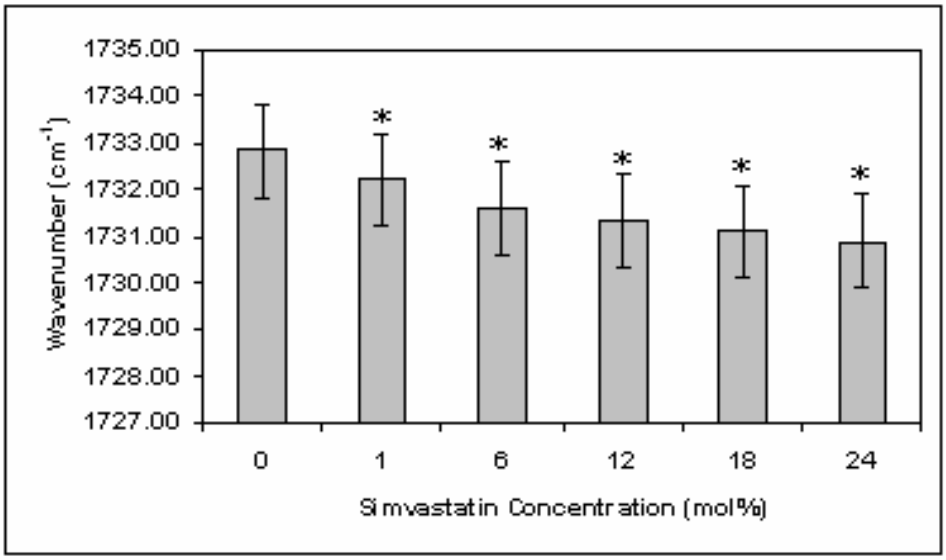

Figure 3.1.2.17 Simvastatin concentration dependence of the frequency of the C=O stretching mode for DMPC liposomes at 10°C. (*) P < 0.05.

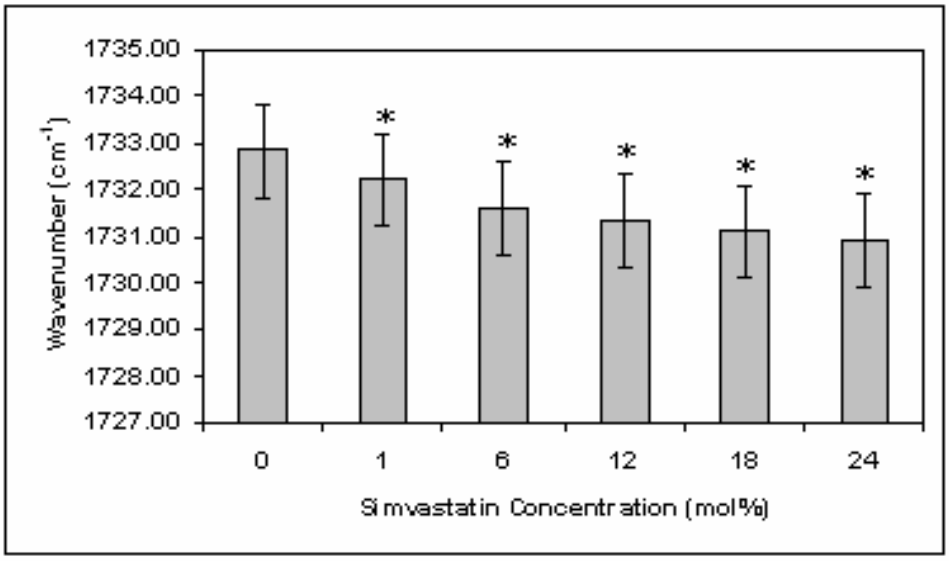

Figure 3.1.2.18 Simvastatin concentration dependence of the frequency of the C=O stretching mode for DPPC liposomes at 29.5°C. (*) P < 0.05.

Figures 3.1.2.19 and 3.1.2.20 show simvastatin dependence of the frequency of the C=O stretching modes of DMPC and DPPC liposomes respectively in their liquid crystalline phase. As it can be seen in both figures, the frequency values of the samples decreased as the simvastatin concentration increased, indicating the strengthening of the existing hydrogen bonds of the glycerol skeleton closer to the head groups or the formation of new hydrogen bonds. Therefore, simvastatin either strengths the existing hydrogen bonds of the glycerol skeleton closer to the head groups or causes new hydrogen bonding. Formation of new hydrogen bonds occur between hydroxyl groups of simvastatin and either carbonyl groups of lipids or water molecules around. The results imply that acyl chain length difference between DMPC and DPPC lipids has no effect on the hydrogen bonding at glycerol backbone near the head group of phospholipids in interfacial region in the liquid crystalline phase in this study.

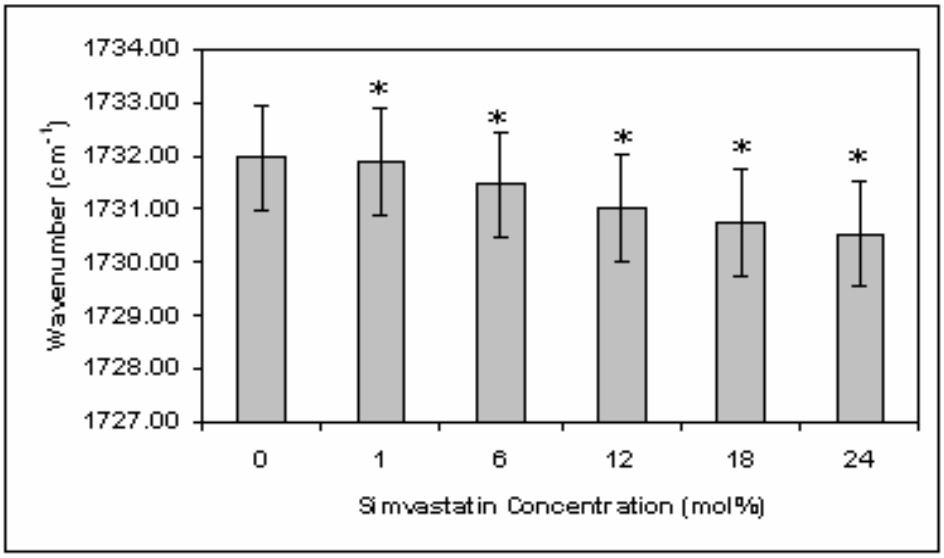

Figure 3.1.2.19 Simvastatin concentration dependence of the frequency of the C=O stretching mode for DMPC liposomes at 35°C. (*) P < 0.05.

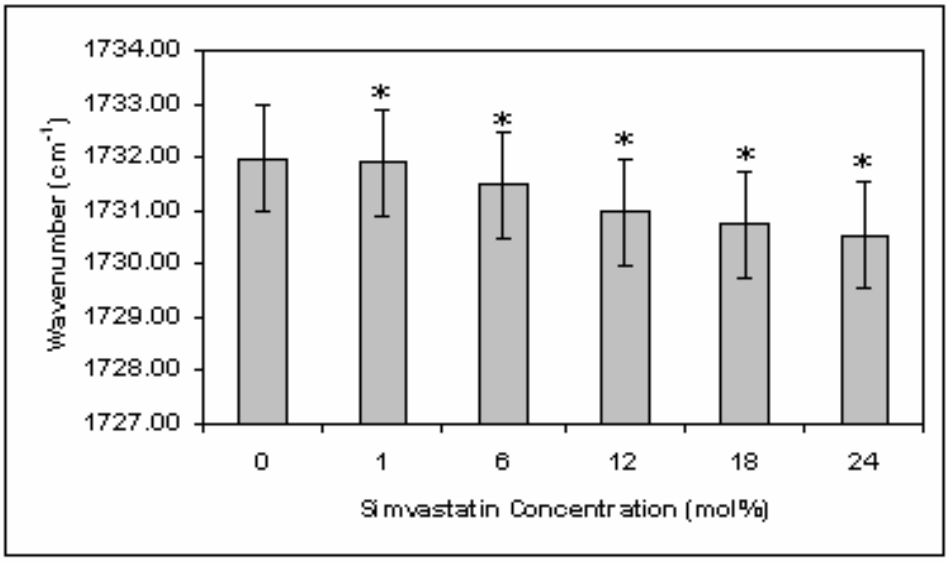

Figure 3.1.2.20 Simvastatin concentration dependence of the frequency of the C=O stretching mode for DPPC liposomes at 54°C. (*) P < 0.05.

The interaction between simvastatin and head group of DMPC or DPPC multilamellar liposomes was monitored by analysing the PO_2^- antisymmetric double stretching band. Figures 3.1.2.21 and 3.1.2.22 show simvastatin dependence of the frequency of the PO_2^- antisymmetric double stretching modes of DMPC and DPPC liposomes respectively in their gel phase. As it can be seen in both figures, the frequency of oscillation shifted to higher values as simvastatin concentration increased. The results imply that increasing simvastatin concentration caused a dehydration around these functional groups in the polar part of the lipids (Toyran and Severcan, 2003). Observing a similar trend in the figures means that the acyl chain length difference between DMPC and DPPC lipids has no effect on the interaction between simvastatin and head group of DMPC or DPPC multilamellar liposomes in the gel phase in this study.

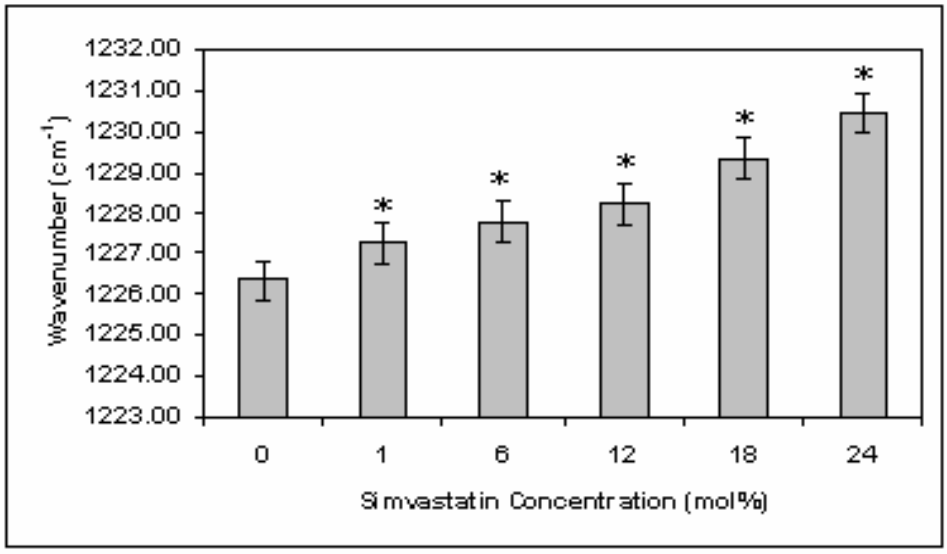

Figure 3.1.2.21 Simvastatin concentration dependence of the frequency of the PO_2^- antisymmetric double stretching mode for DMPC liposomes at 10^oC. (*) $P < 0.05$.

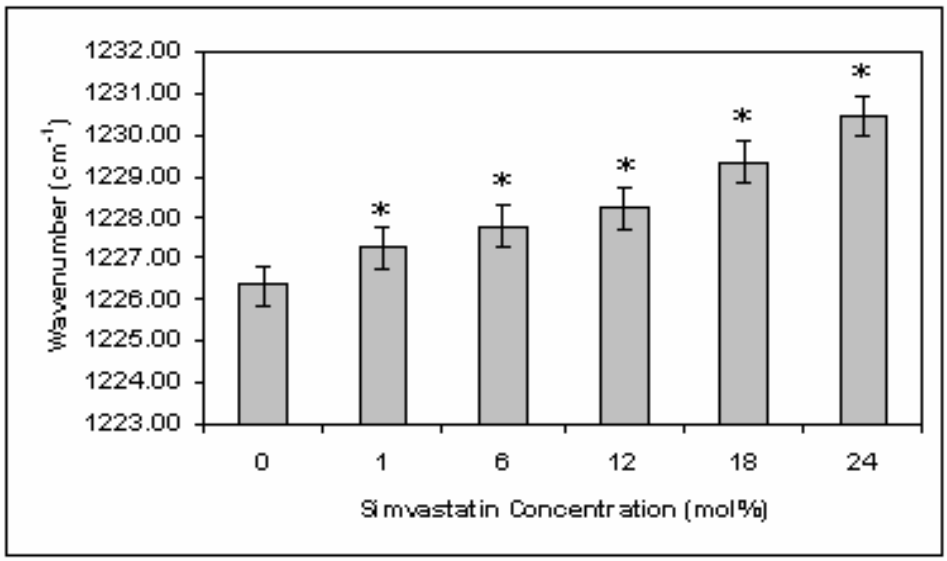

Figure 3.1.2.22 Simvastatin concentration dependence of the frequency of the PO_2^- antisymmetric double stretching mode for DPPC liposomes at 29.5^oC. (*) $P < 0.05$.

Figures 3.1.2.23 and 3.1.2.24 show simvastatin dependence of the frequency of the PO_2^- antisymmetric double stretching modes of DMPC and DPPC liposomes respectively in their liquid crystalline phase. As it can be seen in both figures, the frequency of oscillation shifted to higher values as simvastatin concentration increased. These results imply that increasing simvastatin concentration caused a dehydration around these functional groups in the polar part of the lipids. The comparison of the figures revealed that acyl chain length difference between DMPC and DPPC lipids has no effect on the interaction between simvastatin and head group of DMPC or DPPC multilamellar liposomes in the liquid crystalline phase in this study.

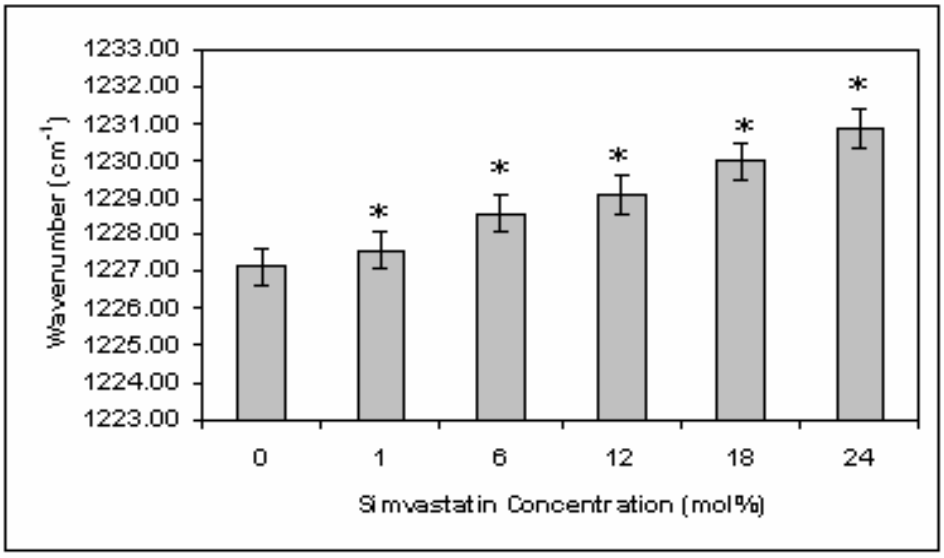

Figure 3.1.2.23 Simvastatin concentration dependence of the frequency of the PO_2^- antisymmetric double stretching mode for DMPC liposomes at 35°C. (*) P < 0.05.

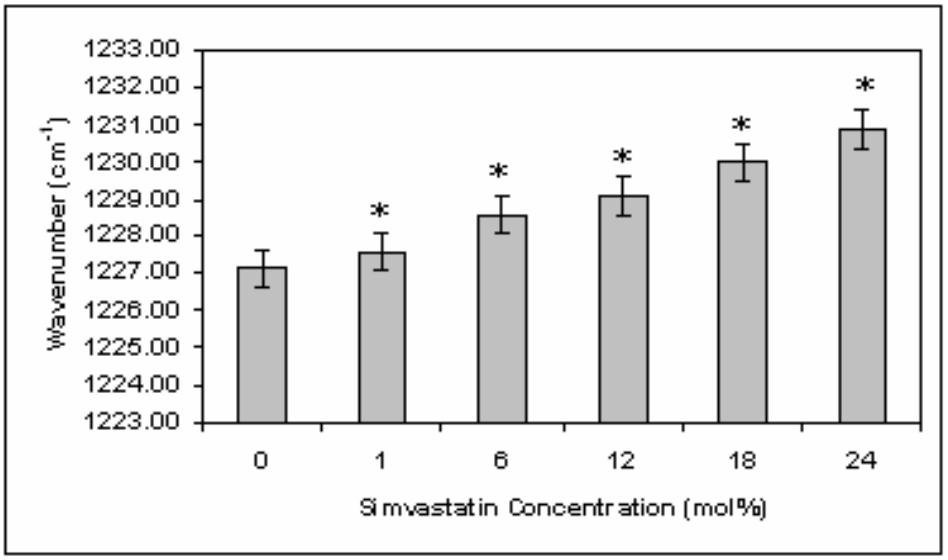

Figure 3.1.2.24 Simvastatin concentration dependence of the frequency of the PO_2^- antisymmetric double stretching mode for DPPC liposomes at 54°C. (*) P < 0.05.

3.2 DSC Studies

Calorimetric investigations of DMPC or DPPC multilamellar liposomes in the presence and absence of simvastatin were carried out for a temperature range of 0-50^{o}C and 20-70^{o}C, respectively. The corresponding heating flow as a function of temperature for DMPC and DPPC liposomes were shown in Figures 3.2.1 and 3.2.2, respectively. As shown in Figure 3.2.1, DMPC liposomes showed the characteristic pretransition with a low-enthalpy change and a sharp main transition at 14.60^{o}C and 22.80^{o}C, respectively (Kiselev *et a*l., 2001). In the current study the pretransition and main transition temperature were determined as 14.20^{o}C and 23.24^{o}C, respectively. The thermotropic properties of hydrated DPPC liposomes have extensively been studied by DSC method (Melchior and Stein, 1976; Huang and Li, 1999). The characteristic parameters used for obtaining information in lipid studies are the transition enthalpy changes, the width of the transition peak at half height and the main phase transition temperature. As shown in Figure 3.2.2, DPPC liposomes showed the characteristic pretransition with a low-enthalpy change and a sharp main transition at 35.20^{o}C and 41.20^{o}C, respectively (Mavramoustakos *et al*., 1997). In our study the pretransition and main transition temperature were determined as 35.47^{o}C and 41.02^{o}C, respectively.

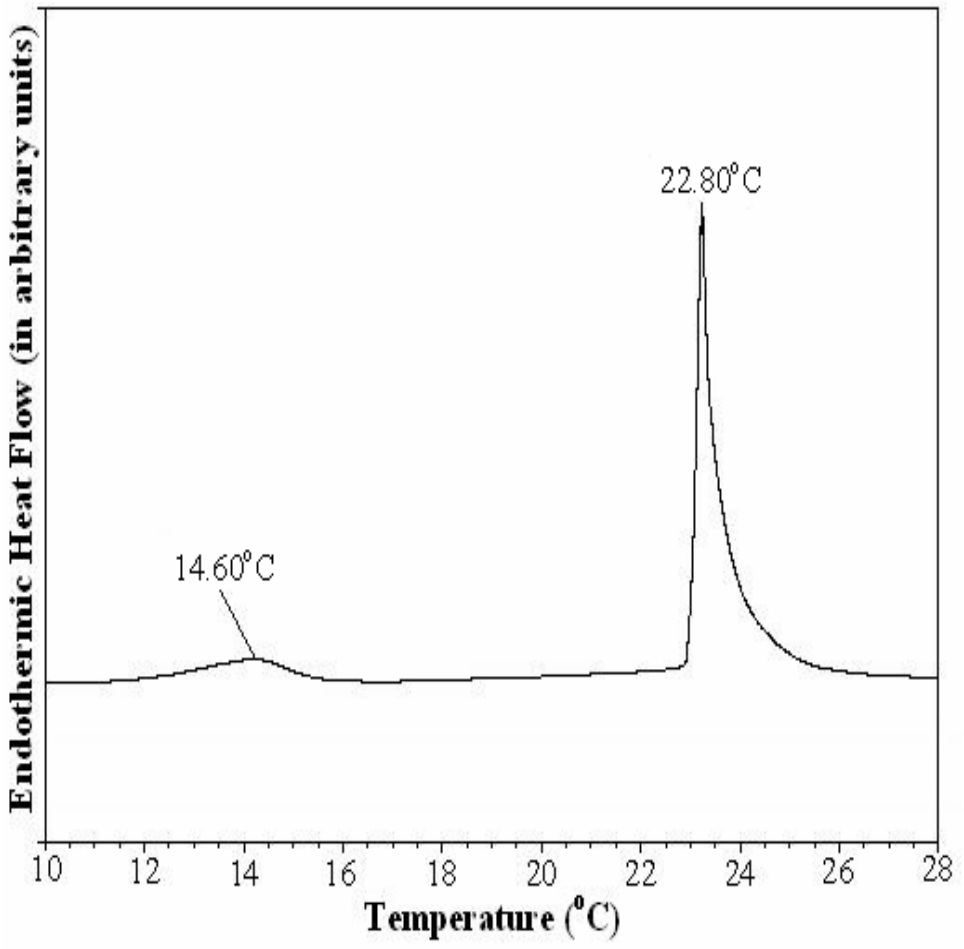

Figure 3.2.1 DSC thermogram of DMPC liposomes (Kiselev *et a*l., 2001).

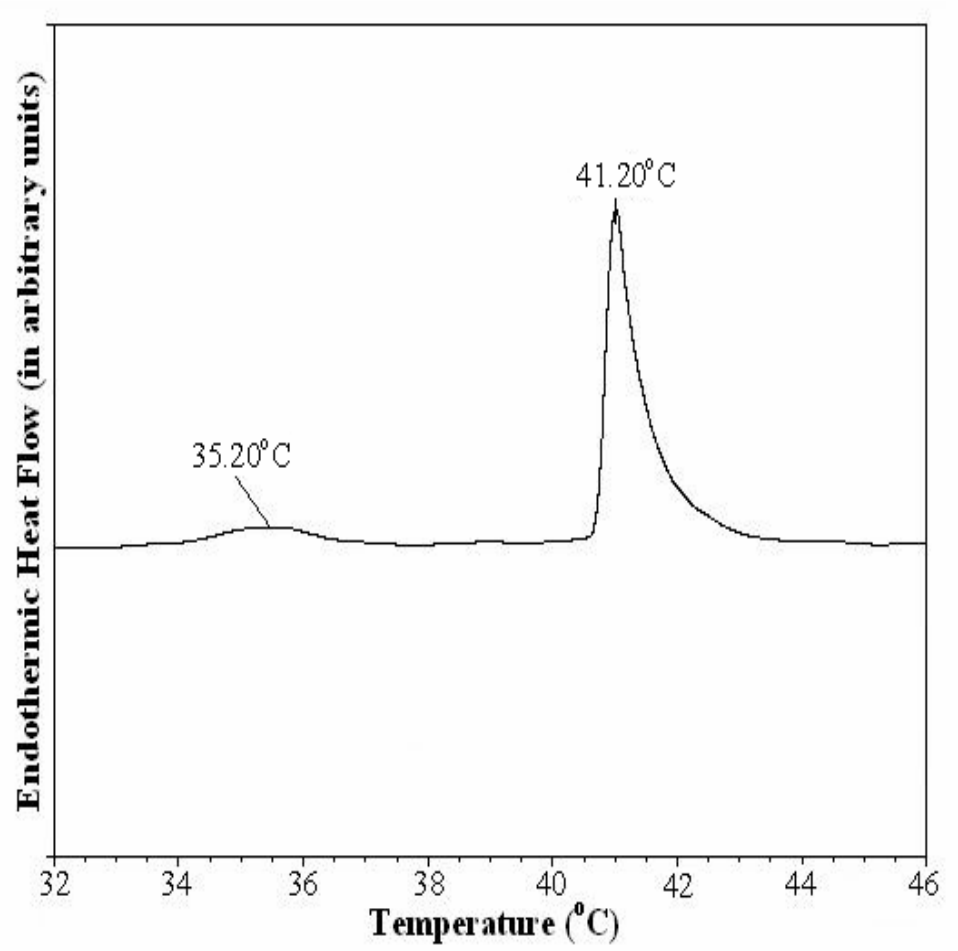

Figure 3.2.2 DSC thermogram of DPPC liposomes (Mavramoustakos *et al*., 1997).

Figures 3.2.3 and 3.2.4 show DSC thermograms of DMPC and DPPC liposomes respectively, in the presence and absence of different simvastatin concentrations. As it can be seen from the figures, the main phase transition temperature of DMPC and DPPC lipids decreased and their pretransition temperature disappeared as simvastatin concentration in the liposomes increased. Moreover, a broadening in the main phase transition peak was observed for both lipids as simvastatin concentration in the liposomes increased. Also more than one peak were observed at 6 mol% simvastatin concentration of DMPC liposomes and 12,18 mol% simvastatin concentrations of DPPC liposomes.

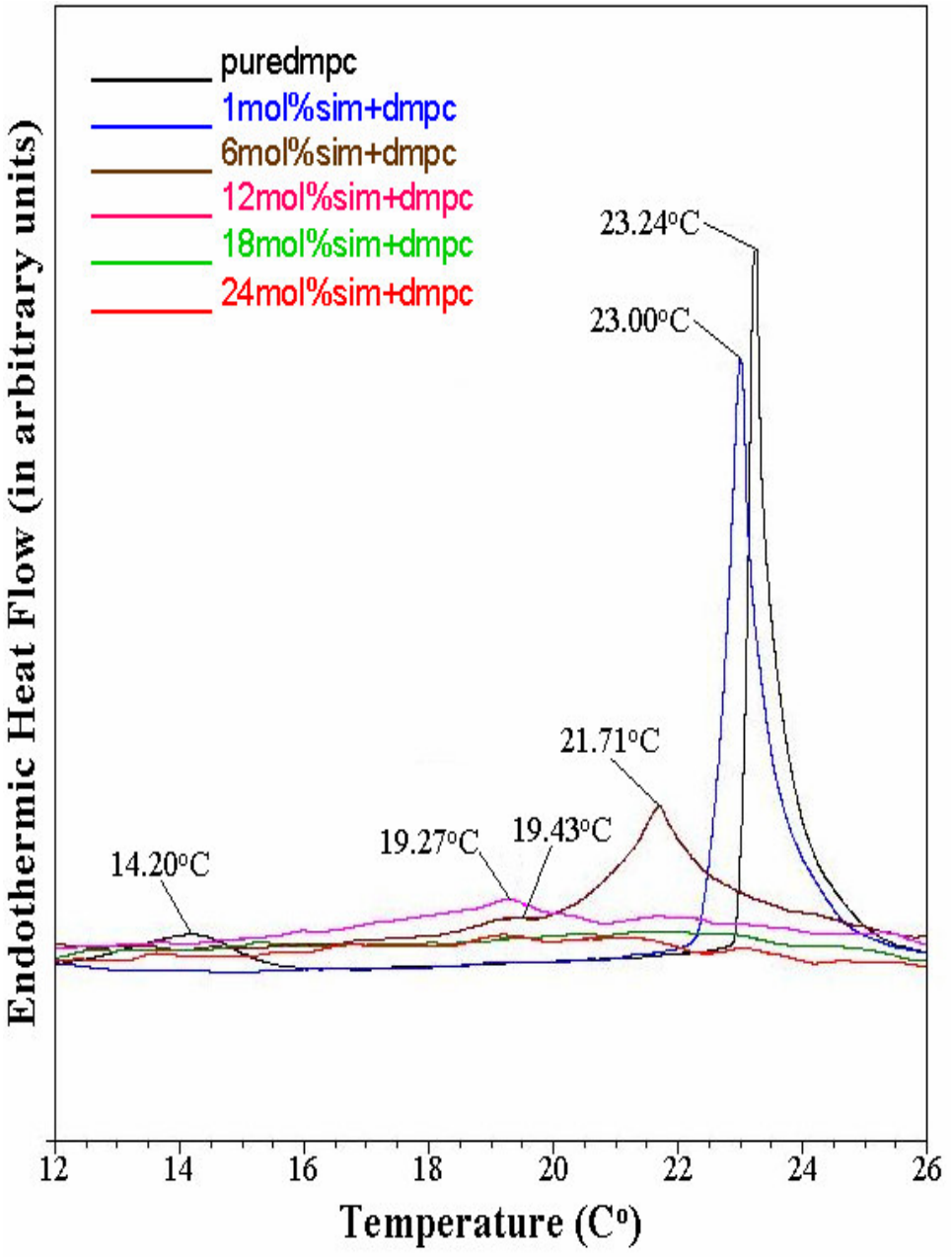

Figure 3.2.3 DSC thermogram of DMPC liposomes in the presence and absence of different simvastatin concentrations in terms of mol%.

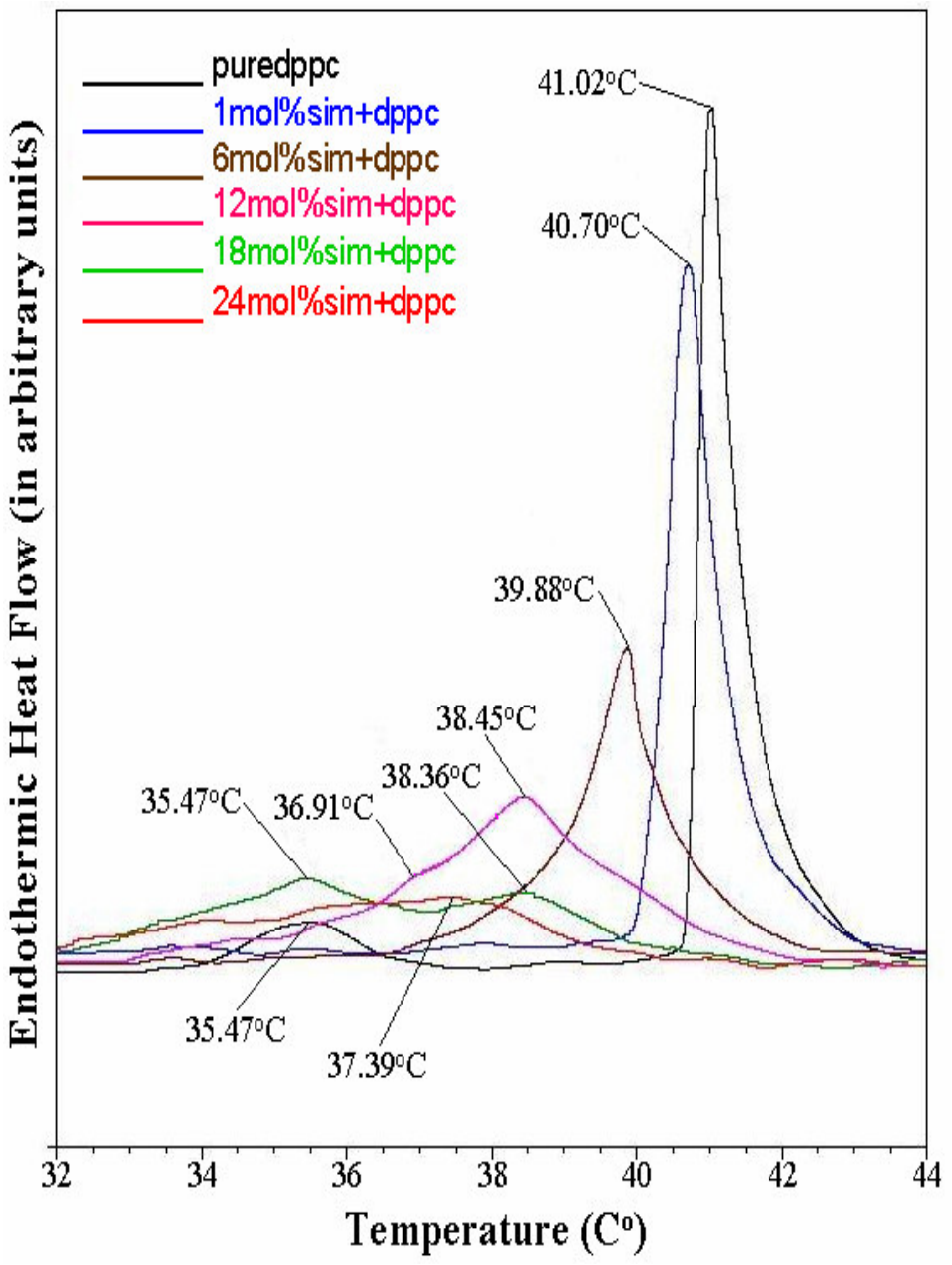

Figure 3.2.4 DSC thermogram of DPPC liposomes in the presence and absence of different simvastatin concentrations in terms of mol%.

The width of the transition peak at half height, the main phase transition temperature values and enthalpy changes at the main transition of DMPC and DPPC samples were given in Tables 3.3.1 and 3.3.2, respectively. The broadening of the main phase transition peak was observed because the width of the transition peak increased as simvastatin concentration in the liposomes increased. When the transition enthalpy changes of DPPC samples were compared, it was found that the enthalpy change of transition was decreased in all simvastatin containing liposomes. Since it was not possible to measure the width of the transition peaks at half height, the main phase transition temperature values and enthalpy changes at the main transition of 18 and 24 mol% simvastatin concentrations of DMPC liposomes, their values were showed by a hyphen in the table 3.3.1.

Table 3.3.1 Width at half height (ΔT), transition temperatures (T_m) and enthalpy of the transitions (ΔH) for DMPC liposomes are given.

Samples	ΔT (^oC) (at half height)	T_m (^oC)	ΔH (cal/g)
DMPC	0.36	23.24	7.72
1mol%sim+DMPC	0.54	23.00	7.02
6mol%sim+DMPC	1.62	21.71	6.18
12mol%sim+DMPC	6.51	19.27	6.23
18mol%sim+DMPC	-	-	-
24mol%sim+DMPC	-	-	-

Table 3.3.2 Width at half height (ΔT), transition temperatures (T_m) and enthalpy of the transitions (ΔH) for DPPC liposomes are given.

Samples	ΔT (^oC) (at half height)	T_m (^oC)	ΔH (cal/g)
DPPC	0.56	41.02	11.57
1mol%sim+DPPC	0.75	40.70	9.90
6mol%sim+DPPC	1.15	39.88	9.71
12mol%sim+DPPC	3.21	38.45	10.06
18mol%sim+DPPC	8.98	38.36	9.25
24mol%sim+DPPC	12.68	37.39	9.64

CHAPTER 4

DISCUSSION

This study can be divided into two parts. In the first part, the effect of simvastatin on the phase transition profile, order, dynamics and hydration states of the head and the region near the aqueous region of zwitterionic DPPC multilamellar vesicles was monitored as a function of temperature and simvastatin concentration. In the second part, studies were carried out to monitor the effect of acyl chain length on the simvastatin-membrane interactions by using two different lipids with different chain length. These lipids are DMPC and DPPC which have molecular formulas of $C_{36}H_{72}NO_8P$ and $C_{40}H_{80}NO_8P$, respectively. For both parts of the study, two non-perturbing techniques, namely Fourier transform infrared (FTIR) spectroscopy and differential scanning calorimetry were used.

We were particularly careful in distinguishing between structural parameters describing molecular order and motion parameters such as bandwidth describing molecular dynamics as suggested by others (Toyran and Severcan, 2003; Severcan *et al*., 2005; Korkmaz and Severcan, 2005; Van Ginkel *et al*., 1989).

4.1 Simvastatin-DPPC Model Membrane Interaction

In the present study, we for the first time investigated the effect of simvastatin on lipid phase transition profile, lipid order, lipid dynamics and hydration states of the head and the region near the aqueous region of zwitterionic DPPC multilamellar vesicles as a function of temperature and simvastatin

concentration varying from 1 to 24 mol%. Furthermore, we for the first time showed that the existence of lateral phase separation in binary mixture of simvastatin and DPPC in this study.

For FTIR spectral analysis, the C-H stretching modes at 3000-2800 cm^{-1}, the C=O stretching band located at 1735 cm^{-1} and PO_2^- antisymmetric double stretching band located at 1240-1220 cm^{-1} were considered. Simvastatin induced shifts in the peak position of the FTIR bands and changes in the bandwidths of several bands in comparison to those of DPPC liposomes. The shifts to higher wavenumbers correspond to an increase in the number of gauche conformers (Toyran and Severcan, 2003; Casal and Mantsch, 1984; Severcan, 1997; Villalain *et al*., 1986). Moreover, the bandwidth of the CH_2 stretching bands give dynamic information about the membrane (Toyran and Severcan, 2003; Villalain *et al*., 1986; Casal *et al*., 1980; Lopez-Garcia *et al*., 1993; Kazancı *et al*., 2001).

FTIR and DSC results revealed that simvastatin eliminates the pre-transition and shifts the main transition to lower temperatures as drug concentration is increased. By monitoring the CH_2 stretching vibrations in FTIR spectra, we showed that simvastatin increases acyl chain flexibility, i.e., increases disorder of DPPC membrane both in the gel and liquid crystalline phase. There is a limited number of studies in the literature about the effects of simvastatin on membrane dynamics. The results of these studies are not in agreement with each other. Koter et al. in 2003, using electron paramagnetic resonance (EPR) spectroscopy, reported that simvastatin increases lipid fluidity in erythrocyte plasma membranes (Koter *et al*., 2003). Djaldetti et al. also observed an increase in the membrane dynamics of macrophages (Djaldetti *et al*., 2006). In contrast to these studies, Rabini et al. reported an initial decrease in the membrane fluidity of erythrocytes (Rabini *et al*., 1993). Moreover, Koter et al. in 2002, using spin label technique reported that atorvastatin, one type of statin

drugs, decreases membrane fluidity of erythrocytes (Koter *et al*., 2002). Our results clearly show that the effects of simvastatin on membrane dynamics are dependent on simvastatin concentration. A dramatic decrease in the dynamics of DPPC membranes is observed in the presence of simvastatin both in the gel and liquid crystalline phase. Our results are in agreement with initial results of Rabini et al. and atorvastatin results of Koter et al. in 2002.

The changes in the frequency and in the bandwidth with respect to temperature are not concerted since simvastatin induces a decrease in the order and at the same time a decrease in the dynamics of the membrane. This type of behaviour has been previously reported for cholesterol (Van Ginkel *et al*., 1989), α-tocopherol (Villalain *et al*., 1986), melatonin (Severcan *et al*., 2005) and progesterone (Korkmaz and Severcan, 2005) containing phospholipid membranes. This controversial effect in between order and dynamics may be an indication of simvastatin-induced lateral phase separation in the binary system. Phase separation can be understood by a shoulder appearing on the main transition peak or by an extra peak around it (Shaikh *et al*., 2001; Bach *et al*., 2001). Our DSC studies revealed that with the addition of simvastatin, the main DSC curve (at around 41^{o}C) decreases in intensity and broadens. This may suggest the co-existence of more than one domain. As simvastatin concentration is increased to 12 mol%, more than one peak appears in the calorimetric profile indicating that lateral phase separation of lipids are indeed occuring probably producing phases with different ratios of simvastatin and phospholipid. In the presence of 18 mol% simvastatin, the main peak is clearly resolved into two components with phase-transition temperatures of 35.47^{o}C and 38.36^{o}C. For higher simvastatin concentration (24mol%), no splitting but a broad signal was obtained. This may also suggest the co-existence of more than one domain. If these domains or one of these domains are sufficiently large, the exchange of lipids between the domains cannot be resolved and the DSC curve will be a superposition of more than one component. We suggest that the peak

observed at a lower temperature most likely represents the transition of the simvastatin rich domain, while the peak located at a higher temperature may arise from simvastatin poor domains similar to previously suggested rich and poor domains in other binary mixtures of DPPC with melatonin (Severcan *et al*., 2005), Vitamin E (Severcan and Cannistraro, 1988), Vitamin D_3 (Bondar and Rose, 1995), Vitamin D_2 (Kazancı *et al*., 2001) ,and progesterone (Korkmaz and Severcan, 2005).

Moreover, FTIR enables us to monitor the hydrophilic part of the bilayer, i.e., the head group and the region closer to the polar head group of the phospholipids (Severcan *et al*., 2000). We found a significant increase in the hydrogen bonding of the C=O group both in the gel and liquid crystalline phase. In other words, simvastatin increased hydrogen bonding in the interfacial region of the bilayer. In our case, the electronegative atom is the oxygen of the hydroxyl group of the simvastatin, which has a partial negative charge. The hydrogen in the O-H group has a partial positive charge. This hydrogen can make hydrogen bonding with the oxygen atoms in the C=O functional groups of the lipids. We should also point out the possibility of simvastatin-induced hydrogen bonding in between the oxygen molecules of both carbonyl and phosphate groups of DPPC and water molecules around these functional groups and/or in between the carbonyl group of simvastatin and nearby water molecules. PO_2^- molecules are highly sensitive to changes in hydration (Severcan *et al*., 2005; Casal and Mantsch, 1987). In the analysis of head group vibrations, simvastatin increases the head group vibration frequency of the membrane both in the gel and liquid crystalline phase, implying a dehydration around the PO_2^- functional groups of the lipids.

A change in the transition temperature of membrane is related with the cooperativity of the lipid molecules of membrane (Güldütuna *et al*., 1997). Loss of cooperativity between the lipid chains means the break down of van

der Waals forces between the lipid molecules. Simvastatin molecules interact with lipids in liposomes by inserting themselves into the bilayer of membrane, disturbing the strong hydrophobic interactions between the lipid molecules, and such an interaction causes simultaneous variation in T_m and transition ΔH values of DSC curves (Lee, 1977; Cater *et al*., 1974). This interaction also causes a broadening in the phase transition profile in FTIR studies (Figures 3.1.1.6 and 3.1.1.7). The broadening of peak profile and lowering of transition temperature demonstrate that both the size and packing of bilayers are modified, and the system is disordered (Jain and Min Wu, 1977; Momo *et al*., 2002). The loss of cooperativity between the lipid chains of DPPC together with the broadening of transition curve in FTIR spectra revealed by the frequency analysis of CH_2 symmetric and antisymmetric stretching modes, imply the penetration of simvastatin into the cooperativity region (C_2-C_8) of the fatty acyl chains (Jain and Min Wu, 1977).

4.2 Effect of Acyl Chain Length

The ideal liposome formulation with optimum stability is important for drug delivery. The physical stability of liposomes has been found to be a function of lipid acyl chain length (Anderson and Omri, 2004). It was also found that the anticellular effects of liposomal amphotericin B (AmB) formed from AmB and small unilamellar vesicles were dependent on saturated acyl chain length difference in phospholipids (Jullien *et al*., 1989). Moreover, it was reported that the rates of ester formation by human plasma lecithin:cholesterol acyltransferase increased or decreased according to acyl chain length of phospholipid classes (Pownall *et al*., 1985). In the present study, we for the first time tested the chain length specificity of simvastatin with DMPC and DPPC lipids. In addition, we for the first time investigated the effect of acyl chain length on simvastatin-membrane interactions by monitoring the membrane properties like membrane fluidity, disorder of the hydrocarbon

chains, and hydrogen bonding around the C=O and PO_2^- functional groups. DMPC and DPPC have molecular formulas of $C_{36}H_{72}NO_8P$ and $C_{40}H_{80}NO_8P$, respectively. These two lipids have the same characteristics in many respects like having two identical saturated acyl chains with an even number of carbons, having a choline head group, and being neutral (Jullien *et al*., 1989). Moreover, their order parameter profiles are essentially similar to each other except for the shorter chains (Kupiainen *et al*., 2005). The molecular structure of DMPC is different from that of DPPC only by a 2-methylene moiety in the acyl chains (Ohki, 2005).

The lateral diffusion rates of lipid molecules depend on the amount of free volume in the bilayer. The possibility of redistributing the free volume is important for diffusion. Thus, increased free volume fluctuations imply faster diffusion. The free area (or volume) fluctuations in the different regions of the bilayer can be quantified by the area compressibility modulus. A high compressibility modulus indicates small free area fluctuations and a low compressibility modulus large fluctuations. The area compressibility moduli for DMPC is slightly lower than that of DPPC so the lateral diffusion rates of DMPC lipids are slightly higher than that of DPPC (Kupiainen *et al*., 2005). In other words, membrane fluidity increases by an increase in the rates of lateral diffusion of lipid molecules. Consequently, DPPC membranes are structurally more stable than DMPC membranes. This result also showed by FTIR studies (Figure 3.1.1.5). Also, acyl chain length of DMPC lipids are shorter than that of DPPC lipids, implying DMPC membranes are more fluid or less stable than DPPC membranes (Karp, 1999). Such a stability difference may explain why simvastatin has more profound effects on the DMPC membranes than DPPC membranes showed by DSC studies (Figures 3.2.3 and 3.2.4). Due to the acyl chain length difference between DMPC and DPPC lipids, liposomes which are formed from these lipids have different stabilities (Betageri, 1993). Transition temperature is an important consideration with liposome stability (Anderson

and Omri, 2004). Gel-like structures of phospholipids with high T_m values and long hydrocarbon chains are more stable than those with low T_m values and short hydrocarbon chains (Gregoriadis, 1991; Crommelin and Schreier, 1994).

Another study comparing the stability of different phospholipids showed that DPPC, which has a large head-group, undergoes hydrolysis more slowly than DMPC with a smaller head-group, making DPPC more stable (Grit and Crommelin, 1993). Also, hydrolysis, one of the mechanisms of liposome destabilization, is increased with short acyl groups which further explains why DMPC liposomes are less stable than DPPC liposomes (Grit and Crommelin, 1993). Moreover, the thickness of the membranes related to the length and average ordering of the hdrocarbon chains (Kupiainen *et al*., 2005). Thus, DPPC membranes are thicker than DMPC membranes.

Relationships between lipid membrane area, hydrophobic thickness, and acyl-chain orientational order was investigated by using a microscopic interaction model for a fully hydrated DPPC lipid bilayer membrane containing cholesterol. Same effects like broadening of the transition curve, shifting of the transition curve towards slightly lower temperatures in the presence of cholesterol were observed on these three parameters (Ipsen *et al*., 1990). Similar trends were also observed in our results.

Furthermore, the transport characteristics on the DLPC, DMPC, and DPPC bilayers were analyzed by using the molecular dynamics method. And the results demonstrated that free energy profiles of small molecules like O_2 and H_2O changed during the permeation process through a lipid bilayer as the acyl chain length of phospholipids changed (Sugii *et al*., 2004).

When we compare the FTIR spectra and DSC thermograms of DMPC and DPPC lipids we observed similar trends on membrane properties, implying

simvastatin, which is a hydrophobic cholesterol reducing agent, did not show chain length specificity between DMPC and DPPC lipids (Söderlund *et al*., 1999). Moreover, effects of simvastatin on the DMPC membranes were more profound than on the DPPC membranes in the DSC thermograms since the main transition peak was so much broadened and nearly it disappeared at higher simvastatin concentrations (18 and 24 mol%) of DMPC liposomes. Thus, it was not possible to measure an apparent T_m temperature and enthalpy change at the main transition. One possible reason of such a result is less stability of DMPC liposomes than DPPC liposomes. Consequently, localization of simvastatin in the cooperativity region of the DMPC bilayer may have a profound effect on disturbing the hydrophobic interactions between the lipid molecules. In addition, simvastatin is a hydrophobic molecule. Thus, penetration of simvastatin into the phospholipid membranes is possible (Higashino *et al*., 2001; Sandaram and Thompson, 1990).

It was previously indicated that a model peptide melittin obtained from bee venom interacts preferentially with DMPC molecules instead of DPPC molecules in mixed phospholipids bilayers. The hydrophobic region of the DMPC bilayer membrane is 3.32 nm in all-*trans* configuration (Sandaram and Thompson, 1990). On the other hand, it has been reported that hydrophobic thickness of DPPC-cholesterol membrane surrounded by melittin is nearly 2.9 nm (Pott and Dufourc, 1995). And the head-to-tail distance of 20 amino acids of melittin except six hydrophilic amino acids is approximately 3.0 nm (Inagaki *et al*., 1989). In the process of the interaction of melittin with DMPC membranes, it is most important that the thickness of the hydrophobic core of the lipid bilayer fits the length of the hydrophobic region of the melittin molecules (Ohki, 2005). Such a case was not observed for simvastatin since similar trends were observed for both lipids in our FTIR and DSC studies.

Furthermore, it was showed that membrane permeability increases with decreasing chain length at a given cholesterol content (testing DPPC, DMPC and DSPC specificity) (Corvera et al., 1992). An increase in the membrane permeability means an increase in the membrane fluidity. Different than found in the case of cholesterol where an increase in the permeability was observed as the chain length decreased, in the current study no significant variations were observed due to the acyl chain length difference in the fluidity or permeability of the membranes.

Finally, similar trends were observed in the FTIR results of DMPC and DPPC membranes both in the gel and liquid crystalline phase for the interaction of simvastatin with the C=O and PO_2^- functional groups of the lipids. Then, it is possible to say that acyl chain length difference between DMPC and DPPC lipids has no effect on the interaction between simvastatin and the hydrogen bonding at glycerol backbone near the head group of phospholipids in interfacial region and head group of DMPC, DPPC lipids.

CONCLUSION

The present work firstly investigated the effect of cholesterol reducing agent, simvastatin, on the physical properties such as phase transition, membrane order and dynamics, of pure neutral DPPC model membranes as a function of simvastatin concentration and temperature. Also this study firstly investigated the effect of acyl chain length on the simvastatin-model membrane interactions by using DMPC and DPPC lipids.

In this study two non-invasive techniques, namely FTIR spectroscopy and DSC were used. By using FTIR we were able to monitor different parts of the membrane such as the head group, acyl chain and the interfacial region. We were able to obtain information about these regions of the membrane in terms of interactions. And DSC enabled us to monitor the main phase transition of the membranes.

Results obtained in this study revealed that there is a strong interaction between simvastatin and the lipid membranes. In the present study, it has been for the first time showed that membrane fluidity decreases as simvastatin concentration increases. Simvastatin also disorders the system in both gel and liquid crystalline phase. Furthermore, we demonstrated for the first time simvastatin induces phase separation in both DMPC and DPPC liposomes. Evidently, these interactions are dependent on simvastatin concentration and temperature. In addition, cooperativity of the lipid molecules is modified by affecting the van der Waals forces among the lipid molecules, thus pretransition of the DMPC and DPPC membranes is completely diminished, and their main phase transition temperature, enthalpy and profile considerably changed. Moreover, simvastatin increased hydrogen bonding in the interfacial

region of the bilayers. Also, a dehydration effect caused by simvastatin around the PO_2^- functional groups in the polar part of the lipids was observed.

Furthermore, the present study firstly monitored the effects of acyl chain length on the simvastatin-model membrane interactions. And any change caused by the difference between the acyl chain length of DMPC and DPPC lipids was not observed. In addition, for both of the lipids similar trends were observed in the FTIR and DSC results. The less stability of DMPC membranes than DPPC membranes is also showed by more profound effects of simvastatin on the DMPC membranes in the DSC thermograms.

REFERENCES

Adamo, P., Taylor, P. B., and Fackrell, H. B. (1989). Staphylococcal alpha toxin induced cardiac dysfunction. *Can J Cardiol*. **5**: 395– 400.

Albert, M. A., Danielson, E., Rifai, N., and Ridker, P. M., PRINCE Investigators. (2001). Effect of statin therapy on C-reactive protein levels: the pravastatin inflammation/CRP evaluation (PRINCE): a randomized trial and cohort study. *JAMA*. **286**: 64-70.

Almuti, K., Rimawi, R., Spevack, D., and Ostfeld, R. J. (2006). Effects of statins beyond lipid lowering: Potential for clinical benefits. *International Journal of Cardiology*. **109**: 7 – 15.

Anderson, M., and Omri, A. (2004). The Effect of Different Lipid Components on the In Vitro Stability and Release Kinetics of Liposome Formulations. *Drug Delivery*. **11**: 33-39.

Anton, P. J., Middelberg, A. P. J., Radke, C. J., and Blanch, H. W. (2000). Peptide interfacial adsorption is kinetically limited by the thermodynamic stability of self association. *Proc Natl Acad Sci USA*. **97**(10): 5054-5059.

Appel, S., and Dingemanse, J. (1996). Clinical pharmacokinetics of fluvastatin with reference to other HMG-CoA reductase inhibitors. *Drugs of Today*. **32**: 39–55.

Attallah, N., Yassine, L., Musial, J., Yee, J., and Fisher, K. (2004). The potential role of statins in contrast nephropathy. *Clin Nephrol*. **62**: 273–278.

Bach, D., Borochov, N., and Wachtel, E. (2001). Phase separation of cholesterol and the interaction of ethanol with phosphatidylserine-cholesterol bilayer membranes. *Chemistry and Physics of Lipids*. **114**: 123-130.

Bauer, D. C., Mundy, G. R., Jamal, S. A., Black, D. M., Cauley, J. A., Ensrud, K. E., van der Klift, M., and Pols, H. A. P. (2004). Use of statins and fracture: results of 4 prospective studies and cumulative meta-analysis of observational studies and controlled trials. *Arch Intern Med*. **164**: 146–152.

Becker, M. W., Reece, B. J., and Poenie, F. M. (1996). In: *The World of the Cell*, Third Edition. pp. 167-192.

Berliner, J. A., Territo, M. C., Sevanian, A., Ramin, S., Kim, J. A., Bamshad, B., Esterson, M., and Fogelman, A. M. (1990). Minimally modified LDL stimulates monocyte endothelial interactions. *J Clin Invest*. **85**(4): 1260–1266.

Betageri, G. (1993). Liposomal encapsulation and stability of dideoxyinosine triphosphate. *Drug Devel Indust Pharm*. **19**: 531-539.

Bhandara, P., Mendelson, Y., Stohr, E., and Peura, R. A. (1994). Comparison of Multivariate Calibration Techniques for Mid-IR Absorption Spectrometric Determination of Blood Serum Constituents. *Appl Spectrosc*. **48**: 271-273.

Bondar, O. P., and Rose, E. S. (1995). Differential scanning calorimetry study of the effect of Vitamin D_3 on the thermotropic phase behaviour of lipid model systems. *Biochim Biophys Acta*. **1240**: 125-132.

Brown, M. S., and Goldstein, J. L. (1980). Multivalent feedback regulation of HMG CoA reductase, a control mechanism coordinating isoprenoid synthesis and cell growth. *J Lipid Research*. **21**: 505–517.

Buerke, M., Sibelius, U., Grandel, U., Buerke, U., Grimminger, F., Seeger, W., Meyer, J., and Darius, H. (2002). Staphylococcus aureus alpha toxin mediates polymorphonuclear leukocyte induced vasocontraction and endothelial dysfunction. *Shock*. **17**: 30–35.

Campbell, I. D. (1984). In: *Biological Spectroscopy*. Edited by: Elias. P. The Benjamin/Cummings Publishing Company, Inc.

Campbell, J. D., and Dwek, R. A. (1984). In: *Biological Spectroscopy*, Chapters 3,4. Edited by: Elias, P. The Benjamin/Cummings Publishing Company, Inc.

Carvalho, A. A. S., Lima, Ü. W. P., and Valiente, R. A. (2004). Statin and Fibrate Associated Myopathy. *Arq Neuropsiquiatr*. **62**(2-A): 257-261.

Casal, H. L., and Mantsch, H. H. (1984). Polymorphic phase behaviour of phospholipid membranes studied by infrared spectroscopy. *Biochim Biophys Acta*. **779**: 381-401.

Casal, H. L., and Mantsch, H. H. (1987). Infrared Studies of Fully Hydrated Saturated Phosphatidylserine Bilayers: Effect of Li^{+} and Ca^{++}. *Biochemistry*. **26**: 4408-4416.

Casal, H. L., Cameron, D. G., Smith, I. C. P., and Mantsch, H. H. (1980). Fourier transform infrared spectra of A. Laidlawii membranes. *Biochemistry*. **19**: 444-451.

Castelli, F., Librando, V., and Sarpietro, M. G. (2001). A calorimetric evidence of the interaction and transport of environmentally carciogenic compounds through the biomembranes. *Thermochimica Acta*. **373**: 133-140.

Cater, B. R., Chapman, D., Hawes, S. M., and Saville, J. (1974). Lipid phase transitions and drug interactions. *Biochim Biophys Act*. **363**(1): 54-69.

Ceckler, T. L., and Cunningham, B. A. (1997). Transition State Thermodynamics of Lipid Bilayers Characterized by Differential Scanning Calorimetry. *The Chemical Educator*. **2**(6): 1-17.

Chan, K. A., Andrade, S. E., Boles, M., Buist, D. S., Chase, G. A., Donahue, J. G., Goodman, M. J., Gurwitz, J. H., LaCroix, A. Z., and Platt, R. (2000). Inhibitors of hydroxymethylglutaryl-coenzyme a reductase and the risk of fracture among older women. *Lancet*. **355**: 2185–2188.

Chapman, D. (1975). Phase transitions and fluidity characteristics of lipids and cell membranes. *Quarterly Reviews of Biophysics*. **8**: 185-235.

Christians, U., Jacobsen, W., and Floren, L. C. (1998). Metabolism and drug interactions of 3-hydroxy-3-methylglutaryl coenzyme A reductase inhibitors in transplant patients: are the statins mechanistically similar? *Pharmacol Ther*. **80**: 1–34.

Connolly, P. J., Westin, C. D., Loughney, D. A., and Minor, L. K. (1993). HMG-CoA reductase inhibitors : design, synthesis, and biological activity of tetrahydroindazole-substituted 3,5-dihydroxy-6-heptanoic acid sodium salts. *J Med Chem*. **36**: 3674–3685.

Corsini, A., Bellosta, S., Baetta, R., Fumagalli, R., Paoletti, R., and Bernini, F. (1999). New insights into the pharmacodynamic and pharmacokinetic properties of statins. *Pharmacol Ther*. **84**: 413–428.

Corvera, E., Mouritsen, O. G., Singer, M. A., and Zuckermann, M. J. (1992). The permeability and the effect of acyl-chain length for phospholipid bilayers containing cholesterol: theory and experiment. *Biochimica et Biophysica Acta*. **1107**: 261-270.

Crommelin, D., and Schreier, H. (1994). Liposomes. In: *Colloidal drug delivery systems*, ed. J. Kreuter. New York: Marcel Dekker.

Çalışkan, S., Çalışkan, M., Kuralay, F., and Önvural, B. (2000). Effect of simvastatin therapy on blood and tissue ATP levels and erythrocyte membrane lipid composition. *Res Exp Med*. **199**: 189-194.

Daniels, T., Bsc, PhD. (1973). In: *Thermal Analysis*, Techniques based on changes in thermal properties. pp. 122.

Datta, D. B. (1987). In: *A Comprehensive Introduction to Membrane Biochemistry*. Flora Publishing, Madison.

Davies, M., Richardson, P., and Woolf, N. (1993). Risk of thrombosis in human atherosclerotic plaques: the role of extracellular lipid, macrophages, and smooth muscle cell content. *Br Heart J*. **69**: 377–381.

Davignon, J. (1997). Atorvastatin: a statin with a large spectrum of action. *Atherosclerosis ID Res Alert*. **2**(6): 243–252.

Dean, J. A. (1995). In: *The Analytical Chemistry Handbook*. McGraw Hill, Inc. New York. pp. 15.1–15.5.

Dimmeler, S., Fleming, I., Fisslthaler, B., Hermann, C., Busse, R., and Zeiher, A. M. (1999). Activation of nitric oxide synthase in endothelial cells by Aktdependent phosphorylation. *Nature*. **399**: 601–605.

Djaldetti, M., Salman, H., Bergman, M., and Bessler, H. (2006). Effect of pravastatin, simvastatin and atorvastatin on the phagocytic activity of mouse peritoneal macrophages. *Experimental and Molecular Pathology*. **80**: 160-164.

Dluhy, R. A., Cameron, D. G., Mantsch, H. H., and Mendelsohn, R. (1983). Fourier Transform Infrared Spectroscopic Studies of the Effect of Calcium Ions on Phosphatidylserine. *Biochemistry*. **22**: 6318-6325.

Downs, J. R., Clearfield, M., Weis, S., Whitney, E., Shapiro, D.R., Peere, P.A., Langendorfer, A., Stein, E.A., Kruyer, W., and Gotto, A. M. Jr. (1998). Primary prevention of acute coronary events with lovastatin in men and women with average cholesterol levels: results of AFCAPS/TexCAPS. *JAMA*. **279**: 1615–1622.

Durazzo, A. E. D. S., Machado, F. S., Ikeoka, D. T., De Bernoche, C., Monachini, M. C., Puech-Leao, P., Caramelli, B., and Powell, J. T. (2004). Reduction in cardiovascular events after vascular surgery with atorvastatin: a randomized trial. *J Vasc Surg*. **39**: 967–976.

Evans, M., and Rees, A. (2002). Effects of HMG-CoA Reductase Inhibitors on Skeletal Muscle. *Drug Safety*. **25**(9): 649-663.

Fassbender, K., Stroick, M., Bertsch, T., Ragoschke, A., Kuehl, S., Walter, S., Walter, J., Brechtel, K., Muehlhauser, F., von Bergmann, K., and Lütjohann, D. (2002). Effects of statins on human cerebral cholesterol metabolism and secretion of Alzheimer amyloid peptide. *Neurology*. **59**: 1257–1258.

Freifelder, D. (1982). In: *Physical Biochemistry*, Chapter 14. W. H. Freeman and Company, New York.

Frengeli, U. P., and Günthard, H. H. (1976). Hydration sites of egg phosphatidylcholine determined by means of modulated excitation infrared spectroscopy. *Biochim Biophys Acta*. **450**: 101-106.

Fuldner, H. H. (1981). Characterization of a third phase transition in multilamellar dipalmitoyllecithin liposomes. *Biochemistry*. **20**: 5707-5710.

Fuller, S. J., Gillespie-Brown, J., and Sugden, P. H. (1998). Oncogenic src, raf and ras stimulate a hypertrophic pattern of gene expression and increase cell size in neonatal rat ventricular myocytes. *J Biol Chem*. **273**: 18146–1852.

Ginsberg, H. N., Le, N. A., Short, M. P., Ramakrishnan, R., and Desnick, R. J. (1987). Suppression of apolipoprotein B production during treatment of cholesteryl ester storage disease with lovastatin: implications for the regulation of apolipoprotein B synthesis. *J Clin Invest*. **80**: 1692–1697.

Golomb, B. A. (2004). Statin Adverse Effects: Implications for the Elderly. *Geriatric Times*. **5**(3).

Gregoriadis, G. (1991). Overview of liposomes. *J Antimicrob Chemother*. **28**(Suppl B): 39-48.

Griffiths, P. R., and de Haseth, J. A. (1986). In: *Fourier Transform Infrared Spectrometry*. Wiley, New York.

Grit, M., and Crommelin, D. J. (1993). Chemical Stability of Liposomes: Implications for their physical stability. *Chem Phys Lipids*. **64**(1-3): 3-18.

Grundy, S. M. (1998). Consensus statement: role of therapy with 'statins' in patients with hypertriglyceridemia. *Am J Cardiol*. **81**: 1B–6B.

Guillot, F., Misslin, P., and Lemaire, M. (1993). Comparison of fluvastatin and lovastatin bloodbrain barrier transfer using in vitro and in vivo methods. *J Cardiovasc Pharmacol*. **21**: 339–346.

Güldütuna, S., Deisinger, B., Weiss, A., Freisleben, H. J., Zimmer, G., Sipos, P., and Leuschner, U. (1997). Ursodeoxycholate stabilizes phospholipid-rich membranes and mimics the effect of cholesterol: investigations on large unilamellar vesicles. *Biochim Biophys Acta*. **1326**: 265-274.

Hamelin, B. A., and Turgeon, J. (1998). Hydrophilicity/lipophilicity: relevance for the pharmacology and clinical effects of HMG-CoA reductase inhibitors. *TiPS*. **19**: 26-37.

Harker, L., Ross, R., and Slichter, S. (1976). Homocystine-induced arteriosclerosis: the role of endothelial cell injury and platelet response in its genesis. *J Clin Invest*. **58**: 731–741.

Heart Protection Study Collaborative Group. (2002). MRC/BHF Heart Protection Study of cholesterol lowering with simvastatin in 20536 high-risk individuals: a randomised placebo-controlled trial. *Lancet*. **360**: 7–22.

Heller, M. R. (1993). *Biochemistry*. **30**: 10472-10483.

Henwood, J. M., and Heel, R. C. (1988). Lovastatin. Apreliminary review of its pharmacodynamic properties and therapeutic use in hyperlipidaemia. *Drugs*. **36**: 429–454.

Hernandez-Perera, O., Perez-Sala, D., and Navarro-Antolin, J. (1998). Effects of the 3-hydroxy-3-methylglutaryl-CoA reductase inhibitors, atorvastatin and simvastatin, on the expression of endothelin-1 and endothelial nitric oxide synthase in vascular endothelial cells. *J Clin Invest*. **101**: 2711–2719.

Higashino, Y., Matsui, A., and Ohki, K. (2001). Membrane Fusion between Liposomes Composed of Acidic Phospholipids and Neutral Phospholipids Induced by Melittin: A Differential Scanning Calorimetric Study. *J Biochem*. **130**: 393-397.

Hobbs, H. H., Brown, M. S., and Goldstein, J. L. (1992). Molecular genetics of the LDL receptor gene in familial hypercholesterolaemia. *Hum Mutat*. **1**: 445–466.

Horwich, T. B., Maclellan, W. R., and Fonarow, G. C. (2004). Statin therapy is associated with improved survival in ischemic and non-ischemic heart failure. *J Am Coll Cardiol*. **43**: 642–648.

Huang, C. H., and Li, S. (1999). Calorimetric and molecular studies of the thermotropic phase behaviour of membrane phospholipids. *Biochim Biophys Acta*. **1422**: 273-307.

Inagaki, F., Shimada, I., Kawaguchi, K., Hirano, M., Terasawa, I., Ikura, T., and Go, N. (1989). Structure of melittin bound to perdeuterated dodecylphosphocholine micelles as studied by two‐dimensional NMR and distance geometry calculations *Biochemistry*. **28**: 5985-5991.

Ipsen, J. H., Mouritsen, O. G., and Bloom, M. (1990). Relationships between lipid membrane area, hydrophobic thickness, and acyl-chain orientational order, The effects of cholesterol. *Biophys J*. **57**: 405-412.

Jackson, M., and Mantsch, H. H. (1993). Biomembrane structure from FT-IR spectroscopy. *Spectrochim Acta Rev*. **15**: 53-69.

Jain, M. K. (1988). In: *Introduction to Biological Membranes*, 2nd Edition. John Wiley and Sons Inc., New York.

Jain, M. K., and Min Wu, N. (1977). Effect of small molecules on the dipalmitoyl lecithin liposomal bilayer: III phase transition in lipid bilayer. *J Membrane Biology*. **34**: 157-201.

Jain, M. K., Wu, N. Y., and Wray, L. V. (1975). Drug-induced phase change in bilayer as possible mode of action of membrane expanding drugs. *Nature*. **255**: 494-496.

Janiak, M. J., Small, D. M., and Shipley, G. G. (1979). Temperature and Compositional Dependence of the Structure of Hydrated Dimyristoyl Lecithin. *J Biol Chem*. **254**: 6068-6078.

Jeppesen, U., Gaist, D., Smith, T., and Sindrup, S. H. (1999). Statins and peripheral neuropathy. *Eur J Clin Pharmacol*. **54**:835-838.

Jick, H., Zornberg, G. L., Jick, S. S., Seshadri, S., and Drachman D. A. (2000). Statins and the risk of dementia. *Lancet*. **356**: 1627–1631.

Joyce, M., Kelly, C., Winter, D., Chen, G., Leahy, A., and Bouchier-Hayes, D. (2001). Pravastatin, a 3-hydroxy-3-methylglutaryl coenzyme A reductase inhibitor, attenuates renal injury in an experimental model of ischemia-reperfusion. *J Surg Res*. **101**: 79–84.

Jullien, S., Contrepois, A., Sligh, J. E., Domart, Y., Yeni, P., Brajtburg, J., Medoff, G., and Bolard, J. (1989). Study of the Effects of Liposomal Amphotericin B on *Candida albicans*, *Cryptococcus neoformans*, and Erythrocytes by Using Small Unilamellar Vesicles Prepared from Saturated Phospholipids. *Antimicrobial Agents and Chemotherapy*. **33**(3): 345-349.

Karp, G. (1999). In: *Cell and Molecular Biology*, 2nd ed, Chapter 4. John Wiley & Sons, Inc.

Kazancı, N., Toyran, N., Haris, P. I., and Severcan, F. (2001). Vitamin D_2 at high and low concentrations exert opposing effects on molecular order and dynamics of dipalmitoyl phosphatidylcholine membranes. *Spectroscopy*. **15**: 47-55.

King, D. S., Jones, D. W., Wofford, M. R., et al. (2001). Cognitive impairment associated with atorvastatin. *Presented at the American College of Clinical Pharmacy Spring Practice and Research Forum*. Salt Lake City; April 22-25.

King, D. S., Wilburn, A. J., Wofford, M. R., Harrell, T. K., Lindley, B. J., and Jones, D. W. (2003). Cognitive impairment associated with atorvastatin and simvastatin. *Pharmacotherapy*. **23**(12): 1663-1667.

Kirsch, C., Eckert, G. P., and Mueller, W. E. (2003). Statin effects on cholesterol micro-domains in brain plasma membranes. *Biochemical Pharmacology*. **65**: 843-856.

Kiselev, M. A., Lesieur, P., Kisselev, A. M., Lombardo, D., Killany, M., Lesieur, S., and Ollivon, M. (2001). A Sucrose Solutions Application to the Study of Model Biological Membranes. *Nuclear Instruments & Methods in Physics Reseach A*. **470**: 409-416.

Kleemann, R., Princen, H. M. G., Emeis, J. J., Jukema, J. W., Fontijn, R. D., Horrevoets, A. J. G., Kooistra, T., and Havekes, L. M. (2003). Rosuvastatin reduces atherosclerosis development beyond and independent of its plasma cholesterol-lowering effect in APOE*3-Leiden transgenic mice: evidence for anti-inflammatory effects of rosuvastatin. *Circulation*. **108**: 1368–1374.

Kobashigawa, J. A., Katznelson, S., Laks, H., Johnson, J. A., Yeatman, L., Wang, X. M., Chia, D., Terasaki, P. I., Sabad, A., Cogert, G. A., Trosian, K., Hamilton, M. A., Moriguchi, J. D., Kawata, N., Hage, A., Drinkwater, D. C., and Stevenson, L. W. (1995). Effect of pravastatin on outcomes after cardiac transplantation. *N Engl J Med*. **333**: 621–627.

Korkmaz, F., and Severcan, F. (2005). Effect of progesterone on DPPC membrane: Evidence for lateral phase separation and inverse action n lipid dynamics. *Archives of Biochemistry and Biophysics*. **440**: 141-147.

Koter, M., Broncel, M., Chojnowska-Jezierska, J., Klikczynska, K., and Franiak, I. (2002). The effect of atorvastatin on erythrocyte membranes and serum lipids in patients with type-2 hypercholesterolemia. *Eur J Clin Pharmacol*. **58**: 501–506.

Koter, M., Franiak, I., Broncel, M., and Chojnowska-Jezierska, J. (2003). Effects of simvastatin and pravastatin on peroxidation of erythrocyte plasma membrane lipids in patients with type 2 hypercholesterolemia. *Can J Physiol Pharmacol*. **81**(5): 485–492.

Koyama, T. M., Stevens, C. R., Borda, E. J., Grobe, K. J., and Cleary D. A. (2000). Characterizing the gel to liquid crystal transition in lipid-bilayer model membranes. *The Chemical Educator*. **5**: 1430-1434.

Koyama, T. M., Stevens, C. R., Borda, E. J., Grobe, K. J., and Cleary, D. A. (1999). Characterizing the Gel to Liquid Crystal Transition in Lipid-Bilayer Model Systems. *Chem Educator*. **4**: 12-15.

Kupiainen, M., Falck, E., Ollila, S., Niemelä, Gurtovenko, A. A., Hyvönen, M. T., Patra, M., Karttunen, M., and Vattulainen, I. (2005). Free Volume Properties of Sphingomyelin, DMPC, DPPC, and PLPC Bilayers. *Journal of Computational and Theoretical Nanoscience*. **2**: 401-413.

Kureishi, Y., Luo, Z., Shiojima, I., Bialik, A., Fulton, D., Lefer, D. J., Sessa, W. J., and Walsh, K. (2000). The HMG-CoA reductase inhibitor simvastatin activates the protein kinase Akt and promotes angiogenesis in normocholesterolemic animals. *Nat Med*. **6**: 1004–1010.

Lacoste, L., Lam, J. Y. T., Hung, J., Letchacovski, G., Solymoss, C. B., and Waters, D. (1995). Hyperlipidemia and coronary disease: correction of the increased thrombogenic potential with cholesterol reduction. *Circulation*. **92**: 3172–3177.

Laufs, U., Endres, M., Stagliano, N., Amin-Hanjani, S., Chui, D-S., Yang, S-X., Simoncini, T., Yamada, M., Rabkin, E., Allen, P. G., Huang, P. L., Böhm, M., Schoen, F. J., Moskowitz M. A., and Liao, J. K. (2000). Neuroprotection mediated by changes in the endothelial actin cytoskeleton. *J Clin Invest*. **106**: 15–24.

Laufs, U., La Fata, J., Plutzky, J., and Liao, J. K. (1998). Upregulation of endothelial nitric oxide synthase by HMG CoA reductase inhibitors. *Circulation*. **97**: 1129–1135.

Lee, A. G. (1977). Lipid phase transitions and phase diagrams. II. Mixtures involving lipids. *Biochim Biophys Acta*. **14**: 472(3-4), 285-344.

Lee, D. C., and Chapman, D. (1986). Infrared spectroscopic studies of biomembranes and model membranes. *Biosci Rep*. **6**: 235-256.

Leung, B. P., Sattar, N., Crilly, A., Prach, M., McCarey, D. W., Payne, H., Madhok, R., Campbell, C., Gracie, J. A., Liew, F. Y., and McInnes, I. B. (2003). A novel anti-inflammatory role for simvastatin in inflammatory arthritis. *J Immunol*. **170**: 1524–1530.

Lewis, R. N. A. H., and McElhaney, R., N. (2002). *Vibrational Spectroscopy of Lipids*, in *Handbook of Vibrational Spectroscopy*, Vol.5, Chalmers, J. M., Griffiths, P. R. (Eds), Wiley, Chichester, UK. pp. 3447-3464.

Liao, J. K. (2002). Beyond lipid lowering: the role of statins in vascular protection. *Int J Cardiol*. **86**: 5–18.

Lindahl, A., Sandström, R., Ungell, A-L., Abrahmsson, B., Knutson, L., Knutson, T., and Lennernäs H. (1996) Jejunal permeability and hepatic extraction of fluvastatin in humans. *Clin Pharm Ther*. **60**: 493-503.

Locatelli, S., Lutjohann, D., Schmidt, H. H., Otto, C., Beisiegel, U., and von Bergmann, K. (2002). Reduction of plasma 24S-hydroxycholesterol (cerebrosterol) levels using high-dosage simvastatin in patients with hypercholesterolemia: evidence that simvastatin affects cholesterol metabolism in the human brain. *Arch Neurol*. **59**: 213–216.

Lodish, H., Berk, A., Matsudaira, P., Kaiser, C. A., Krieger, M., Scott, M. P., and Zipursky, L. (2004). In: *Molecular Cell Biology*, Fifth Edition. W. H. Freeman.

Lopez-Garcia, F., Villalain, J., and Gomez-Fernandez, J. C. (1993). Infrared spectroscopic studies of the interaction of diacylglycerols with phosphatidylserine in the presence of calcium. *Biochim Biohys Acta*. **1169**: 264-272.

Lutgens, E., and Daemen, Mat. J. A. P. (2004). HMG-coA reductase inhibitors: lipid-lowering and beyond. *Drug Discovery Today: Therapeutic Strategies*. **1**(2): 189-194.

Mantsch, H. H. (1984). Biological Applications of Fourier Transform Infrared Spectroscopy: A Study of Phase Transitions in Biomembranes. *J Mol Structure*. **113**: 201-212.

Mantsch, H. H., and Casal, H. L. (1984). The Thermotropic Phase Behaviour of N-Methylated Dipalmitoyl Phosphatidylethanolamines. *Biochim Biohys Acta*. **779**: 381-401.

Maron, D. J., Fazio, S., and Linton, M. F. (2000). Current perspectives on statins. *Circulation*. **101**: 207–213.

Mason, J. T. (1998). Investigation of phase transitions in bilayers membranes. *Methods Enzymol*. **295**: 468–494.

Mathews, C. K., van Holde, K. E., and Ahern, K. G. (2000). In: *Biochemistry*, Third Edition, Chapters 10, 19. Addison Wesley Longman, Inc. Benjamin/Cummings.

Mavramoustakos, T., Theoropoulou, E., and Yang, D-P. (1997). The use of high-resolution solid-state NMR spectroscopy and differential scanning calorimetry to study interactions of anaesthetic steroids with membrane. *Biochimica et Biophysica Acta*. **1328**: 65-73.

Mayor, U., Johnson, C. M., Daggett, V., and Fersht, A. R. (2000). Protein folding and unfolding in microseconds to nanoseconds by experiment and simulation. *Proc Natl Acad Sci USA*. **97**(25): 13518-13522.

Mazeaud, M. M., Driss, F., and Le Quan Sang, K. H. (1992). Biochemical and functional alterations associated with hypercholesterolemia in platelets from hypertensive patients. *Atherosclerosis*. **94**: 201–211.

Mehra, M. R., Uber, P. A., Vivekananthan, K., Solis, S., Scott, R. L., Park, M. H., Milani, R. V., and Lavie, C. J. (2002). Comparative beneficial effects of simvastatin and pravastatin on cardiac allograft rejection and survival. *J Am Coll Cardiol*. **40**: 1609–1614.

Meier, C. R., Schlienger, R. G., Kraenzlin, M. E., Schlegel, B., and Jick, H. (2000). HMG CoA reductase inhibitors and the risk of fractures. *JAMA*. **283**: 3205–3210.

Melchior, D. L., and Stein, J. M. (1976). Thermotropic transitions in biomembranes. *Annu Rev Biophys Bioeng*. **5**: 205-238.

Mendelsohn, R., and Mantsch, H. H. (1986). *Fourier Transform Infrared Studies of Lipid-Lipid Interactions*. In: *Progress in Protein-Lipid Interactions*. (Watts, A., and De Pont, J. J. H. H. M., Eds). Vol. 2. pp. 103-146.

Mendelsohn, R., Davies, M. A., Brauner, J. W., Schuster, H. F., and Dluhy, R. A. (1989). Quantitative determination of conformational disorder in the acyl chains of phospholipid bilayers by infrared spectroscopy. *Biochemistry*. **28**: 8934-8939.

Microcal, Inc. (2002). *DSC Data Analysis in Origin: Tutorial Guide*, Vers. 7. Northhampton, MA. 89-91.

Momo, F., Fabris, S., Bindoli, A., Scutari, G., and Stevanato, R. (2002). EPR and DSC study of the effects of propofol and nitrosopropofol on DMPC multilamellar liposomes. *Current Topics in Biophysics*. **26**: 75-81.

Moreno, P. R., Falk, E., Palacios, I. F., Newell, J. B., Fuster, V., and Fallon, J. T. (1994). Macrophage infiltration in acute coronary syndromes: implications for plaque rupture. *Circulation*. **90**: 775–778.

Muldoon, M. F., Barger, S. D., Ryan, C. M., Flory, J. D., Lehoczky, J. P., Matthews, K. A., and Manuck, S. B. (2000). Effects of lovastatin on cognitive function and psychological well-being. *Am J Med*. **108**: 538-546.

Muldoon, M. F., Ryan, C. M., Flory, J. D., and Manuck, S. B. (2002). Effects of simvastatin on cognitive functioning. *Presented at the American Heart Association Scientific Sessions*. Chicago; Nov. 17-20.

Mundy, G., Garrett, R., Harris, S., Chan, J., Chen, D., Rossini, G., Boyce, B., Zhao, M., and Gutierrez, G. (1999). Stimulation of bone formation in vitro and in rodents by statins. *Science*. **286**: 1946–1949.

Mushayakarara, E., and Levin, I. W. (1982). *J Phys Chem*. **86**: 2324-2327.

Nakagami, H., Jensen, K. S., and Liao, J. K. (2003). A novel pleiotropic effect of statins: prevention of cardiac hypertrophy by cholesterol-independent mechanisms. *Ann Med*. **35**: 398–403.

Nakamura, T., Ushiyama, C., Hirokawa, K., Osada, S., Inoue, T., Shimada, N., and Koide, H. (2002). Effect of cerivastatin on proteinuria and urinary podocytes in patients with chronic glomerulonephritis. *Nephrol Dial Transplant*. **17**: 798–802.

Negre-Aminou, P., van Vliet, A. K., van Erck, M., van Thiel, G. C., van Leeuwen, R. E., and Cohen, L. H. (1997). Inhibition of proliferation of human smooth muscle cells by various HMG-CoA reductase inhibitors; comparison with other human cell types. *Biochim Biophys Acta*. **1345**: 259–268.

Nissen, S. E., Tuzcu, E. M., Schoenhagen, P., Crowe, T., Sasiela, W. J., Tsai, J., Orazem, J., Magorien, R. D., O'Shaughnessy, and C., Ganz, P. Reversal of Atherosclerosis with Aggressive Lipid Lowering (REVERSAL) Investigators. (2005). Statin therapy, LDL cholesterol, C-reactive protein, and coronary artery disease. *N Engl J Med*. **352**: 29–38.

Node, K., Fujita, M., Kitakazi, M., Hori, M., and Liao, J. K. (2003). Short-term statin therapy improves cardiac function and symptoms in patients with idiopathic dilated cardiomyopathy. *Circulation*. **108**: 839–843.

Notarbartolo, A., Davi, G., Averna, M., Barbagallo, C. M., Ganci, A., Giammarresi, C., La Placa, F. P., and Patrono C. (1995). Inhibition of thromboxane biosynthesis and platelet function by simvastatin in type IIa hypercholesterolemia. *Arterioscler Thromb Vasc Biol*. **15**: 247–251.

O'Driscoll, G., Green, D., and Taylor, R. R. (1997). Simvastatin, an HMG-coenzyme A reductase inhibitor, improves endothelial function within 1 month. *Circulation*. **95**: 1126–1131.

Ohara, Y., Peterson, T. E., and Harrison, D. G. (1993). Hypercholesterolemia increases endothelial superoxide anion production. *J Clin Invest*. **91**: 2546–2551.

Ohara, Y., Peterson, T. E., Sayegh, H. S., Subramanian, R. R., Wilcox, J.N., and Harrison, D. G. (1995). Dietary correction of hypercholesterolemia in the rabbit normalizes endothelial superoxide anion production. *Circulation*. **92**: 898–903.

Ohki, K. (2005) Formation of micro-domains as functional regions in biomembranes: specific interactions inferred by differential scanning calorimetry and microscopic imaging of membrane fluidity. *Journal of Physics: Condensed Matter*. **17**: S2957-S2963.

Ohline, S. M., Campbell, M. L., Turnbull, M. T., and Kohler, S. J. (2001). Differential Scanning Calorimetric Study of Bilayer Membrane Phase Transitions: A Biophysical Chemistry Experiment. *J Chem Ed*. **78**(9): 1251-1256.

Orsi, A., Sherman, O., and Woldeselassie, Z. (2001). Simvastatin-associated memory loss. *Pharmacotherapy*. **21**(6): 767-769.

Ostro, M. J. (1983). In: *Liposomes*. Marcel Dekker, Inc., New York.

Päivä, H., Thelen, K. M., Van Coster, R., Smet, J., De Paepe, B., Mattila, K. M., Laakso, J., Lehtimäki, T., von Bergmann, K., Lütjohann, D., and Laaksonen, R. (2005). High-dose statins and skeletal muscle metabolism in humans: A randomized, controlled trial. *Clinical Pharmacology & Therapeutics*. **78**(1): 60-68.

Pedersen, T. R., Berg, K., Cook, T. J., Faergeman, O., Haghfelt, T., Kjekshus, J., Miettinen, T., Musliner, T. A., Olsson, A. G., Pyörälä, K., Thorgeirsson, G., Tobert, J. A., Wedel, H., and Wilhelmsen, L. (1996). Safety and tolerability of cholesterol lowering with simvastatin during 5 years in Scandinavian simvastatin survival study. *Arch Intern Med*. **156**(18): 2085–2092.

Phillips, M. C., Ladbrooke, B. D., and Chapman, D. (1970). *Biochim Biophys Acta*. **196**: 35-44.

Plosker, G. L., and Wagstaff, A. J. (1996). Fluvastatin: A review of its pharmacology and use in the management of hypercholesteraemia. *Drugs*. **51**: 433–459.

Pott, T., and Dufourc, F. J. (1995). Action of melittin on the DPPC-cholesterol liquid-ordered phase: a solid state 2H-and 31P-NMR study. *Biophys J*. **68**(3): 965-977.

Pownall, H. J., Pao, Q., and Massey, J. B. (1985). Acyl Chain and Headgroup Specificity of Human Plasma Lecithin:cholesterol Acyltransferase. *The Journal of Biological Chemistry*. **260**(4): 2146-2152.

Pruefer, D., Makowski, J., Schnell, M., Buerke, U., Dahm, M., Oelert, H., Sibelius, U., Grandel, U., Grimminger, F., Seeger, W., Meyer, J., Darius, H., and Buerke, M. (2002). Simvastatin inhibits inflammatory properties of Staphylococcus aureus alpha-toxin. *Circulation*. **106**: 2104–2110.

Puddu, P., Puddu, G. M., and Muscari, A. (2001). HMG-CoA reductase inhibitors: is the endothelium the main target? *Cardiology*. **95**: 9–13.

Rabini, R. A., Polenta, M., Staffolani, R., Tocchini, M., Signore, R., Testa, I., and Mazzanti, L. (1993). Effect of Hydroxymethylglutaryl-CoA Reductase Inhibitors on the Functional Properties of Erythrocyte Membranes. *Experimental and Molecular Pathology*. **59**(1): 51-57.

Ridker, P. M., Cannon, C. P., Morrow, D., Rifai, N., Rose L. M., and McCabe, C. JUPITER study group.(2004). Rosuvastatin in the primary prevention of cardiovascular disease among patients with low levels of low-density lipoprotein cholesterol and elevated high-sensitivity C-reactive protein. Rationale and design of the JUPITER trial. *Circulation*. **108**: 2292–2297.

Ridker, P. M., Rifai, N., Pfeffer, M. A., Sacks, F., and Braunwald, E. (1999). Long-term effects of pravastatin on plasma concentration of C-reactive protein. *Circulation*. **100**: 230–235.

Ridker, P. M., Cannon, C. P., Morrow, D., Rifai, N., Rose, L. M., McCabe, C. H., Pfeffer, M. A., and Braunwald, E. Pravastatin or Atorvastatin Evaluation Infection Therapy-Thrombolysis in Myocardial Infarction 22 (PROVE IT-TIMI 22) Investigators. (2005). C-reactive protein levels and outcomes after statin therapy. *N Engl J Med*. **352:**20–28.

Rikitake, Y., Kawashima, S., Takeshita, S., Amashita, T., Azumi, H., Yasuhara, M., Nishi, H., Inoue, N., and Yokoyama M. (2001). Anti-oxidative properties of fluvastatin, an HMG-CoA reductase inhibitor, contribute to prevention of atherosclerosis in cholesterol-fed rabbits. *Atherosclerosis*. **154**: 87–96.

Roche, V. F. (2005). Antihyperlipidemic Statins: A Self-Contained, Clinically Relevant Medicinal Chemistry Lesson. *American Journal of Pharmaceutical Education*. **69**(4): 546-560.

Rosenson, R. S. (2004). Current Overview of Statin-Induced Myopathy. *Am J Med*. **116**: 408-416.

Rosoff, M. (1996). In: *Vesicles*. Marcel Dekker, Inc., New York.

Ross, R. (1999). Atherosclerosis: an inflammatory disease. *N Engl J Med*. **340**: 115–126.

Ross, R., (1993). The pathogenesis of atherosclerosis: a perspective for the 1990's. *Nature*. **362**: 801–809.

Roth, B.D., Bocan, T. M. A., Blankley, C. J., Chucholowski, A. W., Creger, P. L., Creswell, M. W., Ferguson, E., Newton, R. S., O'Brien, P., Picard, J. A., Roark, W. H., Sekerke, C. S., Sliskovic, D. R., and Wilson, M. W. (1991). Relationship between tissue selectivity and lipophilicity for inhibitors of HMG-CoA reductase. *J Med Chem*. **34**:463–466.

Ruocco, J. M., and Shipley, G. G. (1982). Characterization of the subtransition of hydrated DPPC bilayers. *Biochim Biophys Acta*. **691**: 309-320.

Sacks, F. M., Pfeffer, M. A., Moye, L. A., Rouleau, J. L., Rutherford, J. D., Cole, T. G., Brown, L., Warnica, J. W., Arnold, J. M., Wun, C. C., Davis, B. R., and Braunwald, E. (1996). The effect of pravastatin on coronary events after myocardial infarction in patients with average cholesterol levels. Cholesterol and Recurrent Events Trial investigators. *N Engl J Med*. **335**(14): 1001-1009.

Sandaram, M. B., and Thompson, T. E. (1990). *Biochemistry*. **29**: 10676-10684.

Sasaki, M., Bharwani, S., Jordan, P., Joh, T., Manas, K., Warren, A., Harada, H., Carter, P., Elrod, J. W., Wolcott, M., Grisham, M. B., and Alexander, J. S. (2003). The 3-hydroxy-3-methylglutaryl-CoA reductase inhibitor pravastatin reduces disease activity and inflammation in dextran-sulfate induced colitis. *J Pharmacol Exp Ther*. **305**: 78– 85.

Scandinavian Simvastatin Survival Study Group. (1994). Randomised trial of cholesterol lowering in 4444 patients with coronary heart disease: the Scandinavian Simvastatin Survival Study (4S). *Lancet*. **344**: 1383–1389.

Schachter, M. (2004). Chemical, pharmacokinetic and pharmacodynamic properties of statins: an update. *Fundamental & Clinical Pharmacology*. **19**: 117-125.

Schneider, F. M., Marsh, D., Jahn, W., Kloesgen, B., and Heimburg, T. (1999). Network formation of lipid membranes: Triggering structural transitions by chain melting. *Proc Natl Acad Sci USA*. **96**(25): 14312-14317.

Schrier, R., and Abraham, W. (1999). Hormones and hemodynamics in heart failure. *N Engl J Med*. **341**: 577–585.

Schwartz, G. G., Olsson A. G., Ezekowitz, M. D., Ganz, P., Oliver, M. F., Waters, D., Zeiher, A., Chaitman, B. R., Leslie, S., and Stern. T. Myocardial Ischemia Reduction with Aggressive Cholesterol Lowering (MIRACL) Study Investigators. (2001). Effects of atorvastatin on early recurrent ischemic events in acute coronary syndromes. The MIRACL study: a randomized controlled trial. *JAMA*. **285**: 1711–1718.

Seelig, A., and Seelig, J. (1974). The dynamic structure of fatty acyl chain in a phospholipid bilayer measured by deuterium magnetic resonance. *Biochem*. **13**: 4839-4845.

Serajuddin, A. T. M., Ranadive, S. A., and Mahoney, E. M. (1991). Relative lipophilicities, solubilities, and structure-pharmacological considerations of 3-hydroxy-3-methylglutaryl-coenzyme A (HMG-CoA) reductase inhibitors pravastatin, lovastatin, mevastatin, and simvastatin. *J Pharmaceut Sc*. **80**: 830–834.

Sever, P. S., Dahlof, B., Poulter, N.R., Wedel, H., Beevers, G., Caulfield, M., Collins, R., Kjeldsen, S. E., Kristinsson, A., McInnes, G.T., Mehlsen, J., Nieminen, M., O'Brien, E., and Ostergren, J. (2003). ASCOT investigators. Prevention of coronary and stroke events with atorvastatin in hypertensive patients who have average or lower-than-average cholesterol concentrations, in the Anglo-Scandinavian Cardiac Outcomes Trial--Lipid Lowering Arm (ASCOT-LLA): a multicentre randomized controlled trial. *Lancet*. **361**: 1149-1158.

Severcan, F. (1997) Vitamin E decreases the order of the phospholipid model membranes in the gel phase: An FTIR study. *Bioscience Reports*. **17**: 231-235.

Severcan, F., and Cannistraro, S. (1988). Direct electron-spin resonance evidence for alpha-tocopherol-induced phase-separation in model membranes. *Chem Phys Lipids*. **478**: 129-133.

Severcan, F., Durmus, H. O., Eker, F., Akınoğlu, B. G., and Haris, I. P. (2000). Vitamin D_2 modulates melittin-membrane interactions. *Talanta*. **53**: 205-211.

Severcan, F., Sahin, I., and Kazancı, N. (2005). Melatonin strongly interacts with zwitterionic model membranes—evidence from Fourier transform infrared spectroscopy and differential scanning calorimetry. *Biochimica et Biophysica Acta*. **1668**: 215-222.

Shaikh, S. R., Dumaual, A. C., Jenski, L. J., and Stillwell, W. (2001). Lipid phase separation in phospholipid bilayers and monolayers modeling the plasma membrane. *Biochimica et Biophysica Acta* **1512**: 317-328.

Shepherd, J., Blauw, G. J, Murphy, M. B., Bollen, E. L. E. M., Buckley, B. M., Cobbe, S. M., Ford, I., Gaw, A., Hyland, M., Jukema, J. W., Kamper, A. M., Macfarlane, P. W., Meinders, A. E., Norrie, J., Packard, C. J., Perry, I. J., Stott, D. J., Sweeney, B. J., Twomey, C., and Westendorp, R. G. J., on behalf of the PROSPER study group. (2002). Pravastatin in elderly individuals at risk of vascular disease (PROSPER): a randomised controlled trial. *Lancet*. **360**: 1623–1630.

Shepherd, J., Cobbe, S. M., Ford, I., Isles, C. G., Lorimer, A. R., MacFarlane, P. W., McKillop, J. H., and Packard, C. J. (1995). Prevention of coronary heart disease with pravastatin in men with hypercholesterolemia. West of Scotland Coronary Prevention Study Group. *N Engl J Med*. **333**(20): 1301-1307.

Sibelius, U., Grandel, U., Buerke, M., Mueller, D., Kiss, L., Kraemer, H-J., Braun-Dullaeus, R., Haberbosch, W., Seeger, W., and Grimminger, F. (2000). Staphylococcal alpha toxin provokes coronary vasoconstriction and loss in myocardial contractility in perfused rat hearts: role of thromboxane generation. *Circulation*. **101**: 78– 85.

Silver, B. L. (1985). In: *The Physical Chemistry of Membranes*, An Introduction to the Structure and Dynamics of Biological Membranes, First Edition. Allen & Unwin, The Solomon Press.

Simons, M., Schwarzler, F., Lutjohann, D., von Bergmann, K., Beyreuther, K., Dichgans, J., Wormstall, H., Hartmann, T., and Schulz, J. B. (2002). Treatment with simvastatin in normocholesterolemic patients with Alzheimer's disease: a 26-week randomized, placebo-controlled, double-blind trial. *Ann Neurol*. **52**: 346–350.

Smilde, T. J., van Wissen, S., Wollersheim, H., Trip, M. D., Kastelein, J. J., and Stalenhoef, A. F. (2001). Effect of aggressive versus conventional lipid lowering on atherosclerosis progression in familial hypercholesterolaemia (ASAP): a prospective, randomised, doubleblind trial. *Lancet*. **357**: 577-581.

Smith, E. L., Robert, L. H., Lehman, I. R., Lefkowitz, R. J., Handler, P., and White, A. (1983). In: *Principles of Biochemistry*, General Aspects, Seventh Edition. Mc-Graw-Hill International Editions.

Song, C., Guo, Z., Ma, Q., Chen, Z., Liu, Z., Jia, H., and Dang, G. (2003). Simvastatin induces osteoblastic differentiation and inhibits adipocytic differentiation in mouse bone marrow stromal cells. *Biochem Biophys Res Commun*. **308**: 458–462.

Söderlund, T., Lehtonen, J. Y. A., and Kinnunen, P. K. J. (1999). Interactions of Cyclosporin A with Phospholipid Membranes: Effect of Cholesterol. *Molecular Pharmacology*. **55**: 32-38.

Sparks, D. L., Sabbagh, M. N., and Connor, D.J., Launer, L. J., Petanceska, S., Baxter, L., Browne, P., Lopez, J., Wassar, D., Lochhead, J., and Ziolwolski, C. (2004). Cholesterol-lowering drug may slow Alzheimer's progression. *American Heart Association meeting report*.

Spika, S., Dey, I., Buda, C., Csongor, J., Szegedi, G., and Farkas, T. (1996). The mechanism of inhibitory effect of eicosapentaenoic acid on phagocytic activity and chemotaxis of human neuthrophil granulocytes. *Clin Immunol Immunopathol*. **79**: 224– 228.

Stuart, B. (2004). In: *Infrared Spectroscopy*, Fundamentals and Applications. John Wiley & Sons, Ltd.

Sturtevant, J. M. (1987). *Biochemical Applications of Differential Scanning Calorimetry*, in *Ann Rev Phys Chem*. Strauss, H. L., Babcock, G. T., and Moore, C. B. Eds., Annual Reviews, Inc, Palo Alto, CA. **38**: 466-476.

Sugii, T., Takagi, S., and Matsumoto, Y. (2004). Molecular Dynamics Study of Permeation Process of Small Molecules Through a Lipid Bilayer. *XXI ICTAM*. Warsaw, Poland.

Szoka, Jr. F., and Papahadjopoulos, D. (1980). Comparative Properties and Methods of Preparation of Lipid Vesicles (Liposomes). *Ann Rev Biophys Bioeng*. **9**: 467-508.

Tahir, A., Grabielle-Madelmont, C., Betrencourt, C., Ollivon, M., and Peretti, P. (1999). A differential scanning calorimetry study of the interaction of Lasalocid antibiotic with phospholipid bilayers. *Cemistry and Physics of Lipids*. **103**: 57-65.

Takemoto, M., Node, K., Nakagami, H., Liao, Y., Grimm, M., Takemoto, Y., Kitakaze, M., and Liao, J. K. (2001). Statins as antioxidant therapy for preventing cardiac myocyte hypertrophy. *J Clin Invest*. **108**(10):1429-1437.

Tchapda, L. N. (2005). *Mechanism of the 3-hydroxyl-3-methylglutaryl-coenzyme A Reductase Inhibitor-Induced Myotoxicity in Human Skeletal Muscle Cell Cultures*. Ph.D. Thesis. Technische Universität Kaiserslautern.

The Long-term Intervention with Pravastatin in Ischemic Disease (LIPID) Study Group. (1998). Prevention of cardiovascular events and death with pravastatin in patients with coronary heart disease and a broad range of initial cholesterol levels. *N Engl J Med*. **339**: 1349–1357.

Tien, H. T., and Ottova, A. L. (2000). In: *Membrane Biophysics*, As Viewed From Experimental Bilayer Lipid Membranes, (Planar Lipid Bilayers and Spherical Liposomes), First edition, Chapters 2,4. Elsevier Science B. V.

Todd, P. A., and Goa, K. L. (1990). Simvastatin. A review of its pharmacological properties and therapeutic potential in hypercholesterolaemia. *Drugs*. **40**(4): 583–607.

Tolman, K. G. (2002). The Liver and Lovastatin. *Am J Cardiol*. **89**: 1374-1380.

Torre-Amione, G. (1999). The syndrome of heart failure: emerging concepts in the understanding of its pathogenesis and treatment. *Curr Opin Cardiol*. **14**: 193–195.

Toyran, N., and Severcan, F. (2003). Competitive effect of Vitamin D_2 and Ca^{2+} on phospholipid model membranes: an FTIR study. *Chemistry and Physics of Lipids*. **123**: 165-176.

Tsujita, Y., and Watanabe, Y. (1989). Pravastatin sodium: a novel cholesterol-lowering agent that inhibits HMG-CoA reductase. *Cardiovasc Drug Rev*. **7**(2): 110–126.

Usui, H., Shikata, K., Matsuda, M., Okada, S., Ogawa, D., Yamashita, T., Hida, K., Satoh, M., Wada, J., and Makino, H. (2003). HMG-CoA reductase inhibitor ameliorates diabetic nephropathy by its pleiotropic effects in rats. *Nephrol Dial Transplant*. **18**: 265–272.

Van der Wal, A. C., Becker, A. E., Van der Loos, C. M., and Das, P. K. (1994). Site of intimal rupture or erosion of thrombosed coronary atherosclerotic plaques is characterized by an inflammatory process irrespective of the dominant morphology. *Circulation*. **89**: 36–44.

Van Ginkel, G., van Langen, H., and Levine, Y., K. (1989). The membrane fluidity concept revisited by polarized fluorescence spectroscopy on different model membranes containing unsaturated lipids and sterols. *Biochimie*. **71**: 23-32.

Vasudevan, A. R., Hamirani, Y. S., and Jones, P. H. (2005). Safety of statins: Effects on muscle and the liver. *Cleveland Clinic Journal of Medicine*. **72**(11): 990-1001.

Vaughan, C. J., Gotto, A. M., and Basson, Jr. C. T. (1999). The evolving role of statins in the management of atherosclerosis. *J Am Coll Cardiol*. **35**: 1–10.

Vevera, J., Fisar, F., Kvasnicka, T., Zdenek, H., Starkova, L., Ceska, R., and Papezova, H. (2005). Cholesterol-lowering therapy evokes time-limited changes in serotonergic transmission. *Psychiatry Research*. **133**: 197-203.

Villalain, J., Arranda, F. J., and Gomez-Fernandez, J. C. (1986). Calorimetric and infrared spectroscopic studies of the interaction of α-tocopherol and α-tocopheryl acetate with phospholipid vesicles. *Eur J Biochem*. **158**: 141-147.

von Haehling, S., Anker, S., and Bassenge, E. (2003). Statins and the role of nitric oxide in chronic heart failure. *Heart Fail Rev*. **8**: 99–106.

Wagstaff, L. R., Mitton, M. W., Arvik, B. M., and Doraiswamy, P. M. (2003). Statin-associated memory loss: analysis of 60 case reports and review of the literature. *Pharmacotherapy*. **23**(7): 871-880.

Watts, A., and De Pont, J. J. H. H. M. (1986). (Eds). In: *Progress in Protein-Lipid Interactions*, 2. Elsevier, Amsterdam, The Netherlands.

Weber, P. C., and Salemme, F. R. (2003). Applications of calorimetric methods to drug discovery and the study of protein interactions. *Current Opinion in Structural Biology*. **13**: 115-121.

Werner, N., Nickenig, G., and Laufs, U. (2002). Pleiotropic effects of HMG-CoA reductase inhibitors. *Basic Res Cardiol*. **97**(2):105-116.

White, H. D., Simes, R. J., Anderson, N. E., Hankey, G. J., Watson, J. D.G., Hunt, D., Colquhoun, D. M., Glasziou, P., MacMahon, S., Kirby, A. C., West, M. J., and Tonkin, A. M. (2000). Pravastatin therapy and the risk of stroke. *N Engl J Med*. **343**: 317–326.

Wierzbicki, A. S., Poston, R., and Ferro, A. (2003). The lipid and non-lipid effects of statins. *Pharmacology & Therapeutics*. **99**: 95-112.

Willerson, J., Hillis, M., Winniford, M., and Buja, L. M. (1986). Speculation regarding mechanisms responsible for acute ischemic heart disease syndrome. *J Am Coll Cardiol*. **8**: 245–250.

Wilson, H. L., Schwartz, D. M., Bhatt, H. R., McCulloch, C. E., and Duncan, J. L. (2004). Statin and aspirin therapy are associated with decreased rates of choroidal neovascularization among patients with age-related macular degeneration. *Am J Ophthalmol*. **137**: 615–624.

Xu, C., Stenman, E., and Edvinsson, L. (2002). Reduction of bFGF-induced smooth muscle cell proliferation and endothelin receptor mRNA expression by mevastatin and atorvastatin. *Biochem Pharmacol*. **64**: 497–505.

Yi, P. N., and MacDonald, R. C. (1973). Temperature-dependence of optical properties of aqueous dispersions of phosphatidylcholine. *Chem Phys Lipids*. **11**: 114-134.

Yokota, N., O'Donnell, M., Daniels, F., Burne-Taney, M., Keane, W., Kasiske, B., and Rabb, H. (2003). Protective effect of HMGCoA reductase inhibitor on experimental renal ischemia-reperfusion injury. *Am J Nephrol*. **23**: 13–17.